CHAPTER V

RESULTS AND DISCUSSIONS

This chapter illustrates and discusses results of the optimization of WAG process results obtained from both black oil and compositional reservoir models. The effects of horizontal permeability, vertical to horizontal permeability ratio, and distance between producer and injector were thoroughly investigated. In addition, the impact of using different relative permeability hysteresis models on WAG process was also examined.

5.1 Optimum WAG process using Black oil model

Several studies have been conducted on optimizing the WAG process in specific reservoirs, and different production and injection scenarios have been reported. Thus, it is difficult to indicate the best strategy from these studies. In this study, we first investigated a base case model and then varied a few reservoir parameters to study their effect on the recovery factor.

In this section, the study also includes waterflood since it has been suggested before that WAG process can achieve higher recovery factor than conventional waterflood. The waterflood cases are created with the same input data of PVT and relative permeability function as WAG process. Only difference is at the injection strategy in which only water will be injected continuously until reaching the economic limit.

5.1.1 Results of base case model

Before optimizing the WAG process, a base case reservoir model was constructed. The PVT properties, relative permeability function, initial condition, production and injection strategy for the base case were already mentioned. The results of the base case model are presented in Figures 5.1 to 5.14.

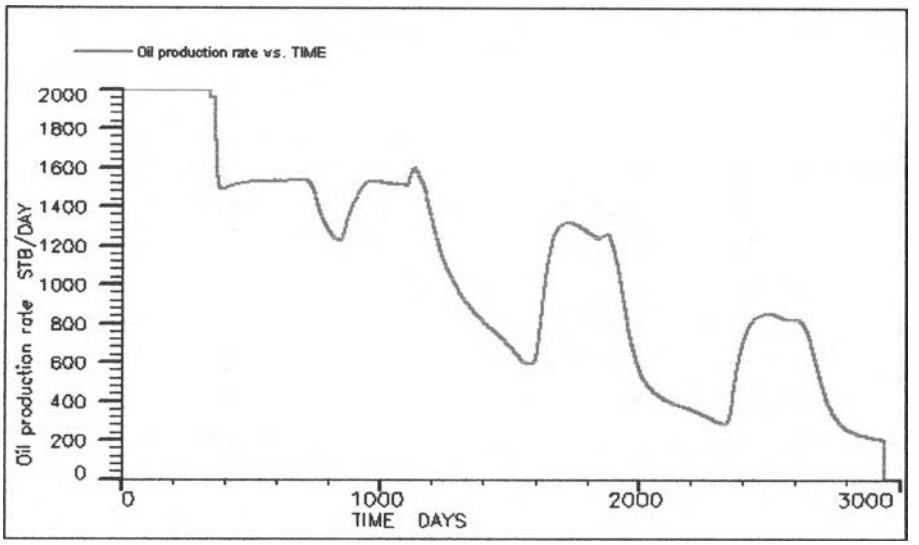

Figure 5.1: Oil production rate vs. producing time for the base case model.

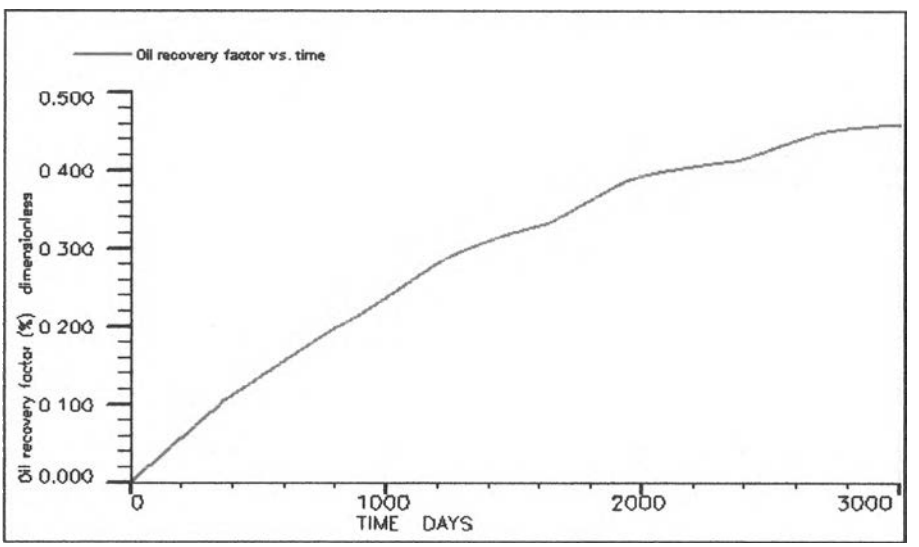

Figure 5.2: Oil recovery factor vs. producing time.

The oil production profile is shown in Figure 5.1. It can be seen that the reservoir can maintain the maximum allowable at 2,000 STB/day for about 380 days. This plateau period should be longer if the maximum allowable is set to a lower value. After 380 days, the oil rate drops rapidly. This can be explained by the limited capability of the reservoir to produce at such a high rate. Then, the oil rate declines and increases in a cyclic fashion and follows a declining trend throughout the producing time following the decrease of reservoir pressure. The cyclic type of oil production comes from the fact that water and gas are injected alternately for a period of 12 months each (24-month cycle size). When water is injected, the reservoir pressure increases, resulting in the increasing of oil production rate. On the other

hand, the reservoir pressure decreases when gas is injected, resulting in a decrease of oil production rate. The production ends when the oil production rate reaches 200 STB/day economic rate, after producing for 2,950 days. It can be observed that the production profile can generate another new oil rate peak if the economic rate is set to a lower value. From this production profile, this WAG base case reservoir model has 45.74 % oil recovery factor as shown in Figure 5.2.

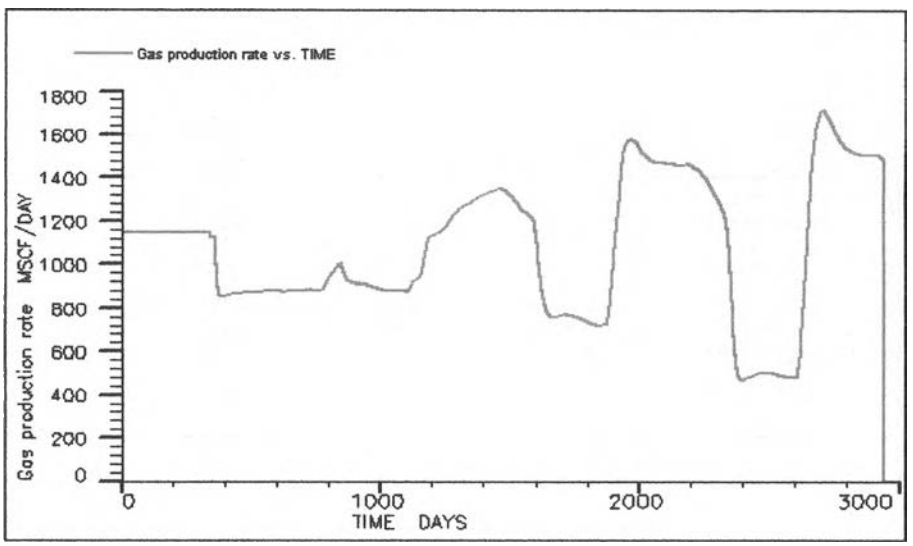

Figure 5.3: Gas production rate vs. producing time.

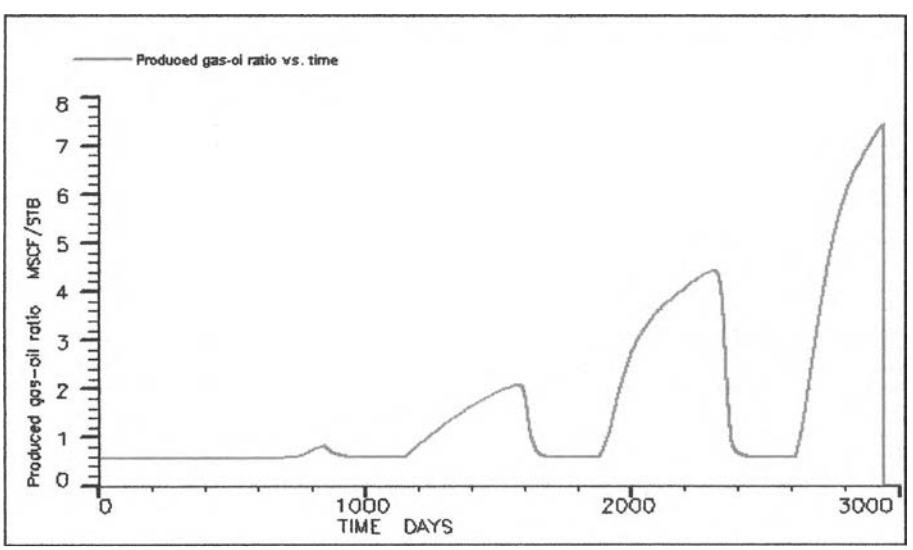

Figure 5.4: Gas-oil ratio vs. producing time.

The gas production rate shown in Figure 5.3 and the gas-oil ratio shown in Figure 5.4 during the first 770 days have the same trend as the oil production rate shown in Figure 5.1. The gas production during the early time comes from the solution gas only since there is no initial gas saturation. In this period, gas-oil ratio is constant at 0.537 MSCF/STB. At day 770, the injected gas slug reaches the production well. The gas production and gas-oil ratio increases in a cyclic manner due to alternate injection of water and gas. The gas production rate increases when injected gas slug reaches the production well and decreases when the injected water slug reaches the production well. In this case, it can be seen that three gas slugs have reached the production well. The gas-oil ratio increases to higher values at late producing times. Since the water and gas are steadily injected, the reservoir pressure is constant. However, the oil rate still declines. This is due to the reduction of oil relative permeability. The gas production rate increases in a cyclic fashion as a result of gas injection.

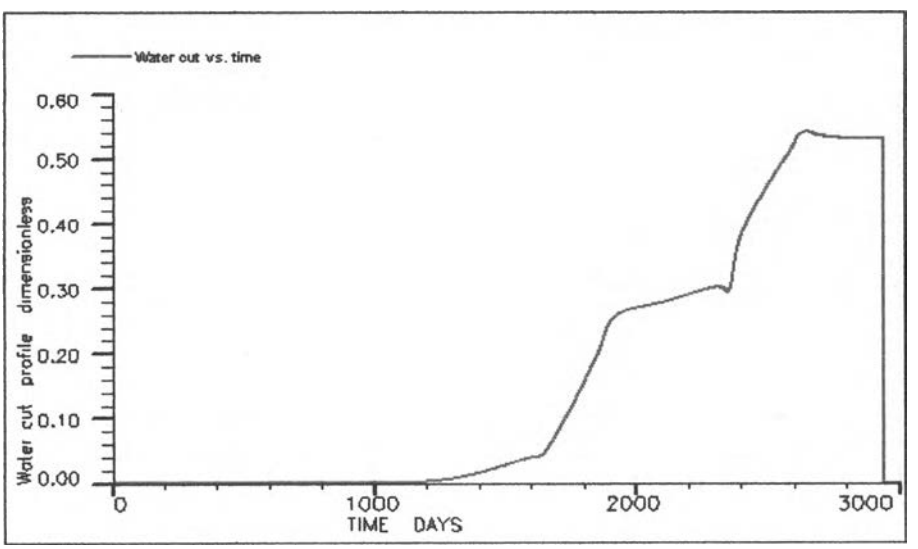

Figure 5.5: Water cut vs. producing time.

Figure 5.5 shows that water does not breakthrough until the well produces for 1,200 days. After the water reaches the production well, water production dramatically increases. The water cut profile does not fluctuate in a cyclic manner as the gas production whereas the water production does follow a similar trend as the oil production profile. This is because water cut is a ratio of produced water to produced

liquid (oil and water). During the period that the oil production increases, the water cut increases at a higher rate than that when the oil production decreases.

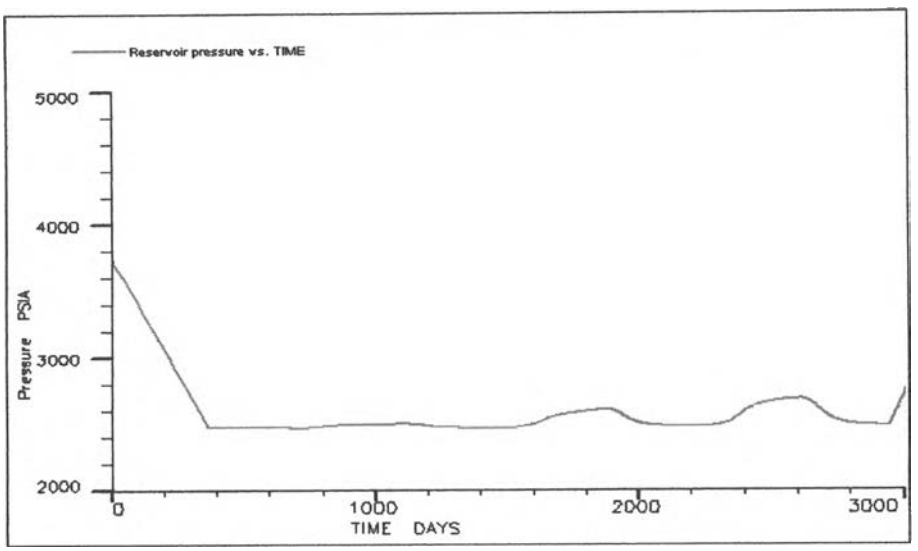

Figure 5.6: Reservoir pressure vs. producing time.

The average reservoir pressure is shown in Figure 5.6. The plateau production at the beginning causes a rapid drop of reservoir pressure. After that, the reservoir pressure fluctuates slightly in the range of 2,440 to 2,650 psia due to the alternation of fluid injection. The reservoir pressure increases when water is injected but decreases when gas is injected.

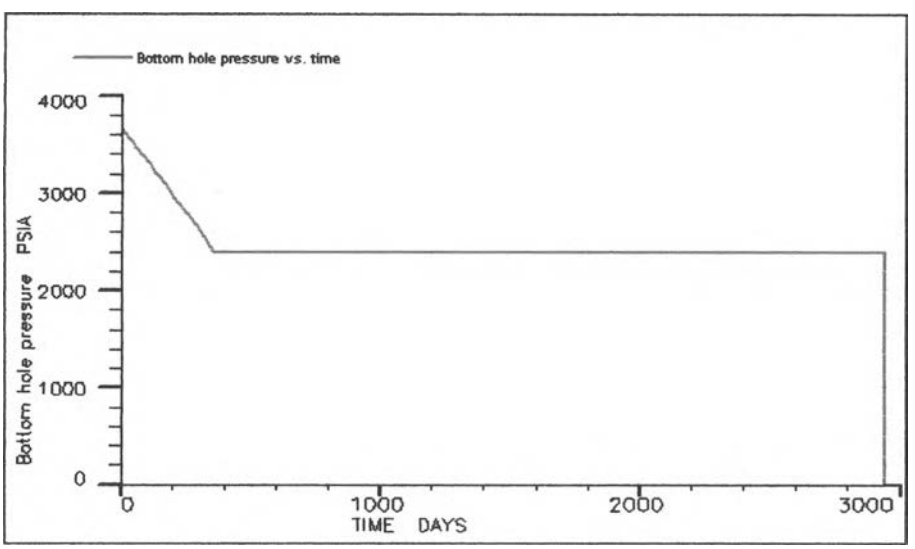

Figure 5.7: Bottom hole pressure of production well vs. producing time.

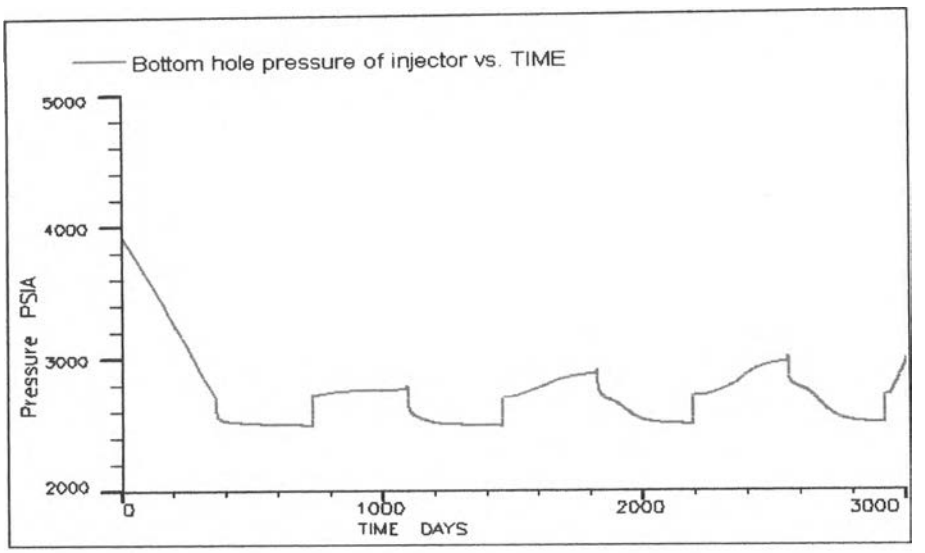

Figure 5.8: Bottom hole pressure of injection well vs. time.

The bottom hole pressure profiles of the production and injection wells are plotted in Figures 5.7 and 5.8, respectively. As seen in Figure 5.7, the bottom hole pressure of the production well decreases as oil is produced from the reservoir until it reaches 2400 psia which is the minimum allowable bottom hole pressure. The production well has to adjust the bottom hole pressure in order to achieve a plateau rate of 2000 STB/day at initial period of production. After that, oil is produced at bottom hole pressure of 2400 psia. In Figure 5.8, the bottom hole pressure of the injection well at the beginning of the injection is about 3,850 psia. while the average reservoir pressure is 3,745 psia. The bottom hole pressure of the injection well generally increases during water injection but decrease during gas injection. Since gas has higher compressibility than water, gas injection does not create a large amount of pressure increase when compared with water. At the same time, the producer is still producing. Thus, the bottom hole pressure of the injector reduces during gas injection.

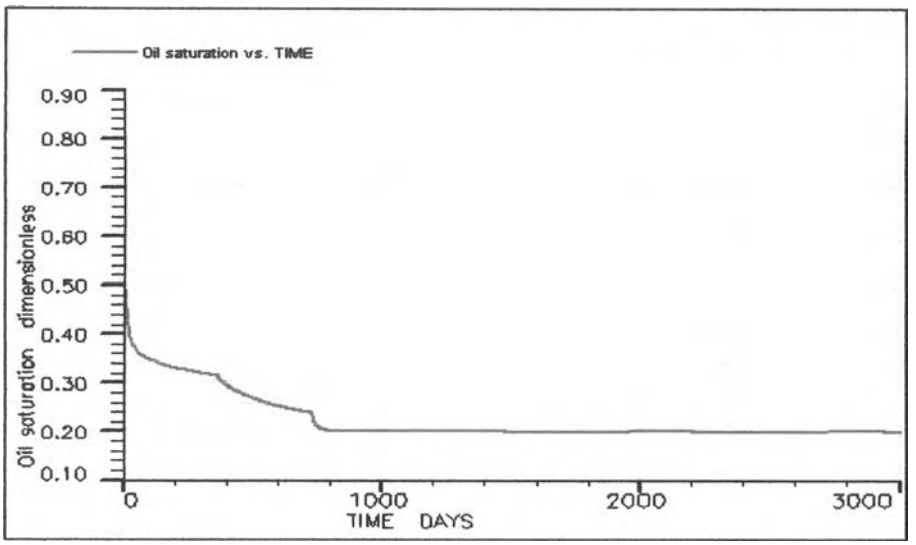

Figure 5.9: Oil saturation of one of injection well blocks vs. time.

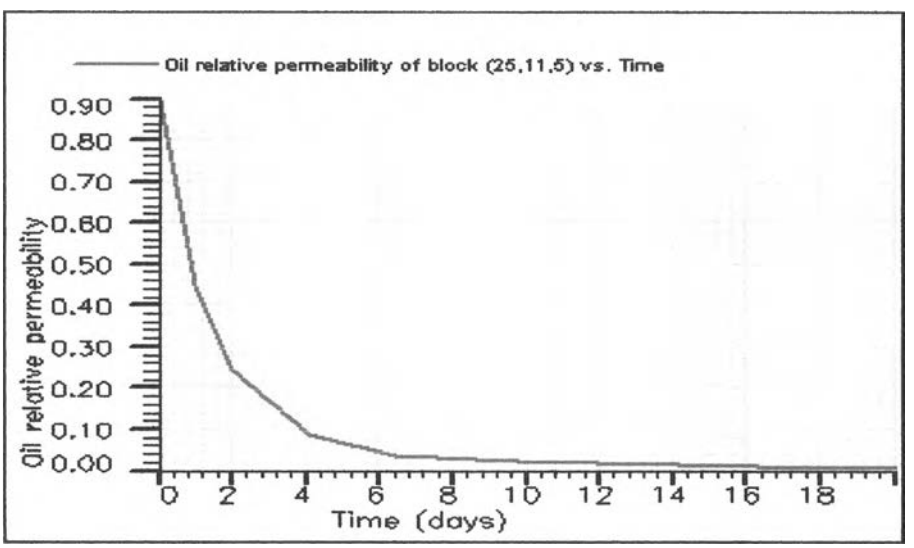

Figure 5.10: Oil relative permeability of one of injection well blocks vs. time.

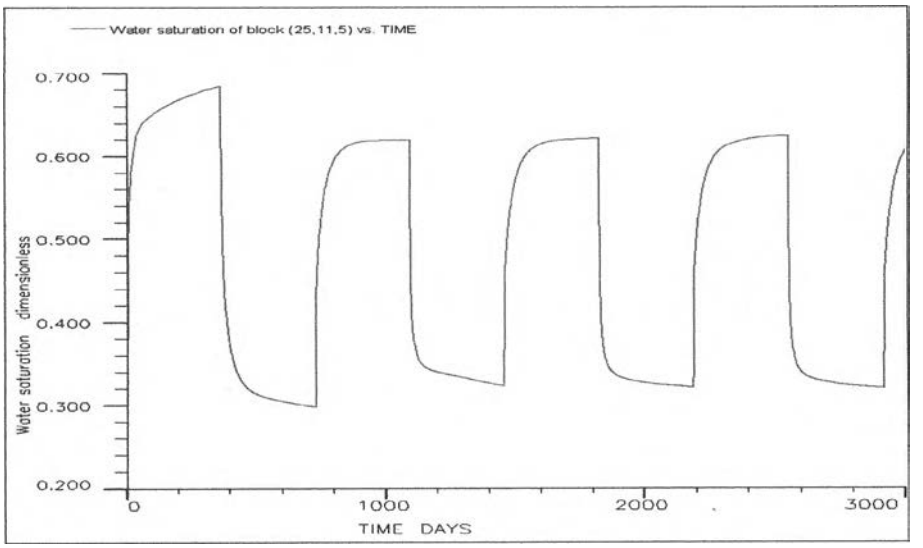

Figure 5.11: Water saturation of one of injection well blocks vs. time.

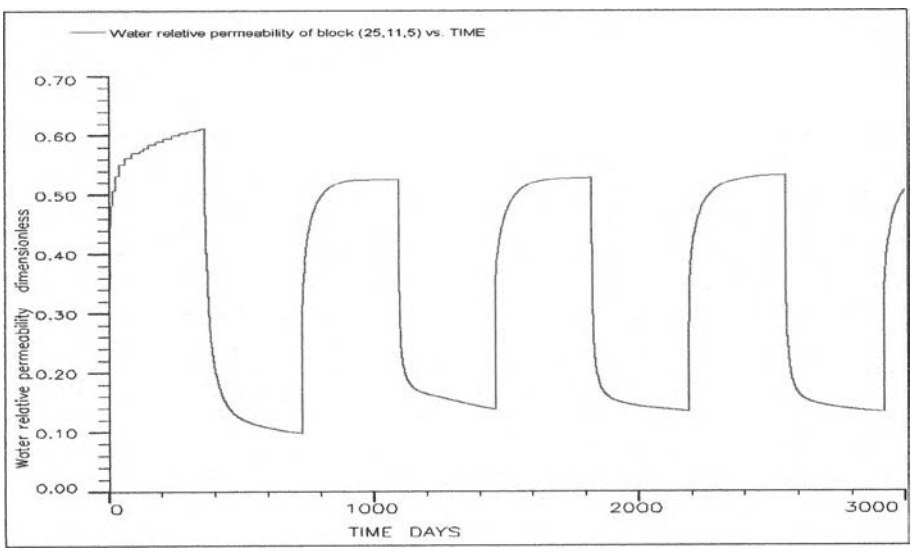

Figure 5.12: Water relative permeability of one of injection well blocks vs. time.

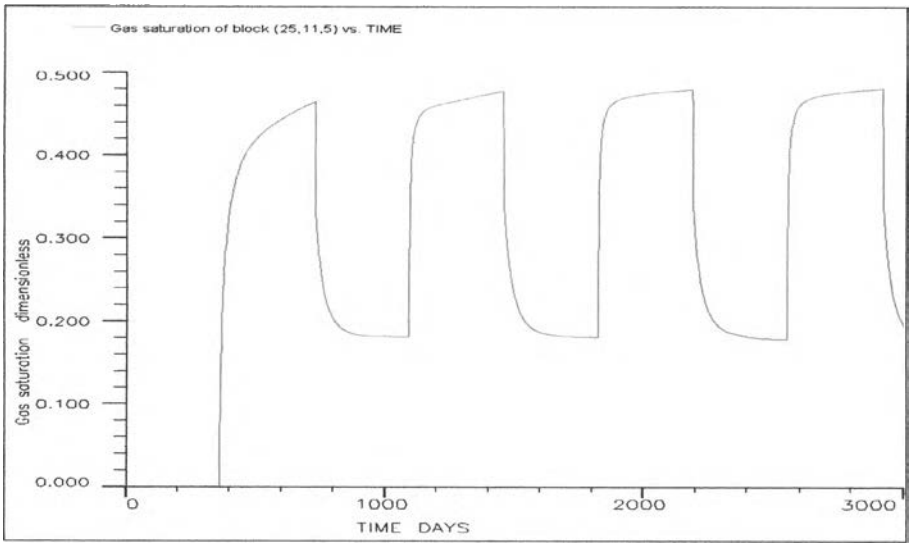

Figure 5.13: Gas saturation of one of injection well blocks vs. time.

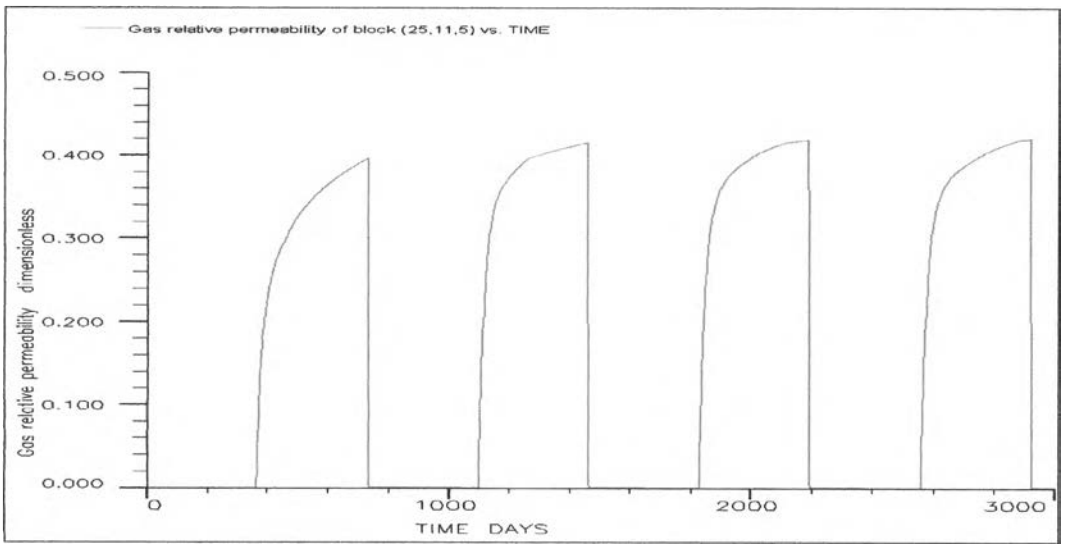

Figure 5.14: Gas relative permeability of one of injection well block vs. time.

Apart from the results that represent the entire reservoir output, some of the grid block properties are also presented such that we have better understanding of the WAG process. In this case, the grid block at coordinate (25,11,5) is chosen because it is the block where the injection well is located. Figure 5.9 shows that the initial oil saturation of 0.8 reduces to 0.32 when the first water slug is injected. The following gas and water slugs further reduce the oil saturation to the irreducible oil saturation at 0.2. This is confirmed by the profile of the relative permeability to oil in Figure 5.10. The relative permeability to oil decreases from 0.9 to 0 in a very short time. The

saturations and relative permeabilities to water and gas are shown in Figures 5.11 to 5.14. Saturation and relative permeability of water and gas increases when that particular phase is injected and decreases when another phase is injected. The maximum value of saturation and relative permeability will follow the value input relative permeability function in the reservoir model. Note that the effect of Killough relative permeability hystersis model is taken into account in this model but cannot be seen from these plots. The effect of relative permeability hysteresis effect will be discussed in detail later in this chapter.

5.1.2 Optimization study

The water-gas ratio and cycle size are considered to be the most important parameters in a WAG process. In order to optimize these parameters, a set of simulation runs using various water-gas ratios and cycle sizes was performed. The values of water-gas ratio used in this study are 0.25, 0.5, 1, 2 and 4. These water-gas ratios were coupled with a series of cycle sizes which are 3, 6, 12, 24, and 36 months. This set of water-gas ratios and cycle sizes was chosen because they were reasonably implemented in many literatures.

5.1.2.1 Effect of horizontal permeability

The horizontal permeability is considered to be one of reservoir properties that mostly affects the flow of the fluid. The set of horizontal permeability to be investigated in this study is 50, 100, 200, 500, and 1,000 md. A simulation for a waterflood process was also performed.

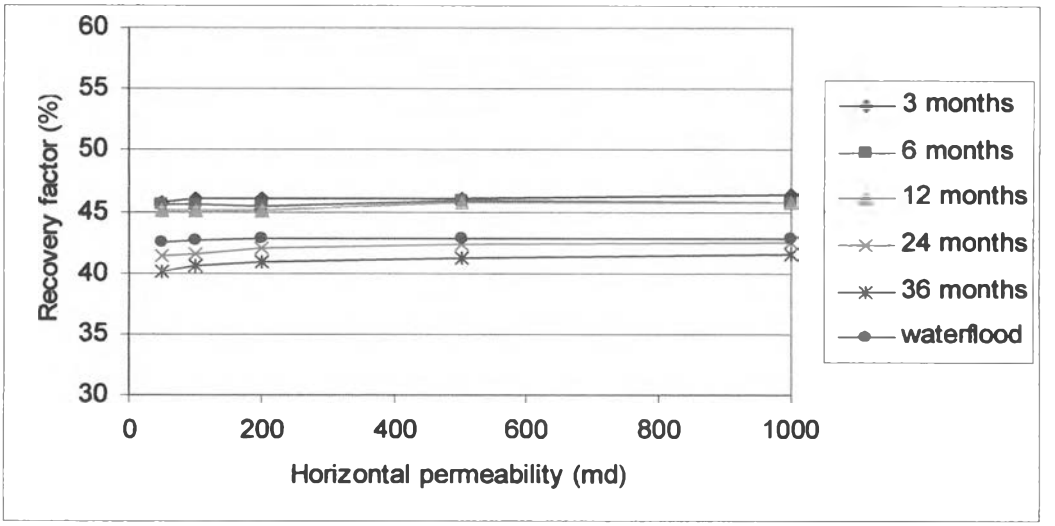

Figure 5.15: Recovery factor of WAG process with water-gas ratio = 0.25 when varying horizontal permeability.

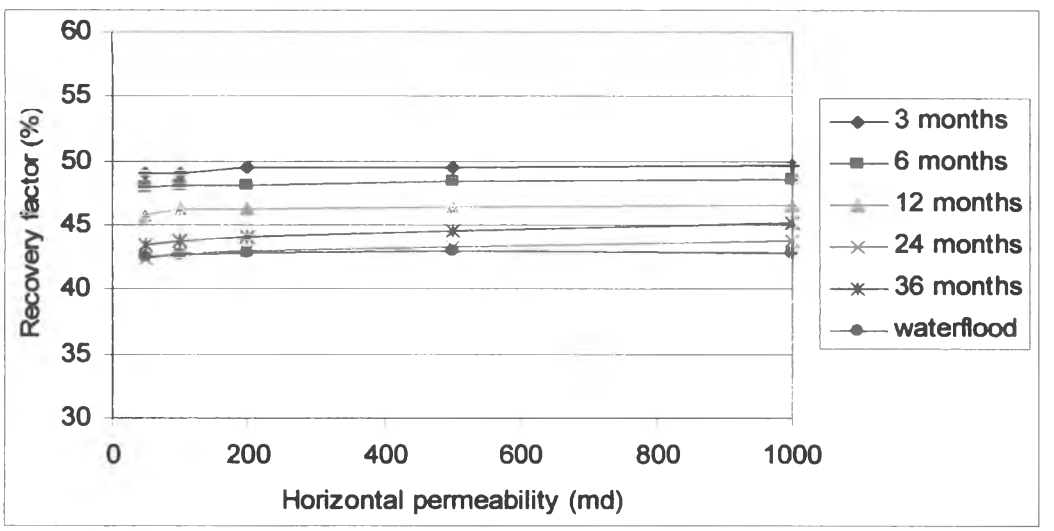

Figure 5.16: Recovery factor of WAG process with water-gas ratio = 0.5 when varying horizontal permeability.

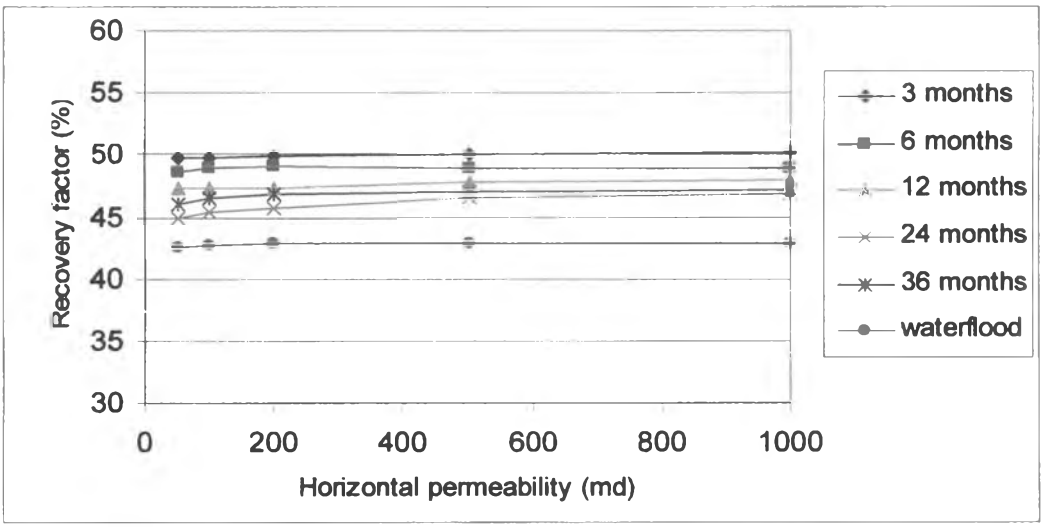

Figure 5.17: Recovery factor of WAG process with water-gas ratio = 1 when varying horizontal permeability.

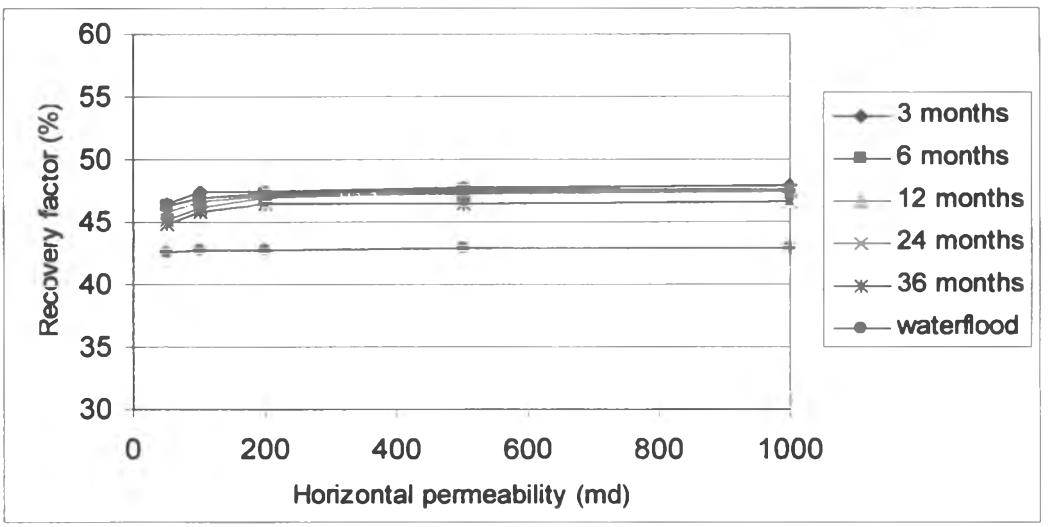

Figure 5.18: Recovery factor of WAG process with water-gas ratio = 2 when varying horizontal permeability.

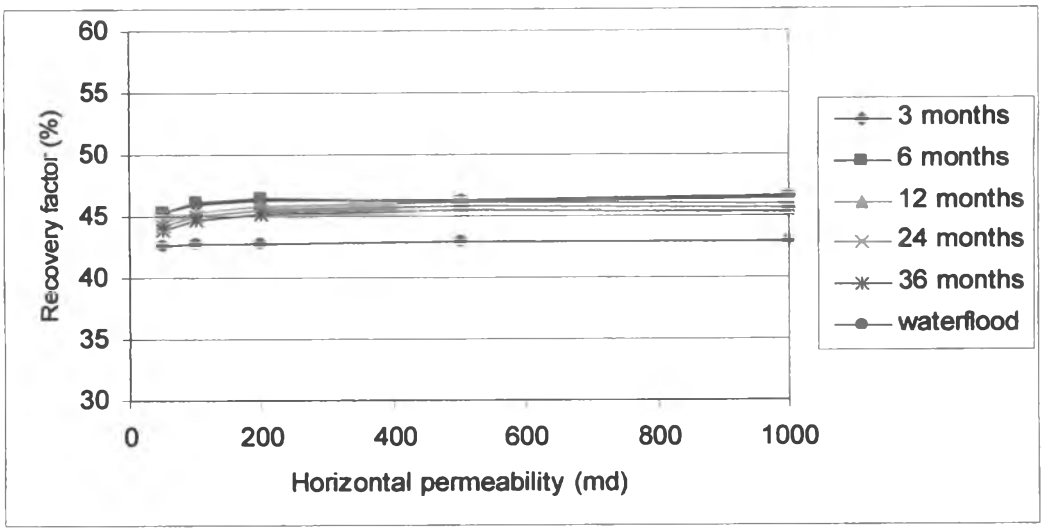

Figure 5.19: Recovery factor of WAG process with water-gas ratio = 4 when varying horizontal permeability.

Figures 5.15-5.19 show the effect of horizontal permeability on the recovery factor of WAG cases with different cycle sizes. It is found from these plots that the recovery factor slightly increases when the horizontal permeability increases from 50 to 100 and 200 md because the ability to allow fluid to flow increases resulting in an increase of oil production. When the horizontal permeability increases from 200 to 500 and 1000 md, recovery factor is almost constant. This seems to come from the fact that the microscopic displacement efficiency becomes stable after reaching the threshold value of permeability.

In addition, as can be seen from these figures, a case with a smaller cycle size provides a higher recovery factor. With a large cycle size, water and gas injections cannot fully complement each other like WAG cases with smaller cycle sizes because large water slug can cause water underriding whereas large gas slug can cause gas overriding. It is seen that the optimum cycle size which is 3-month does not change with horizontal permeability. The horizontal permeability has no effect on the optimum cycle size.

As can be observed from Figure 5.15, WAG cases with cycle sizes of 24 and 36 months have less recovery factor than waterflood cases. This is because too low amounted of water was injected (water-gas ratio = 0.25) and cycle sizes are too large. These WAG cases nearly perform like gas injection.

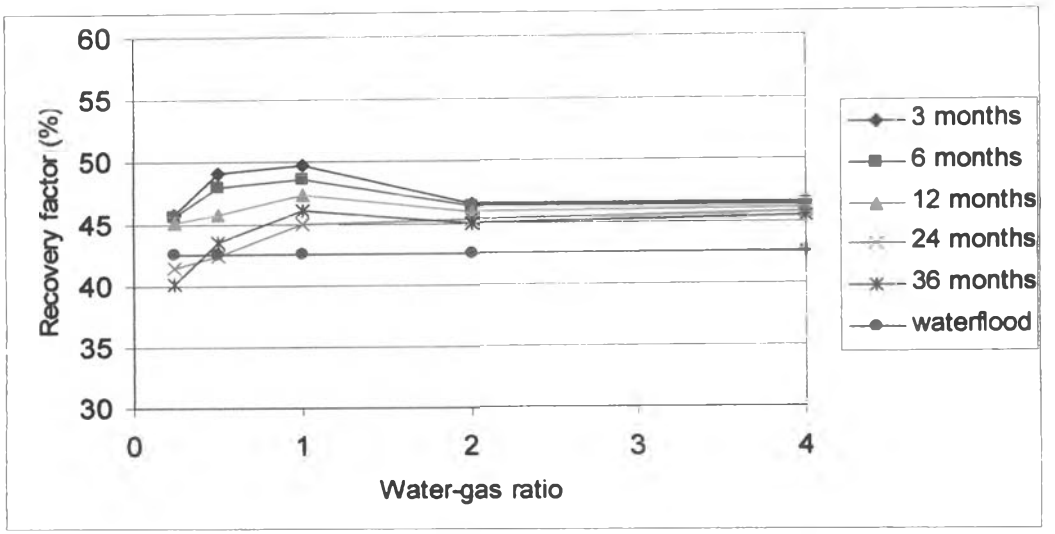

Figure 5.20: Recovery factor of WAG process with k_h = 50 md when varying water-gas ratio.

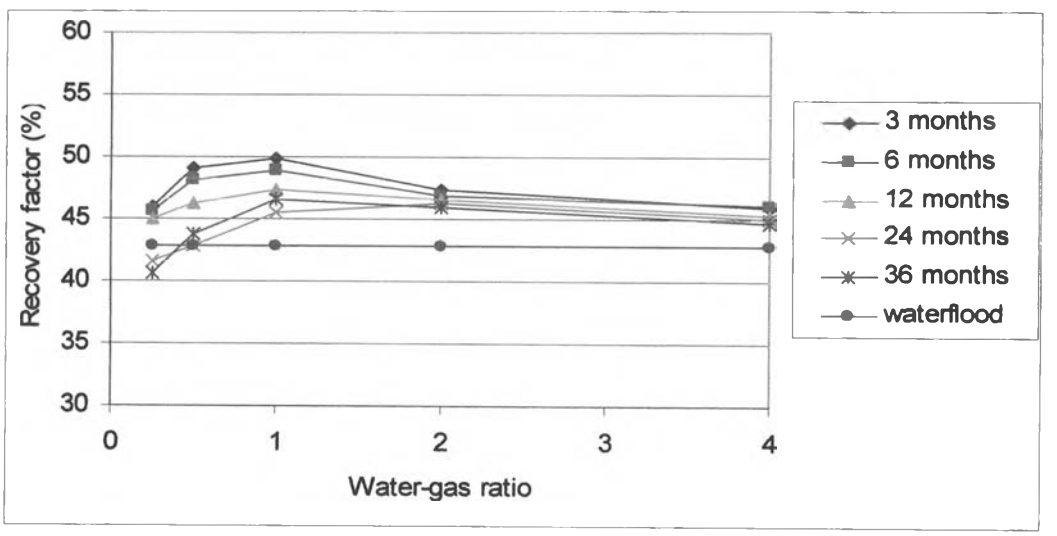

Figure 5.21: Recovery factor WAG process with k_h = 100 md when varying water-gas ratio.

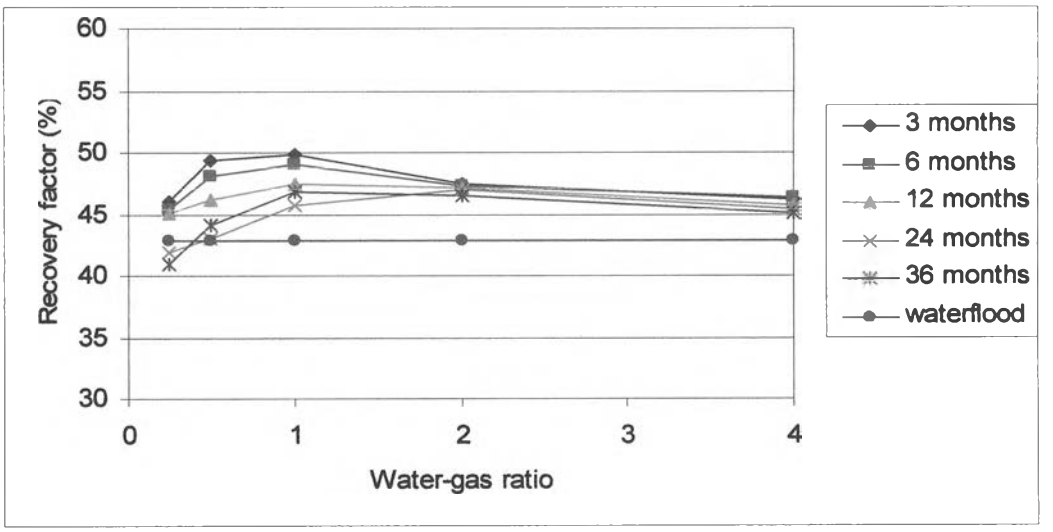

Figure 5.22: Recovery factor of WAG process with k_h = 200 md when varying water-gas ratio.

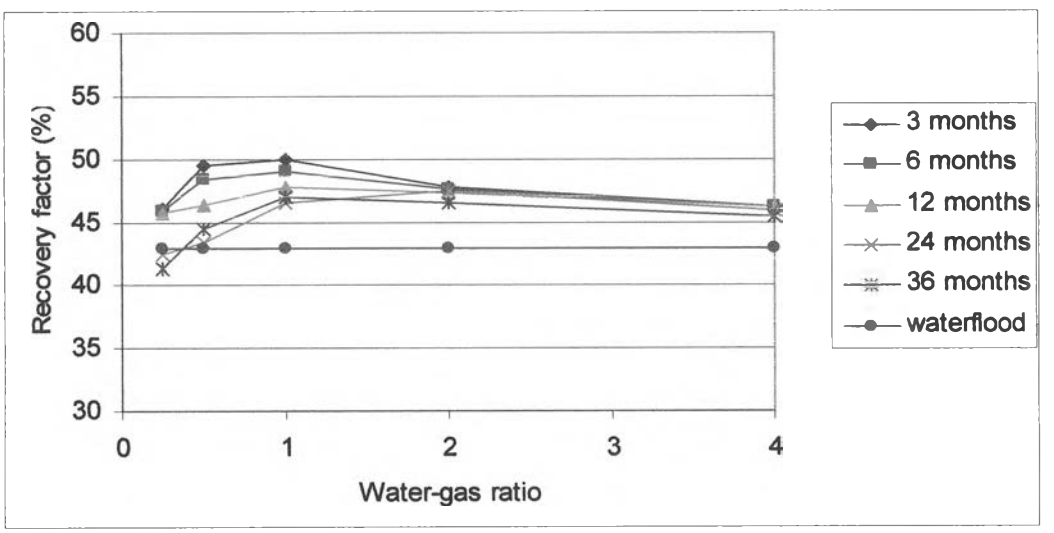

Figure 5.23: Recovery factor of WAG process with k_h = 500 md when varying water-gas ratio.

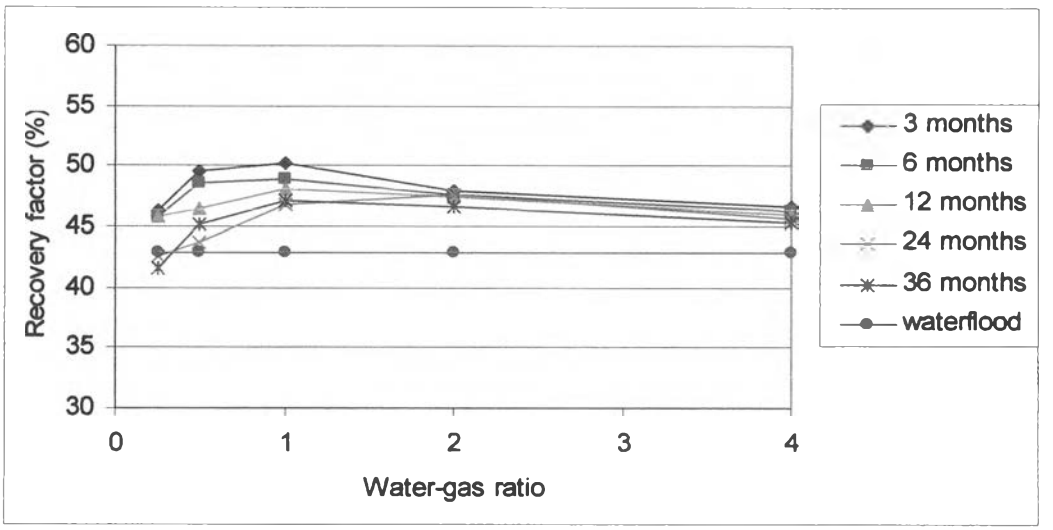

Figure 5.24: Recovery factor of WAG process with k_h = 1,000 md when varying water-gas ratio.

In order to optimize the water-gas ratio, recovery factor is plotted as a function of water-gas ratio for different cases. Figures 5.20 – 5.24 show the effect of cycle size on the recovery factor as a function of water-gas ratio for different values of horizontal permeability. It is seen that each figure shows similar characteristics. The recovery factor varies in the range of 40 – 51 %. Most WAG cases have higher recovery factor than waterflood, which has the recovery factor around 43 %. The recovery factor increases as the water-gas ratio is changed from 0.25 to 0.5 and 1. As the water-gas ratio increases from 1 to 2 and 4, the recovery factor generally decreases for all the cases except when the cycle size is 24 months. All WAG cases with water-gas ratio of 1 and cycle size of 3 months for all values of horizontal permeability, has the highest recovery factor at about 50 % even if the values of horizontal permeability are different. These results are summarized in Table 5.1. Variation in the horizontal permeability does not have an effect on the production strategy. It is also found that for WAG cases with cycle sizes smaller than 24 months, WAG cases with smaller cycle sizes will achieve higher recovery than WAG cases with larger cycle size. Another observation is that WAG cases with water-gas ratio =1 do not show the highest recovery factor when coupled with all the cycle sizes.

Table 5.1: Summary of Optimum WAG cases for each horizontal permeability.

k_h (md)	Optimum water-gas ratio	Optimum cycle size (months)
50	1	3
100	1	3
200	1	3
500	1	3
1000	1	3

Figure 5.25 is a plot of duration of plateau rate as a function of horizontal permeability when the cycle size is 24 months. As seen in the figure, cases with higher horizontal permeability have longer plateau rate because oil can flow at the maximum allowable rate better in reservoir with higher horizontal permeability. Moreover, WAG cases with lower water-gas ratio can maintain the plateau rate longer than case with higher water-gas ratio.

Figure 5.26 shows the effect of horizontal permeability on the water breakthrough time. As seen in the figure, cases with higher horizontal permeability show earlier water breakthrough than cases with lower horizontal permeability because water can flow better at higher horizontal permeability. In addition, cases with lower water-gas ratio produce for a longer period before water breakthrough because they have lower volume of injected water.

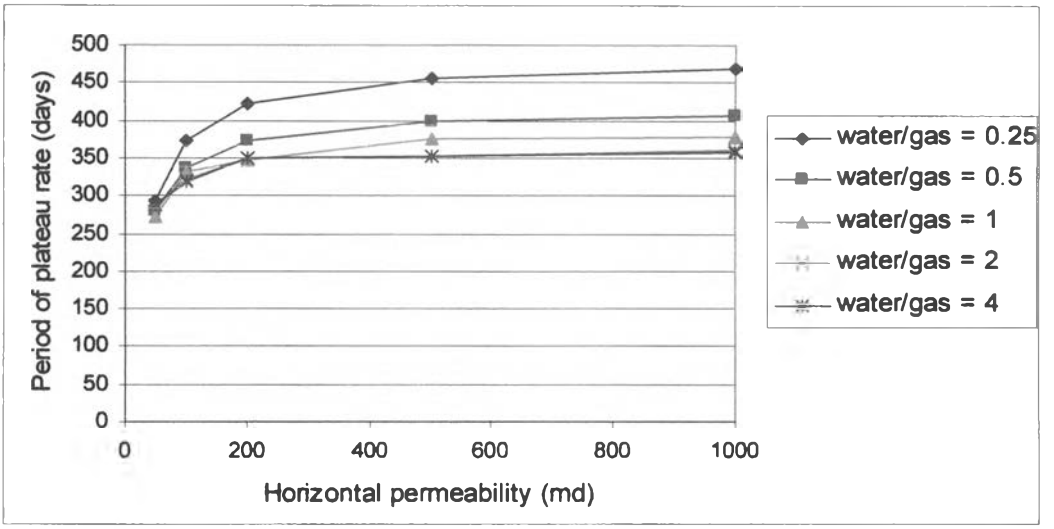

Figure 5.25: Effect of horizontal permeability on period of plateau rate for WAG cases with 24 months cycle size.

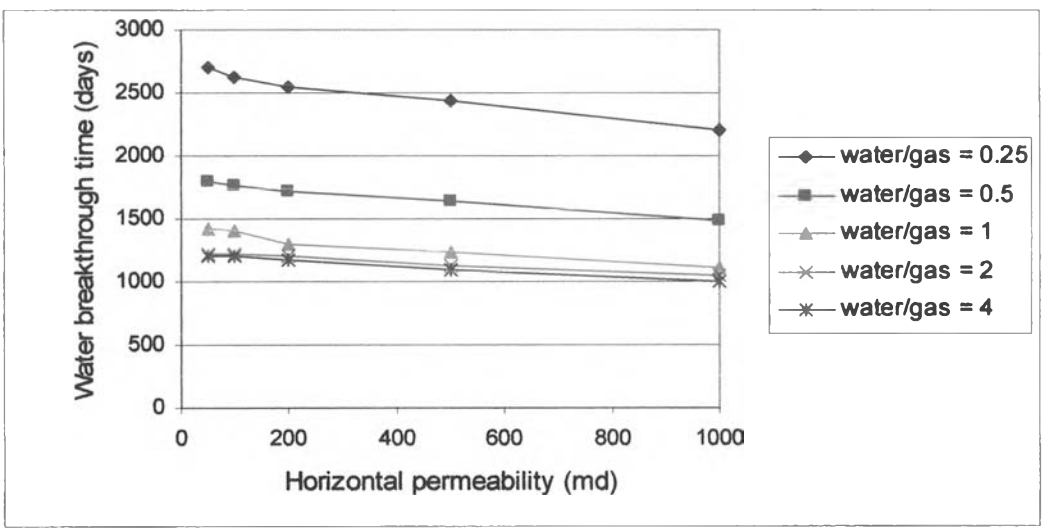

Figure 5.26: Effect of horizontal permeability on water breakthrough time for WAG cases with 24 months cycle size.

However, cases having large amount of injected water such as the cases when water–gas ratio is 2 and 4 were terminated by a water cut limit of 0.7 while cases with water gas ratio of 0.25, 0.5, and 1 were terminated by economic limit. This is because more water is injected in case with high water-gas ratio, giving rise to a higher water cut. Table 5.2 presents the results observed from the WAG cases with k_h = 200 md and k_v = 2 md. The water cut at the time of abandonment is lower for cases

with a small water-gas ratio due to a lower amount of injected water. Another observation is that cases with lower water-gas oil ratio can produce longer although they do not yield the highest recovery factor. This could raise up an arguement whether the economic limit has an effect on the optimal results. In order to investigate the effect of economic criteria, two additional criteria were considered. The first one was to use only the 200 STB/day economic rate without considering the water cut. Another one was to perform the WAG process for an equal duration.

Table 5.2: Results of WAG cases with 2-year cycle size k_h = 200 md and k_v = 2 md terminated by oil rate = 200 STB/day and water cut = 0.7.

Water-gas ratio	Recovery factor (%)	Water cut (%)	Period of production (days)
0.25	41.97	24.63	4,400
0.5	43.05	29.64	3,030
1	45.74	53.06	2,950
2	47.44	70	2,870
4	45.47	70	2,520

The effect of using only 200 STB/day economic limit can be presented in Figure 5.27. It's found that the optimum WAG process is still the case with water-gas ratio equal to 1 and cycle size equal to 3 months . However, the recovery factors for WAG cases with water-gas ratio of 2 and 4 and the waterflood are higher than those in Figure 5.20 because these cases can produce longer when there is no constraint on the water cut. As seen in Figure 5.27, the recovery factor of water flood increases to 47.36 %. Several WAG cases provide lower recovery than the water flood. However, the water cut for cases with water-gas ratio of 2 and 4 and the waterflood definitely exceeds 0.7. The optimal water-gas ratio for WAG cases with 12, 24, and 36 months in Figure 5.27 is 4 while that in Figure 5.22 the optimal water-gas ratio for cases with 3 and 6 months is 1. Therefore, it can be suggested that changing the economic criteria from constraining both oil rate and water cut to only oil rate affects the optimization of WAG cases with large cycle sizes but not affect the true optimal case.

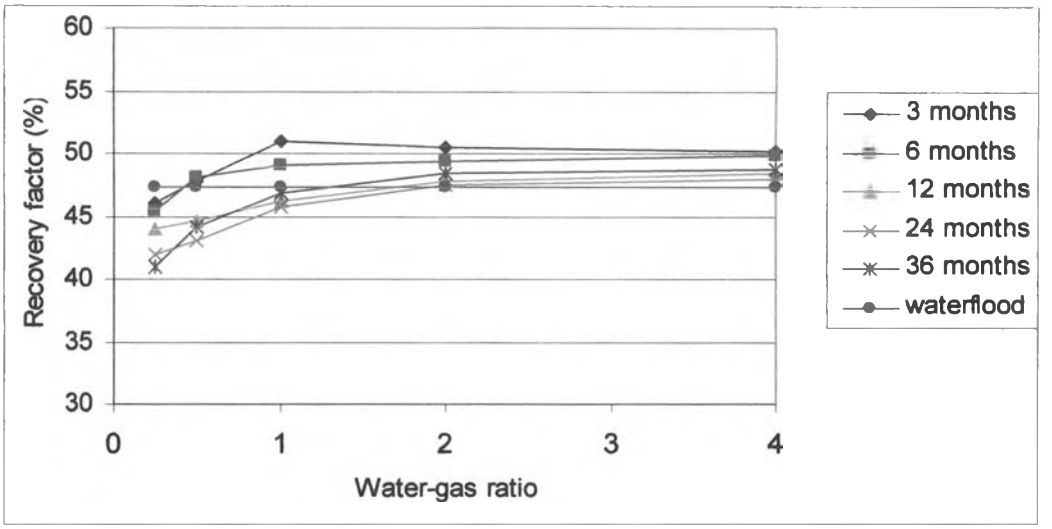

Figure 5.27: Recovery factor of WAG process with k_h = 200 md when varying water-gas ratio using only oil rate as an economic limit.

In these figures, there is one observation that most WAG cases with 36 months cycle size achieve more recovery than cases with 24-month cycle size. This observation does not follow the trend that recovery factor increases when the cycle size is smaller. In order to make a further investigation for this result, additional cases with water-gas ratio of 1 and k_h of 200 md were simulated with cycle size varied from 2 – 48 months. Figure 5.28 is a plot of recovery factor as a function of cycle size. It can be seen from the figure that for cases with a cycle size smaller than 20 months, recovery factor decreases as the cycle size increases. For the cases with cycle size larger than 20 months, the recovery factor fluctuates with the increasing cycle size and does not show a single trend. This can be explained by the fact that for cases with large cycle sizes, oil production rate fluctuates in a wider range as shown in Figures 5.29-5.33. It is seen that cases with 32 – 40 months cycle size, the peak oil production rate gradually becomes larger and results in longer producing time. But for the case with 40 months cycle, the peak of oil production rate is too wide and reaches the economic limit with fewer peak of oil rate resulting in having much lower recovery factor. This upward trend of the recovery factor continues as the cycle size increases until it reaches 38 months. Note that WAG cases with a cycle size larger than 36 months in this investigation was constructed in order to help analyze the trend only. In the literature, WAG process with a cycle size larger than 36 months have not been implemented.

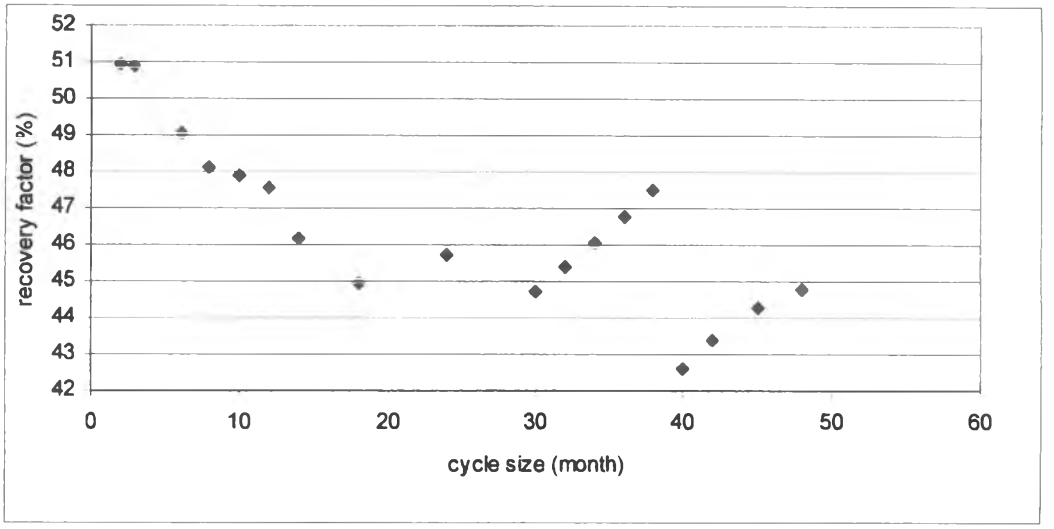

Figure 5.28: Recovery factor WAG cases with water-gas ratio = 1 for investigating the effect of cycle size.

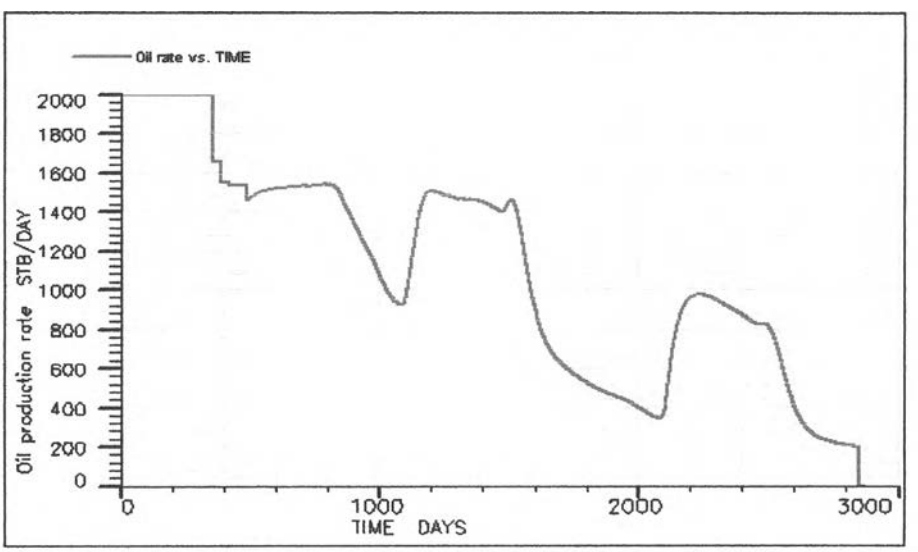

Figure 5.29: Production profile for WAG case with water-gas ratio = 1 for case with 32 month -cycle size.

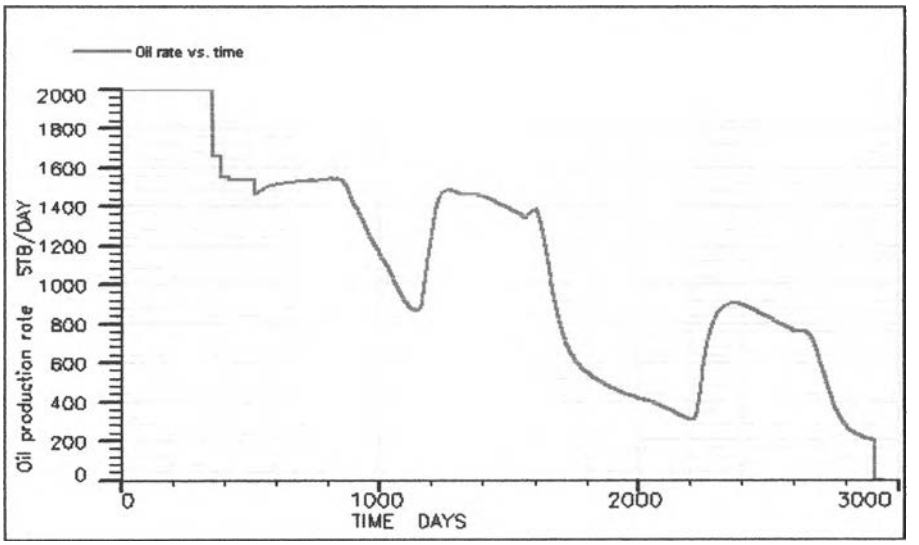

Figure 5.30: Production profile for WAG case with water-gas ratio = 1 for case with 34 month -cycle size.

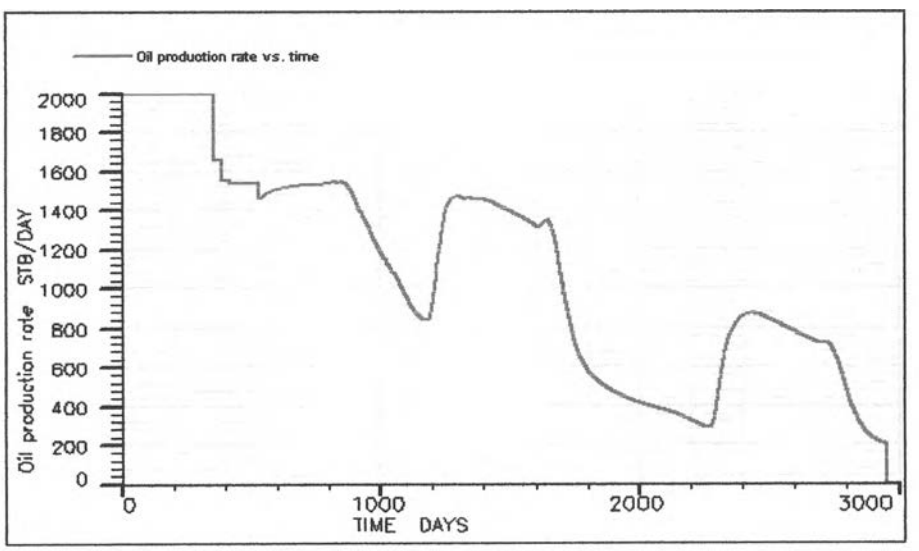

Figure 5.31: Production profile for WAG case with water-gas ratio = 1 for case with 36 month -cycle size.

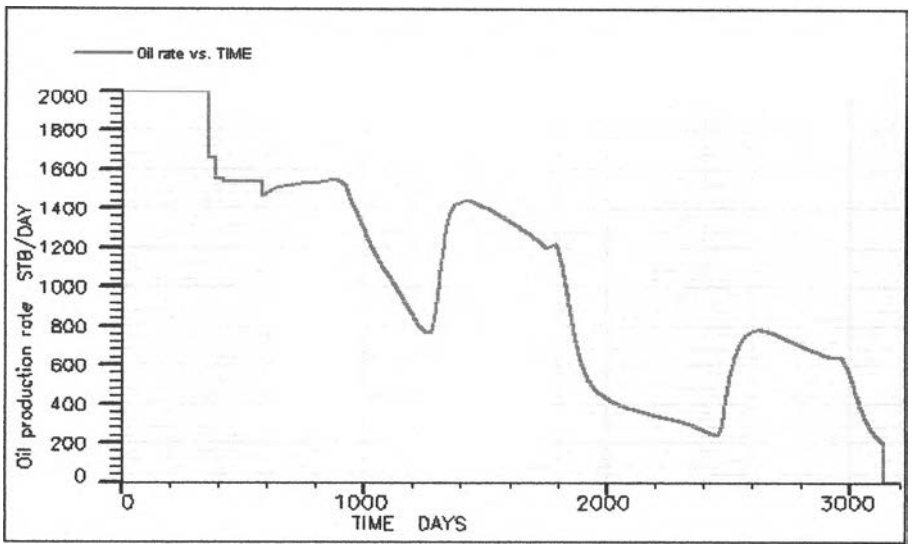

Figure 5.32: Production profile for WAG case with water-gas ratio = 1 for case with 38 month -cycle size.

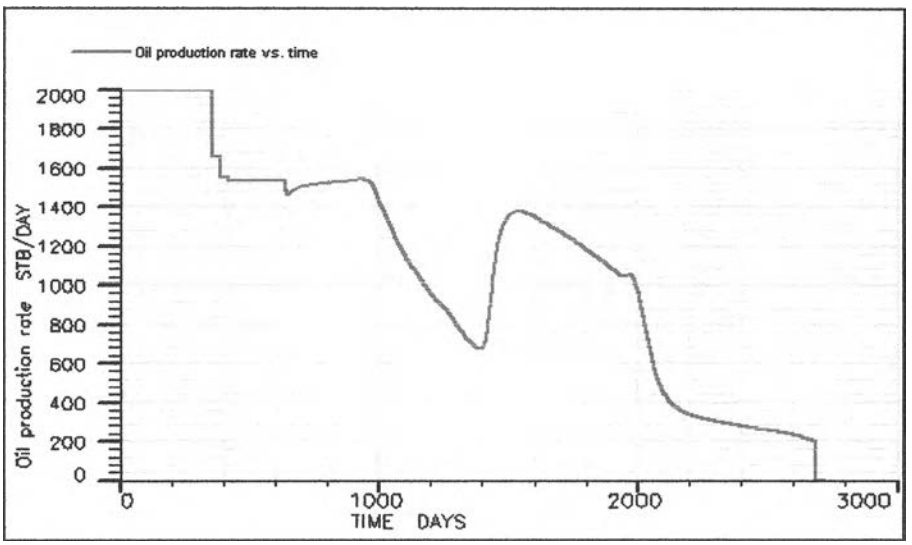

Figure 5.33: Production profile for WAG case with water-gas ratio = 1 for case with 40 month -cycle size.

As presented in Table 5.2 that time to reach the economic limit is different for different cases, it is interesting to investigate the effect of time of production. In this study, recovery factors of WAG cases were computed when producing time reaches 6 years or 2,190 days, since every cases completes the injected cycle of injection in 6 years. The result is illustrated in Figure 5.34. Apparently, it is found that the cases with higher water-gas ratios and larger cycle sizes provide higher recovery factor than cases with lower water-gas ratios. This is because cases with higher water-gas ratios

and larger cycle size has wider oil rate peak. If the producing time is fixed, such cases can produce oil more than case with lower water-gas ratios and smaller cycle size. When comparing the recovery factor after implementing WAG process for 6 years, WAG case with water-gas ratio of 4 and cycle size of 36 months is the optimum process. This is drastically different from the WAG cases terminated by oil economic rate and water cut constraint.

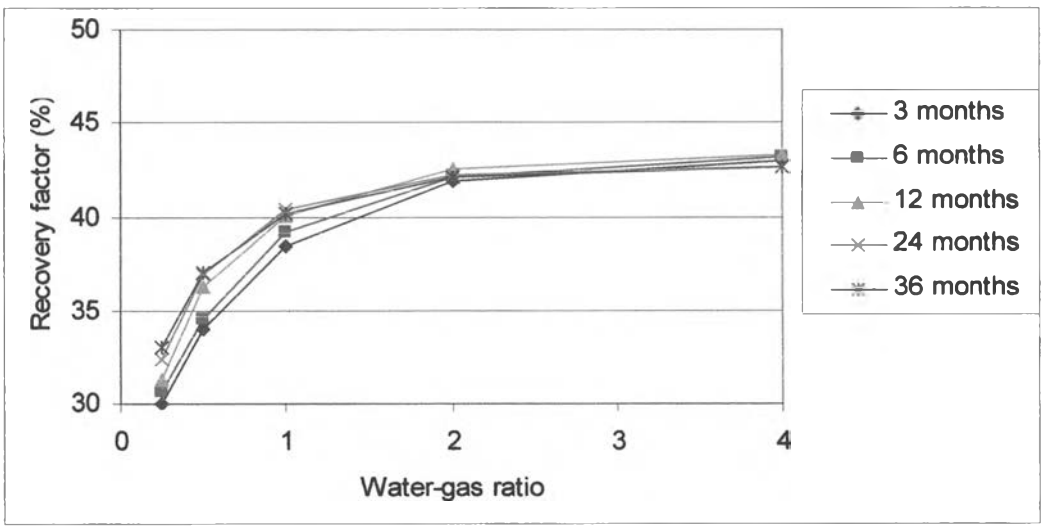

Figure 5.34: Percent recovery of WAG process with k_h = 200 md computed at 6 years.

From the investigations in this study, it can be said that the horizontal permeability does not have any effect on optimum WAG process but have an effect on the production profile of each case. In addition, it is found that fixing a producing time in short period have a significant effect on optimum WAG process.

5.1.2.2 Effect of vertical to horizontal permeability ratio

Vertical to horizontal permeability (k_v/k_h) ratio is another important reservoir property. In this part of the study, WAG cases were simulated with varying vertical to horizontal ratios which are 0.01, 0.1, 0.5, and 1. The results are presented in Figures 5.35-5.39. As seen in these figures, the smaller the cycle size, the higher recovery factor is obtained. It is found that the recovery factors of all cases are nearly the same for all vertical to horizontal permeability ratios. Thus, if the recovery factor of each case is constant, the optimum WAG process does not change either. In order to thoroughly investigate the effect of vertical to horizontal permeability ratio, additional WAG cases with water and gas injection rate of 500 and 10,000 RB/day were simulated. Cases with water-gas ratio of 1 and 24-month cycle size were chosen for this additional run. The results presented in Figure 5.40 shows the same behavior as those for the injection rate of 2,000 RB/day. Thus, it can be concluded that vertical to horizontal permeability ratio does not have any effect on optimizing WAG process when the injection rate is in the range of 500-10,000 RB/day.

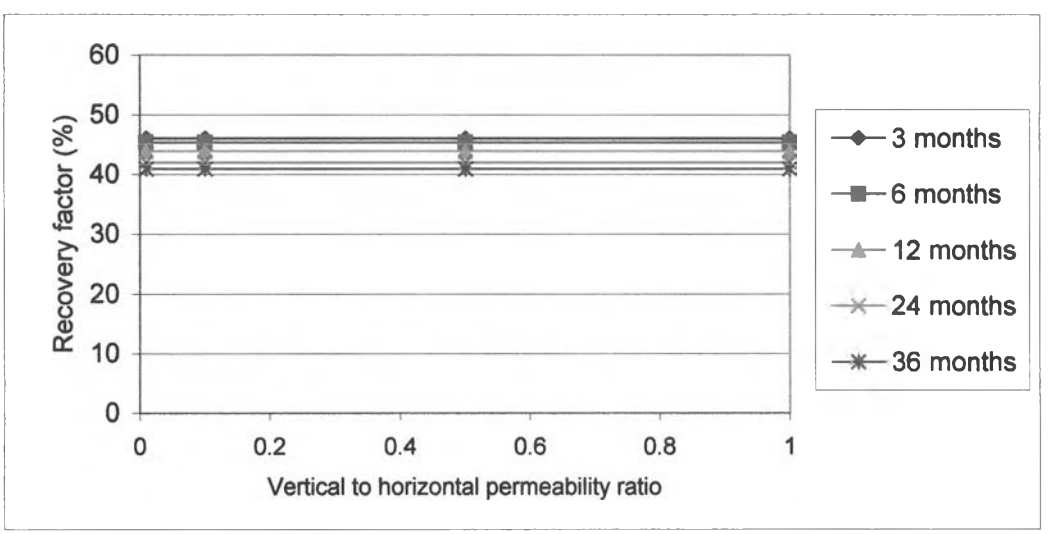

Figure 5.35: Effect of k_v/k_h on WAG cases with water-gas ratio = 0.25, k_h = 200 md.

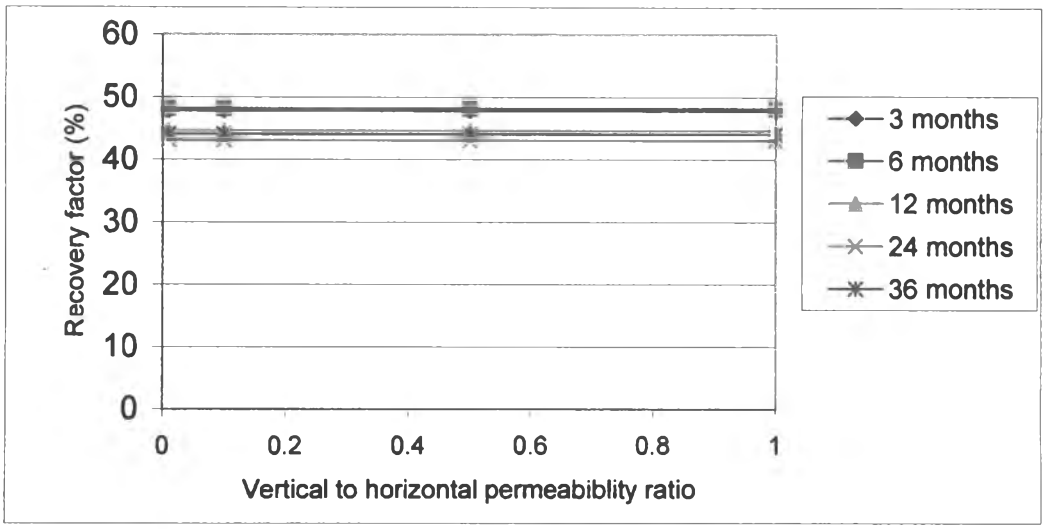

Figure 5.36: Effect of k_v/k_h on WAG cases with water-gas ratio = 0.5, k_h = 200 md.

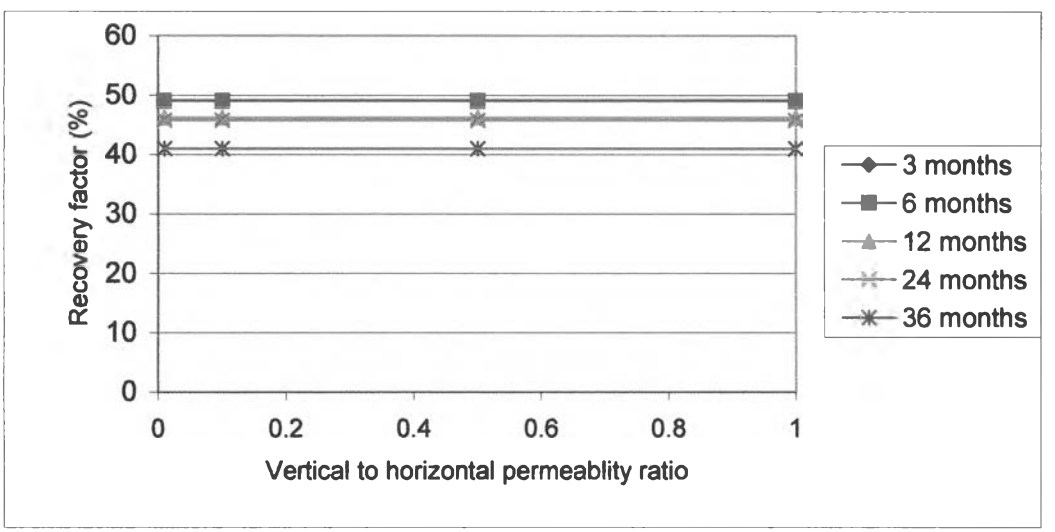

Figure 5.37: Effect of k_v/k_h on WAG cases with water-gas ratio = 1, k_h = 200 md.

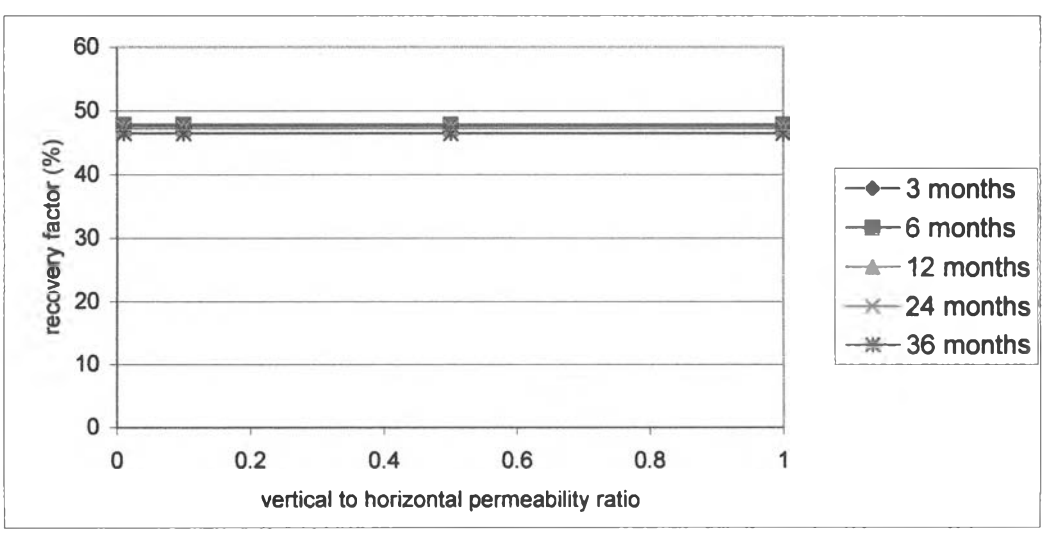

Figure 5.38: Effect of k_v/k_h on WAG cases with water-gas ratio = 2, k_h = 200 md.

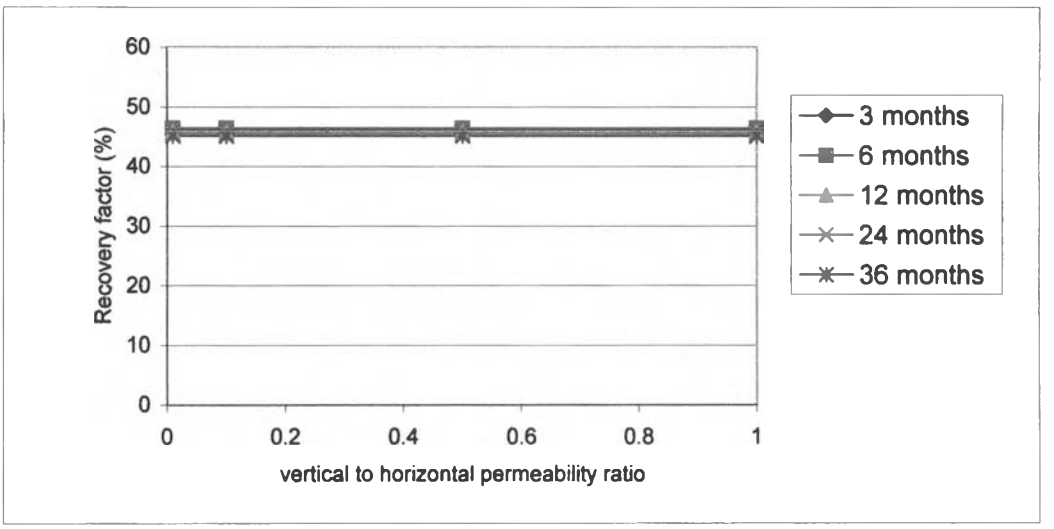

Figure 5.39: Effect of k_v/k_h on WAG cases with water-gas ratio = 4, k_h = 200 md.

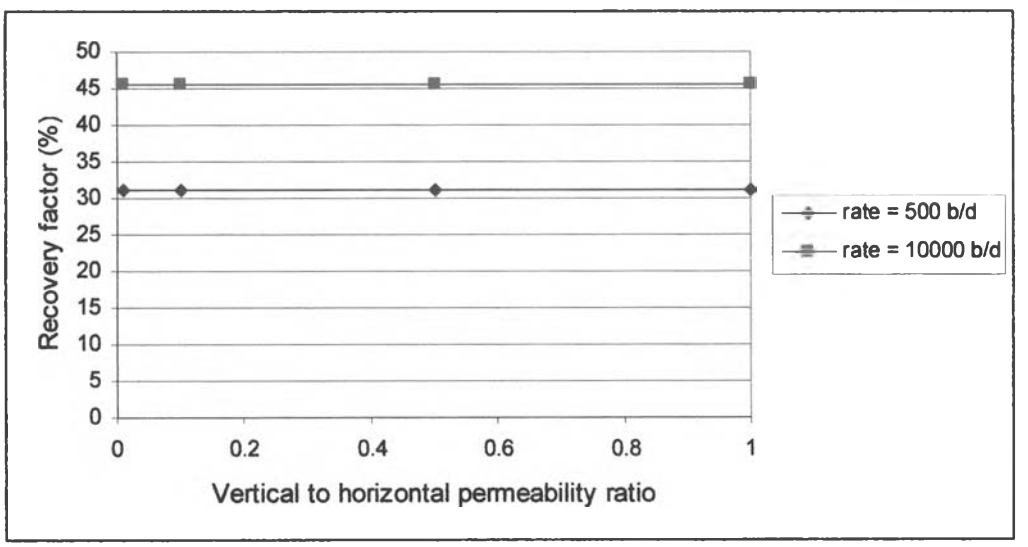

Figure 5.40: Effect of k_v/k_h on WAG cases with injection rate = 500 and 10000 barrel/day.

5.1.2.3 Effect of locations of producer and injector

Since the locations of the producer and injector affects the time of water breakthrough, well positioning may have an effect on the optimization process as well. In this study, three different locations of the producer and injector as shown in Table 5.3 were studied. Figure 5.41 helps illustrate these scenarios. Note that scenario 2 is the base case model as mentioned in Chapter 4. In scenario 1, the distance is reduced to 900 ft while the distance is increased to 2,800 ft in scenario 3. The cases with k_h = 200 md and k_v = 2 md were selected for this investigation.

Table 5.3: Scenario for studying the effect of locations of the producer and injector.

Scenario	Location of producer (x,y)	Location of injector (x,y)	Distance between producer and injector (ft)
1	(11,11)	(20,11)	900
2	(6,11)	(25,11)	1,900
3	(1,11)	(30,11)	2,800

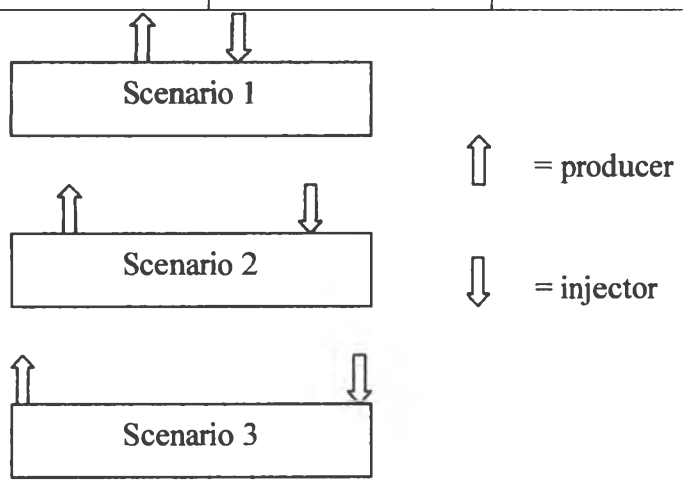

Figure 5.41: Configuration of three different well locations.

Figures 5.42-5.44 present the effect of the locations of the production and injection wells. The optimum case is still the case with water-gas ratio of 1 and cycle size of 3 months. Most of WAG cases still perform better than waterflood. It can be observed that in scenario 1, cases with a cycle size of 24 and 36 months achieve the highest recovery at the water-gas ratio of 4. When the distance between producer and injector decreases, cases with large cycle size provide more recovery by injecting more water. This may come from the reason that cases with a large cycle size and lower water-gas ratio behaves like a gas injection (gas is not as effective as water in displacing oil saturated between wells and boundary) if the distance between the producer and injector is not far enough. Gas will breakthrough before the next water slug is injected, resulting in low sweep efficiency. Thus, cases with higher water-gas ratio performs better in scenario 1. This is confirmed by the recovery of waterflood process shown in Figure 5.42. The waterflood has higher recovery factor than many WAG cases with low water-gas ratio. It can also be noticed that cases in scenario 3 have higher recovery factor than cases in scenario 1 and 2, respectively. The

waterflood cases also follow this trend. This observation means that the longer distance between producer and injector is, the less amount of oil is left between the well and along the boundaries. When the two wells are located near the boundaries of the resevoir, the more amount of oil is swept by water. Table 5.4 helps illustrate the fact that a longer distance between two wells results in a longer time for water to reach the production well. Figures 5.45-47 help illustrate this observation. The oil production rate before water breakthrough in scenario 3 fluctuates with higher peaks than that in scenario 1 and 2.

Table 5.4: Water breakthrough time for WAG cases with water-gas ratio = 1 And 3 month-cycle size.

Scenario	Water breakthrough time (days)
1	220
2	1,330
3	2,045

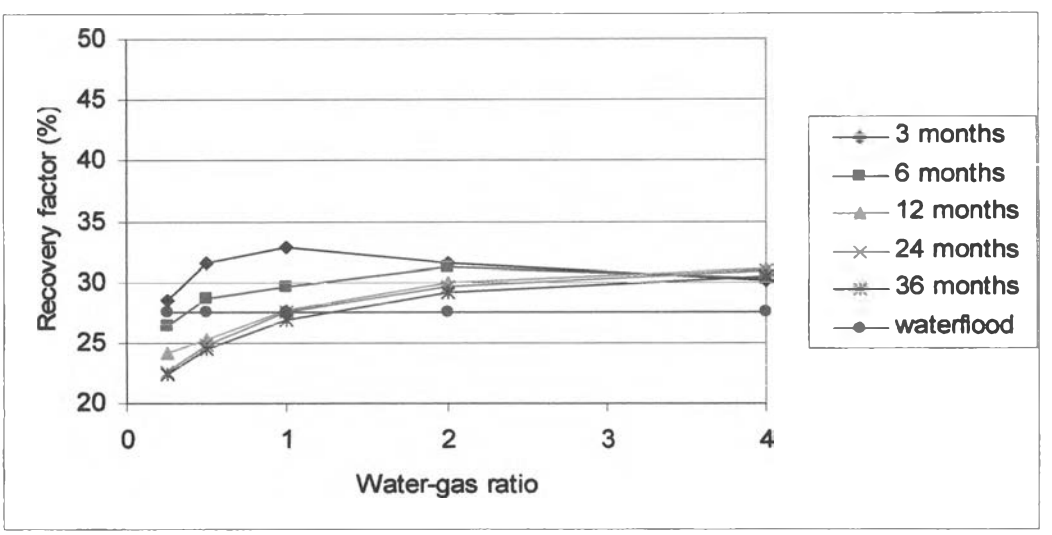

Figure 5.42: Recovery factor of WAG process when varying water-gas ratio when distance between the injector and producer is 900 ft.

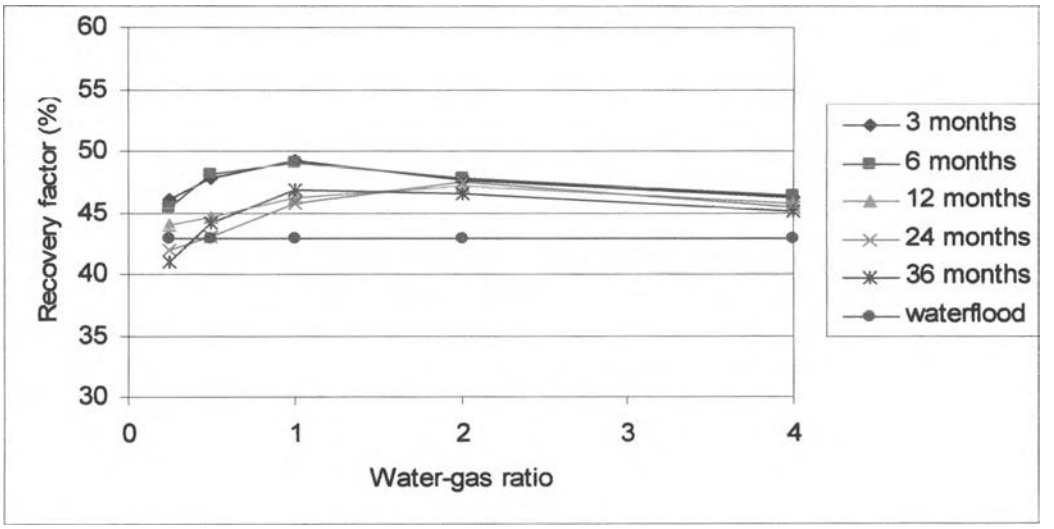

Figure 5.43: Recovery factor of WAG process when varying water-gas ratio when distance between the injector and producer is 1900 ft.

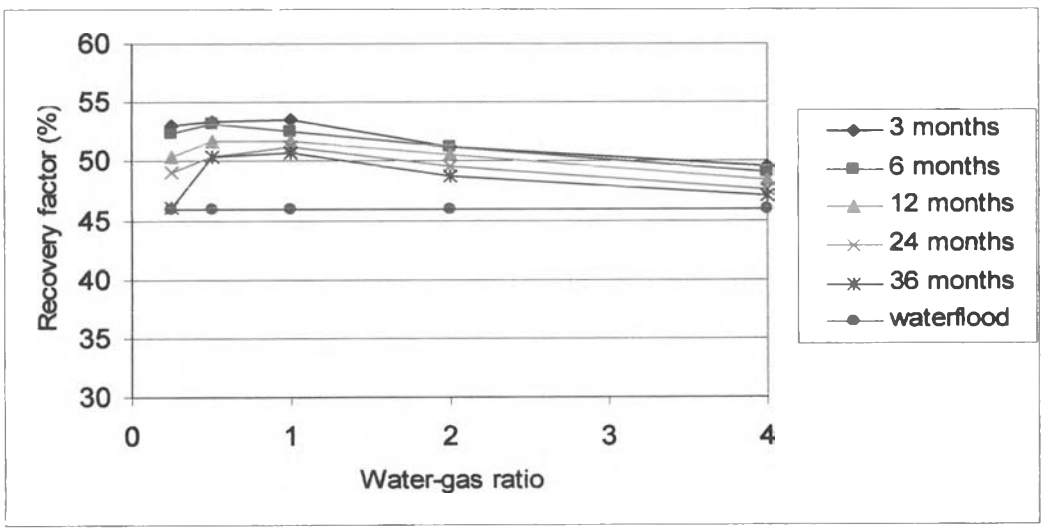

Figure 5.44: Recovery factor of WAG process when varying water-gas ratio when distance between injector and producer is 2800 ft.

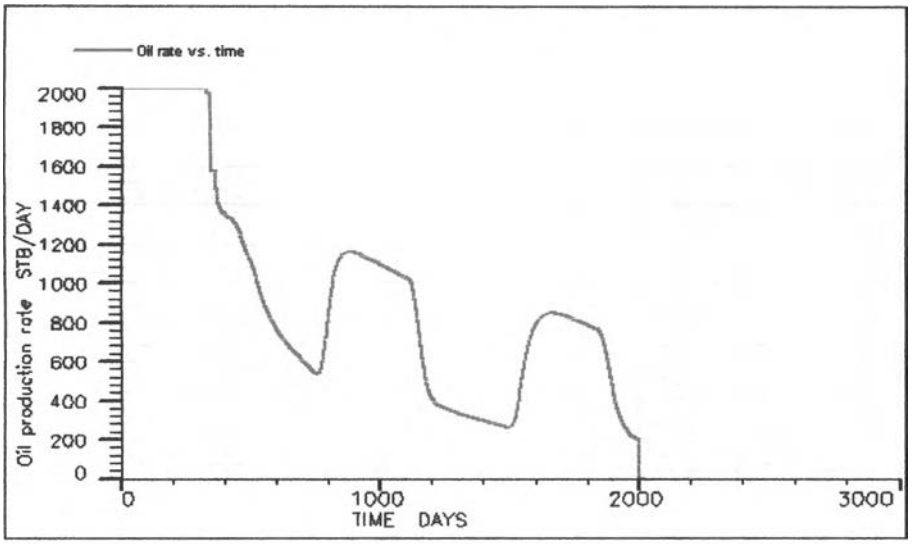

Figure 5.45: Production profile of scenario 1.

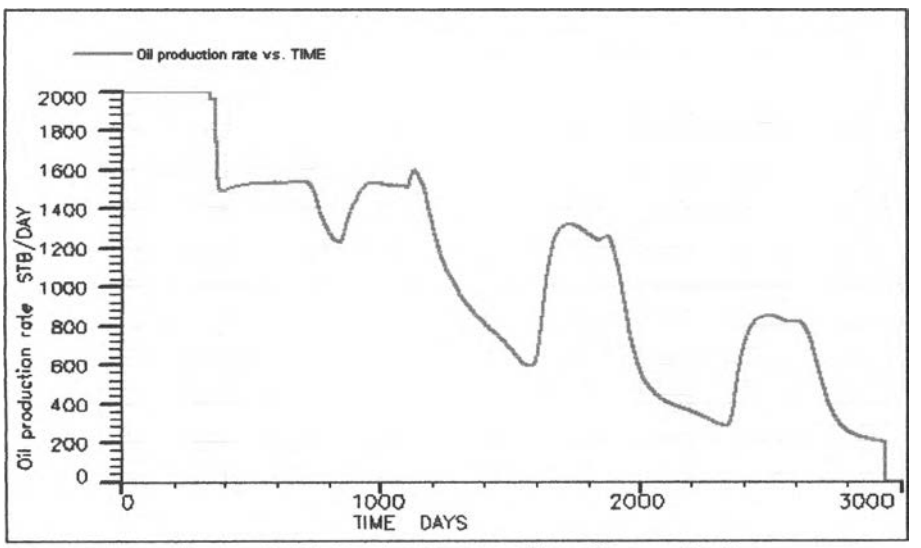

Figure 5.46: Production profile of scenario 2.

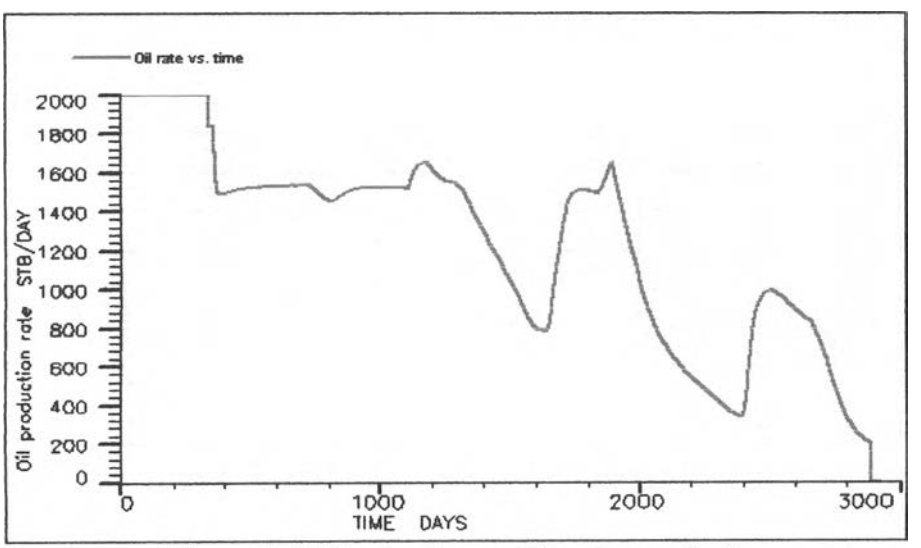

Figure 5.47: Production profile of scenario 3.

From the investigation using black oil model in this section, it can be concluded that horizontal permeability, vertical to horizontal permeability, and location of the production and injection well do not have any effect on the optimization of WAG process. That is, the optimal value for water-gas ratio and cycle size is the same when these parameters are changed. However, the actual values of recovery efficiency are different as these parameters are changed.

5.2 Optimum WAG process using compositional model

In the previous section, the optimization of WAG process was conducted using a black oil reservoir model. Nevertheless, the black oil simulator is unable to handle the composition exchange between oil and gas phases whereas the compositional simulator has an ability to do it. In this study, we choose to use injected gas that has the same components as the light components of the reservoir oil.

In order to compare the results with those obtained from the black oil model, common input parameters for both models are kept the same. Additional parameters needed in the compositional model are one involving with the equation of state. With the same injection strategy, differences between the results of the black oil and compositional models can be considered as the effect of composition exchange or miscibility. This section discusses the optimization of the WAG process in the same manner as the previous section, i.e., the effect of horizontal permeability, vertical to horizontal permeability ratio, and distance between the production and injection well on the best cycle size and water-gas ratio. Waterflood cases were also run in this section for comparison purposes.

5.2.1 Results of base case model

Like the black oil model, the results of the base case of compositional model were thoroughly investigated. Figures 5.48 to 5.61 show the results of the base case model which is a WAG process with water-gas ratio of 1, cycle size of 24 months, k_h of 200 md, and k_v of 2 md.

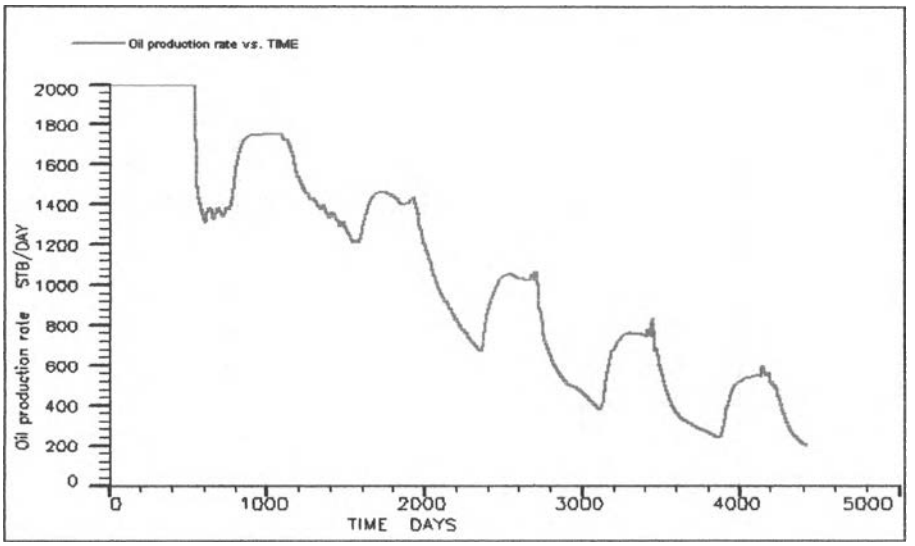

Figure 5.48: Oil production profile.

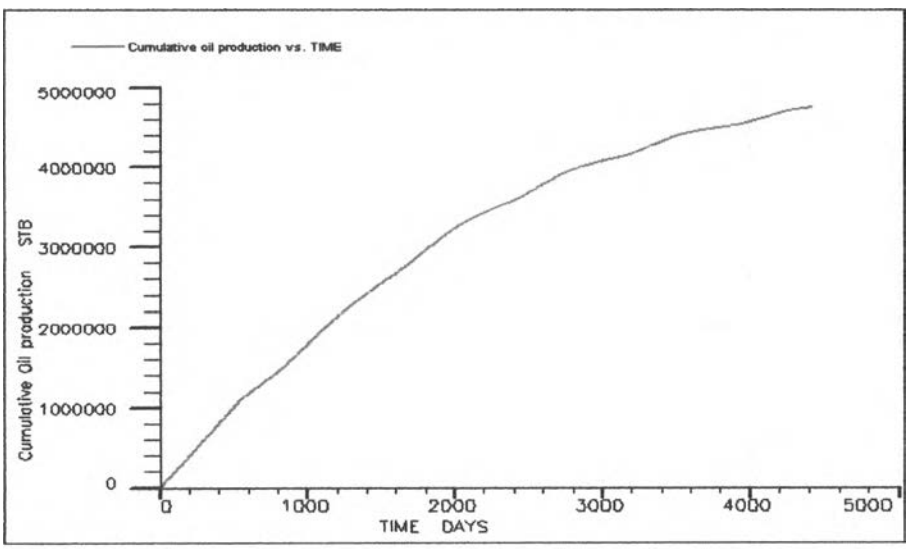

Figure 5.49: Cumulative oil production profile.

The oil production profile is shown in Figure 5.48. It can be seen that the reservoir can maintain a plateau rate of 2000 STB/day for about 550 days. This period in the compositional model is longer than that in the black oil model (380 days). After this plateau rate, the oil production then increases and decreases in a cyclic manner throughout the producing time. The production ends when the oil production rate reaches 200 STB/day. It can be observed that the producing time of the compositional base case is 4,400 days, which is much longer than producing time of the black oil base case model (2,950 days). Figure 5.49 illustrates that the cumulative oil production of the base case compositional model is 4,600,000 STB. Since the compositional simulator is unable to summarize the recovery factor directly, such calculation is done separately.

In this case, the recovery factor is 58.54 % which is higher than that obtained from the black oil base case model (45.74 %). The increment in the recovery can be explained by the fact that oil viscosity in the compositional model is lower than that in the black oil model. This can be shown in Figures 5.50 and 5.51. It is seen that after producing for 400 days, the gas slug reaches block (20,11, 5). The miscibility of gas results in lower oil viscosity in the compositional model. The reason for choosing block (20,11, 5) is that the block is located far away from the injector. Thus, there is oil left in this block. If the block at injector is chosen, oil can be flooded to a saturation of 0. Then, we cannot see the viscosity value.

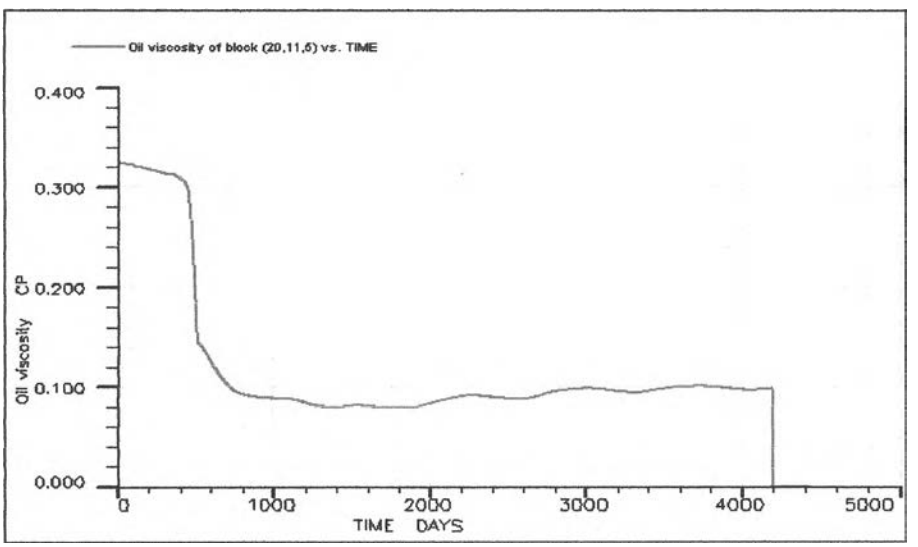

Figure 5.50: Oil viscosity of block (20,11,5) profile from compositional model.

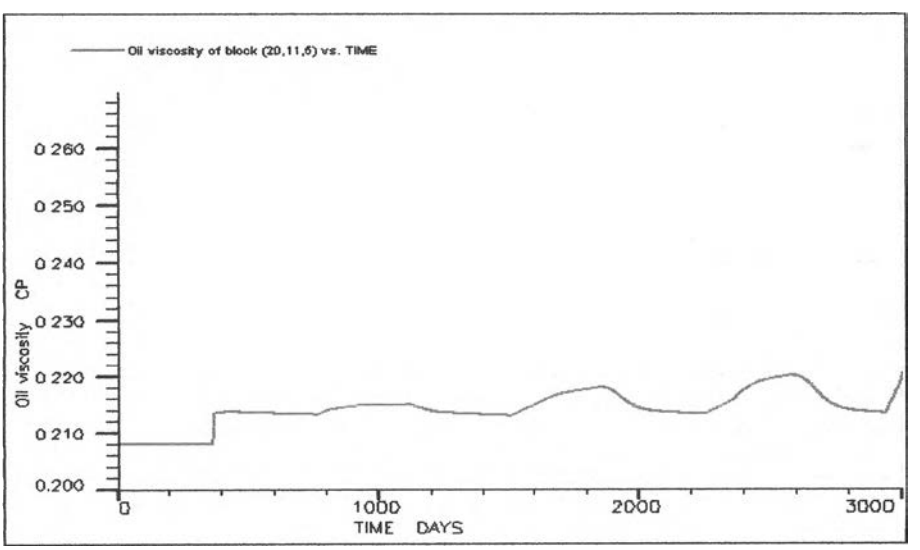

Figure 5.51: Oil viscosity of block (20,11,5) profile from black oil model.

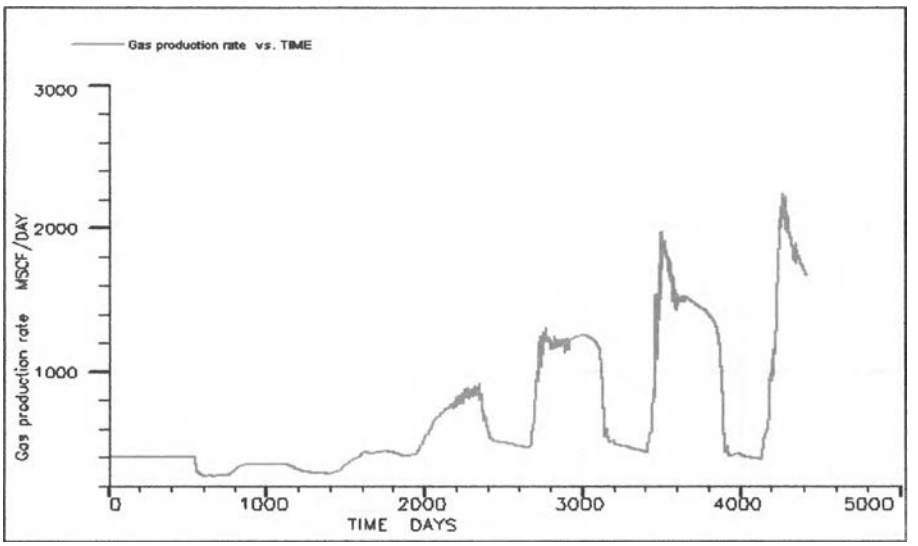

Figure 5.52: Gas production profile.

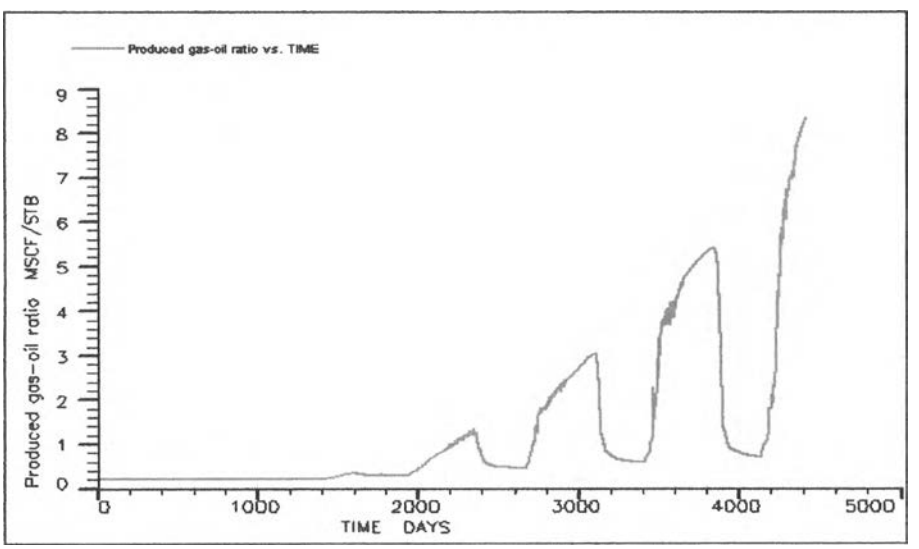

Figure 5.53: Gas-oil ratio profile.

The apparent difference between compositional and black oil models is found on gas production and gas-oil ratio profile as shown in Figures 5.52 and 5.53, respectively. These two plots show similar trend as those for the black oil case. In Figure 5.52, the initial gas-oil ratio is 0.202 MSCF/STB whereas the initial gas-oil ratio in base case black oil model is 0.537 MSCF/STB which follows the value specified in the input data. This much lower initial gas-oil ratio for the base case compositional model may come from the miscibility of the injected gas. The hydrocarbon gas partially condenses into reservoir oil at such a high pressure. It can be seen from Figure 5.53 that gas breakthrough time is 1,450 days which is much slower than that in black oil model.

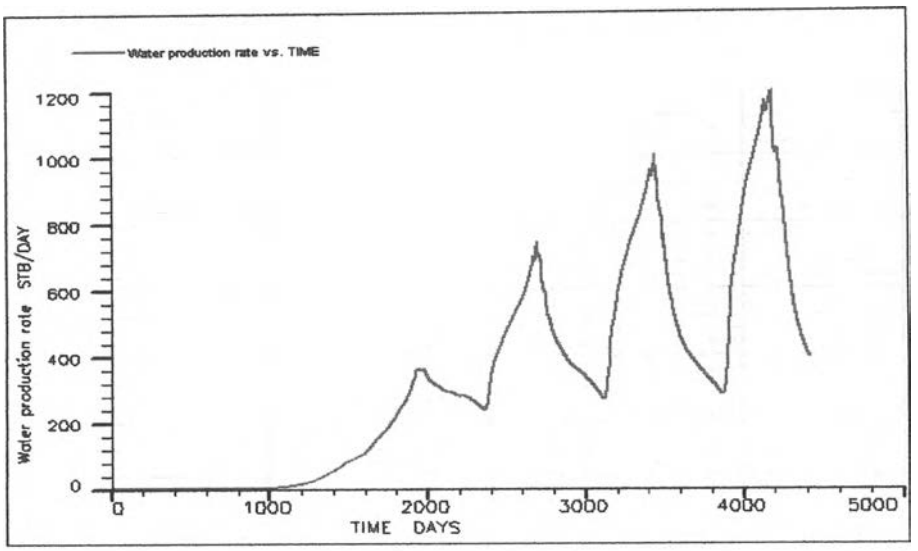

Figure 5.54: Water production profile.

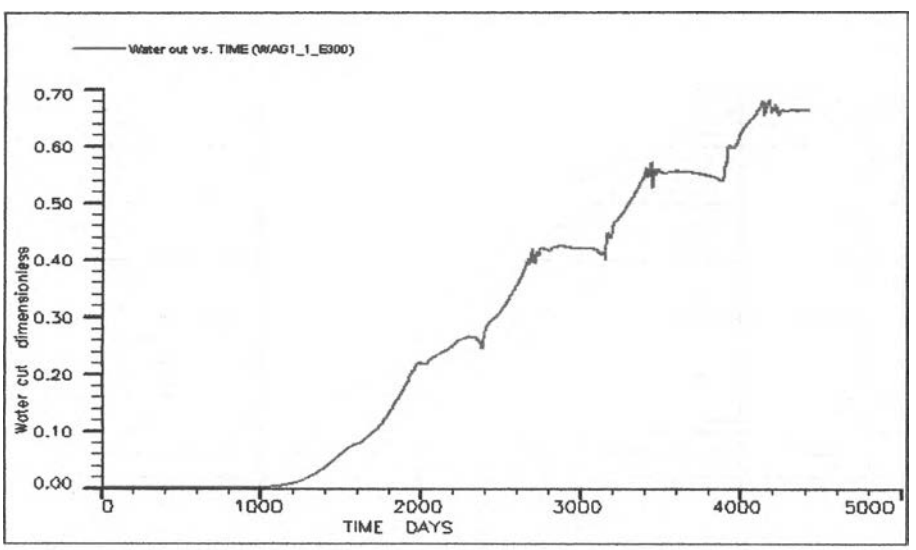

Figure 5.55: Water cut profile.

Figure 5.54 and 5.55 show that the water breakthrough time is 1,100 days which is 100 days earlier than the breakthrough time in the base case black oil model. This is due to the fact that the reduction in oil viscosity helps increase the displacement rate of oil by water. The water cut profile is similar to the one in the black oil model.

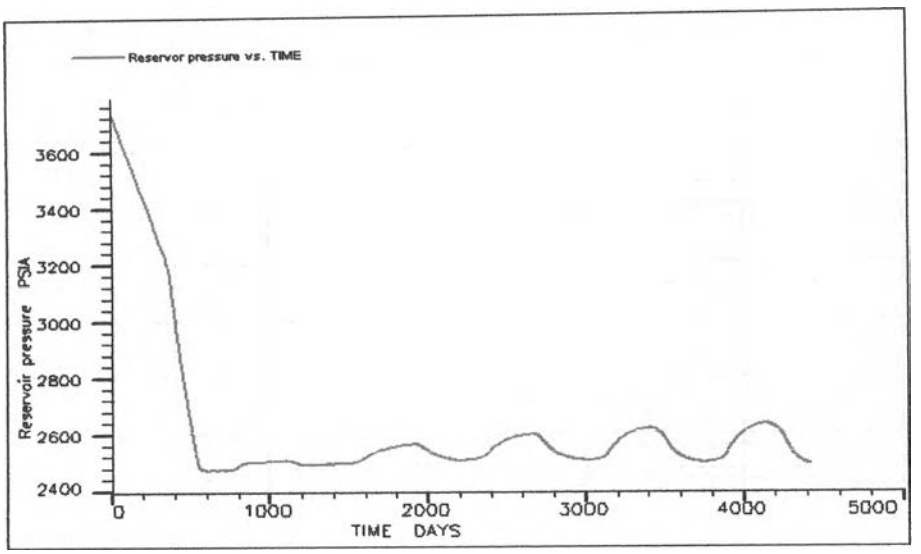

Figure 5.56: Average reservoir pressure profile.

The average reservoir pressure of the compositional model is shown in Figure 5.56. The pressure rapidly drops from 3,745 psia to 2,440 psia during the period of plateau production and then fluctuates in the range of 2,440 to 2,640 psia. This behavior is similar to the black oil model.

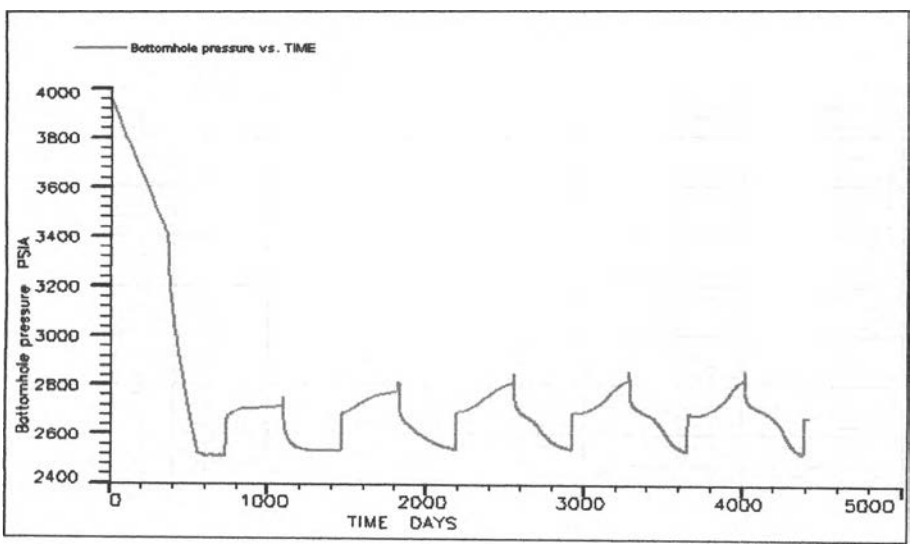

Figure 5.57: Bottom hole pressure profile of injection well.

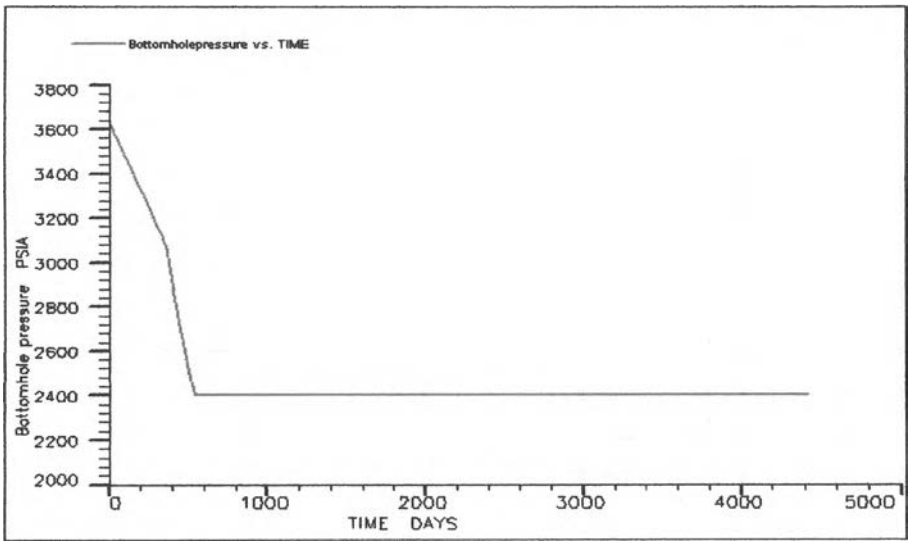

Figure 5.58: Bottom hole pressure profile of production well.

The bottom hole pressure profiles of the injection and production wells are plotted in Figures 5.57 and 5.58, respectively. For the injection well, the pressure drops from 3,900 to 3,400 psia during the injection of the first slug of water for 1 year. When the first gas slug is injected, the bottom hole pressure of the injector drops again to 2,440 psia and stays constant at this pressure until the second water slug is injected. The bottom hole pressure of the injector generally increases when injecting water and decreases when injecting gas. This occurs alternately throughout the producing time. In Figure 5.58, the bottom hole pressure of the production well decrease from 3,600 to 2,400 psia during the period of plateau production. The bottom hole pressure profiles of the two wells are similar to those in the black oil model.

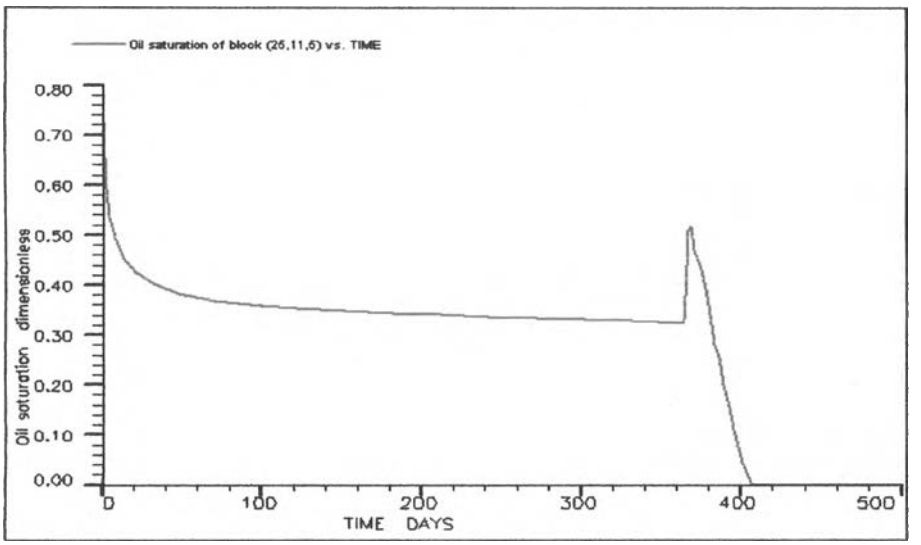

Figure 5.59: Oil saturation profile of one of injection well blocks.

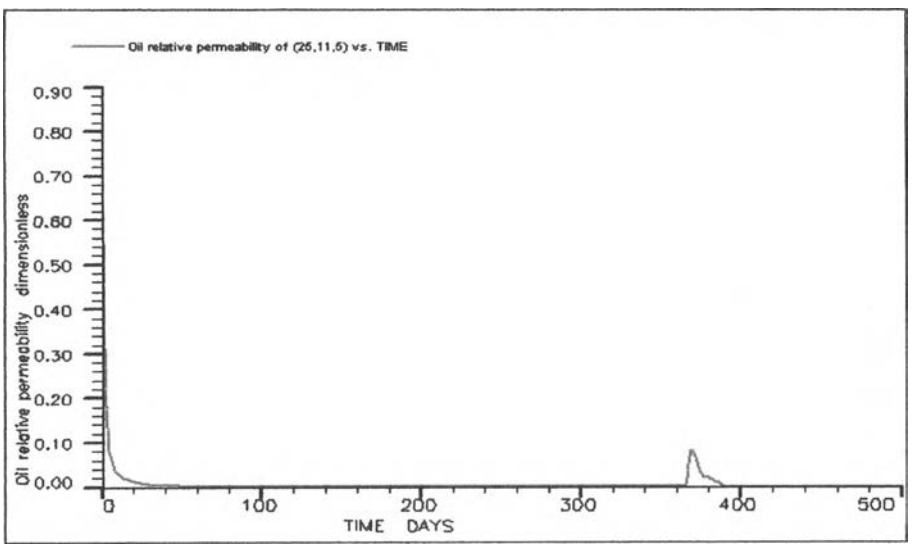

Figure 5.60: Oil relative permeability profile of one of injection well blocks.

The properties of grid block at location (25,11,5) which is one of injection well blocks are shown as in the black oil model. Figure 5.59 presents the oil saturation profile of the grid block. It is seen that the oil saturation decreases from 0.8 to 0.32 during the first slug of water injection. This behavior is similar to the black oil model. However, when the first gas slug is injected, the oil saturation increases instantly to 0.5 and then decreases to 0 in 40 days. The behavior during gas injection is very different from the black oil model. In the black oil model, the oil saturation stays at 0.2 which is the residual oil saturation for the rest of the producing time. The residual oil saturation of 0.2 was specified in both models. In the compositional

model, miscibility develops in this block during the initial period of gas injection at which the pressure of the block is still high. Thus, the oil saturation increase to 0.5. After that, the pressure of the block reduces to a low value. As oil is displaced by the injected gas, the oil saturation becomes zero as a result of vaporization. Figure 5.60 illustrates the oil relative permeability of block (25,11,5) which is seen that oil relative permeability follows the relative permeability function specified in the model.

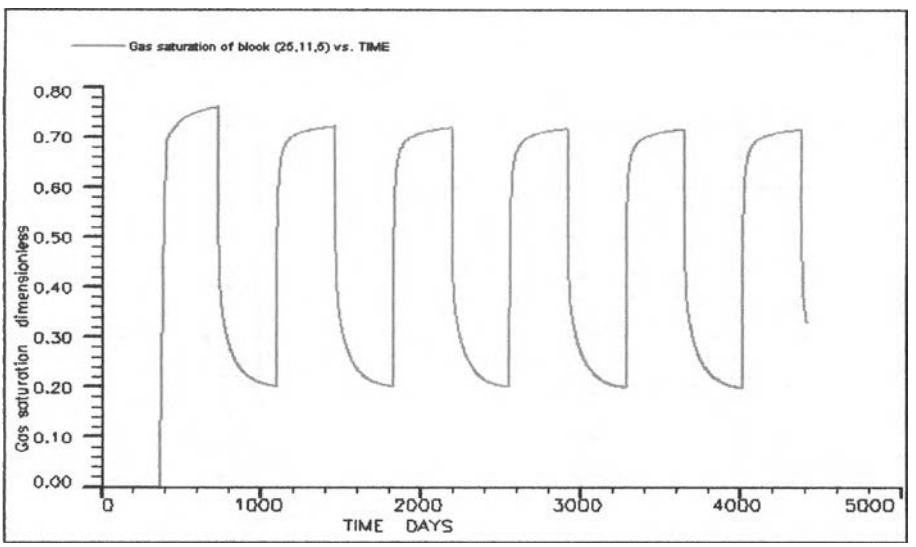

Figure 5.61: Gas saturation profile of one of injection well blocks.

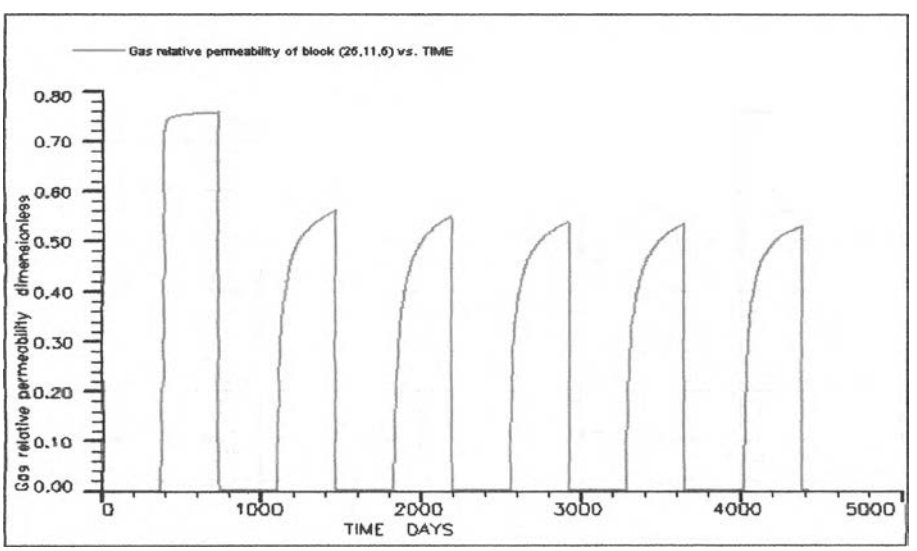

Figure 5.62: Gas relative permeability profile of one of injection well blocks.

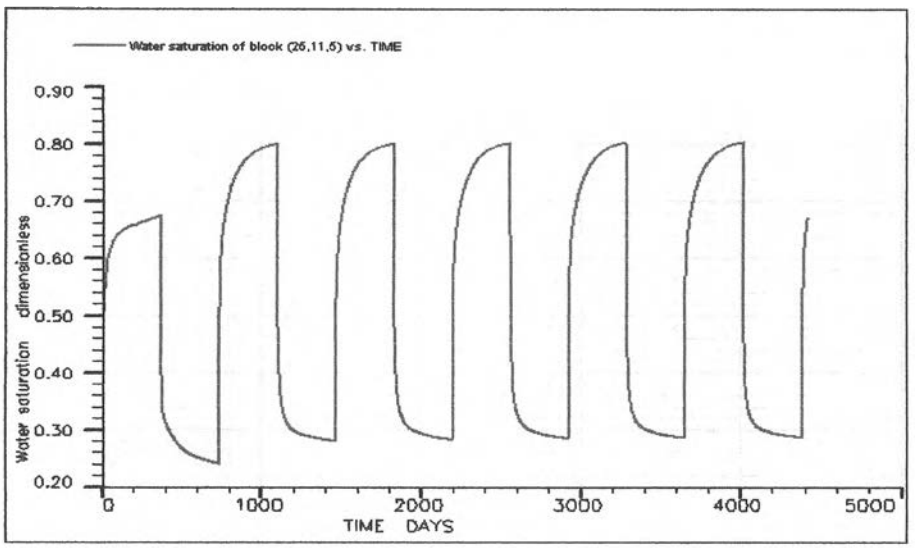

Figure 5.63: Water saturation profile of one of the injection well blocks.

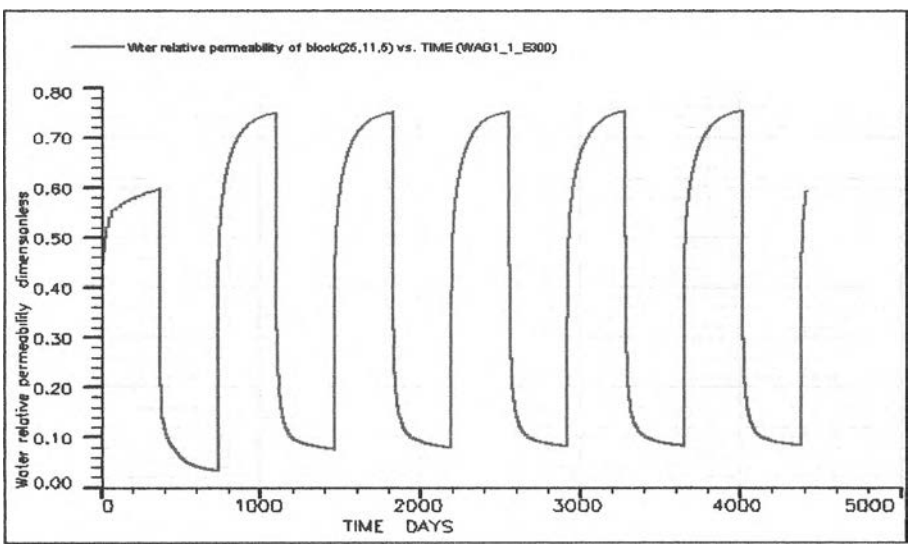

Figure 5.64: Water relative permeability profile of one of the injection well blocks.

The saturation and relative permeability of water and gas are shown in Figures 5.61 to 5.64. The saturation and relative permeability of water and gas increase when that particular phase is injected and decrease when the other phase is injected. The differences from the black oil model are at the maximum values of saturation and relative permeability of both phases. The maximum gas saturation in Figure 5.61 is 0.75 whereas the maximum water saturation is 0.8. Both values are higher than the values in the black oil model. This is a result of having residual oil saturation reduced to 0. This means water and gas can occupy more space when each phase is injected since there is no residual oil.

5.2.2 Optimization study

5.2.2.1 Effect of horizontal permeability

As it was concluded in the previous section that the horizontal permeability does not have any effect on the optimization of the WAG process, it is interesting to investigate if the same result will be obtained in the compositional reservoir model. The set of horizontal permeability used in this part is the same as that in the black oil reservoir model.

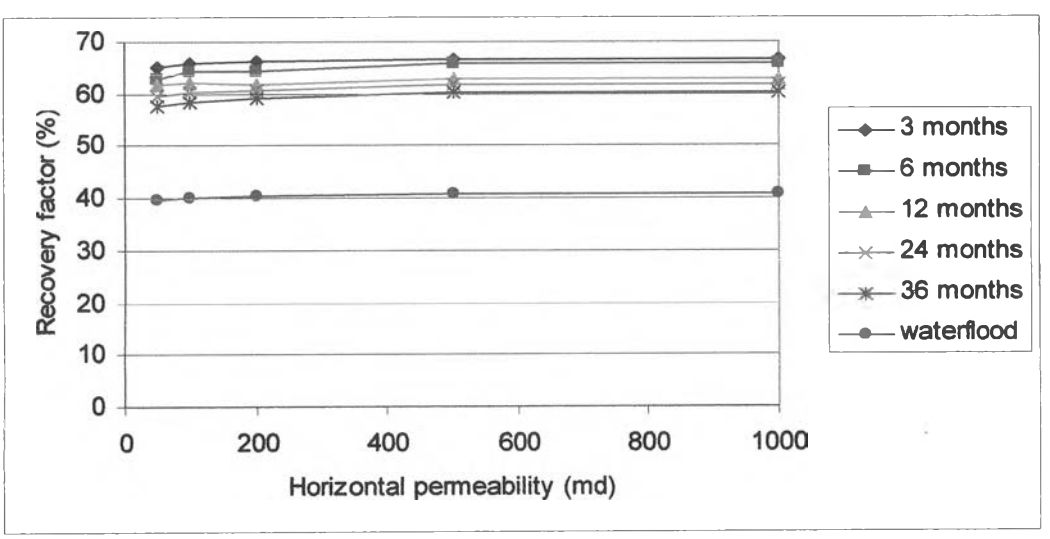

Figure 5.65: Recovery factor of WAG process when varying horizontal permeability for cases with water-gas ratio = 0.25.

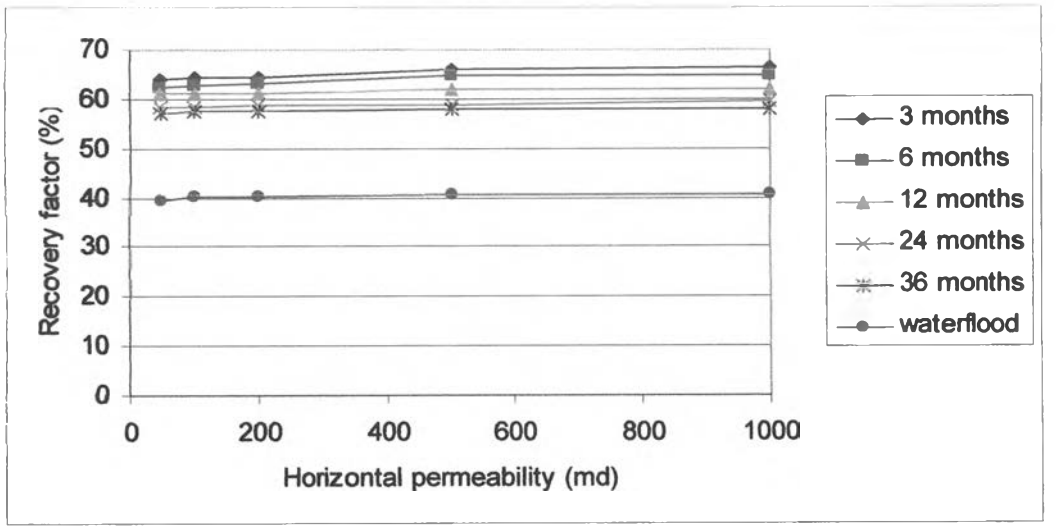

Figure 5.66: Recovery factor of WAG process when varying horizontal permeability for cases with water-gas ratio = 0.5.

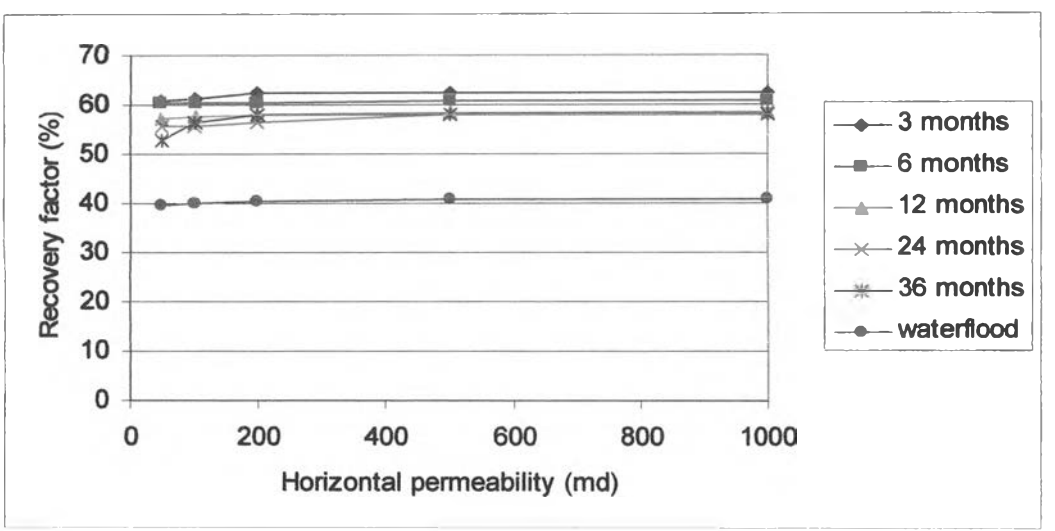

Figure 5.67: Recovery factor of WAG process when varying horizontal permeability for cases with water-gas ratio = 1.

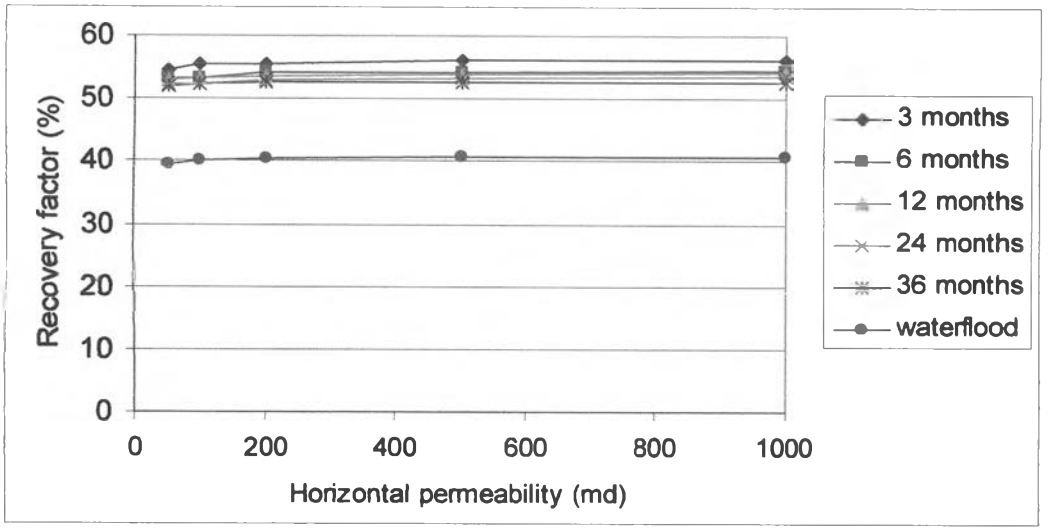

Figure 5.68: Recovery factor of WAG process when varying horizontal permeability for cases with water-gas ratio = 2.

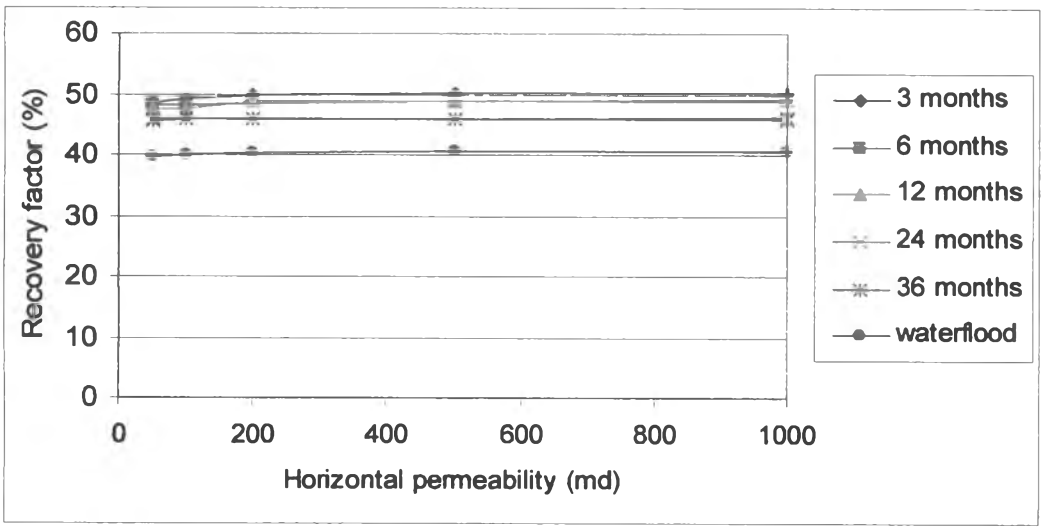

Figure 5.69: Recovery factor of WAG process when varying horizontal permeability for cases with water-gas ratio = 4.

Figures 5.65-5.69 show the effect of horizontal permeability on the recovery factor of WAG cases with different cycle sizes in the compositional model. It is found that the effect of horizontal permeability is similar to that in the black oil model. The recovery factor slightly increases from horizontal permeability of 50 to 100 and 200 md. Since the ability to allow fluid to flow increases, oil production also increases. Increasing the horizontal permeability from 200 to 500 and 1000 md, the recovery factor is almost constant. Cases with a smaller cycle size provide a higher recovery factor than those with a larger cycle size. Changing the horizontal permeability does not change the optimum cycle size value which is 3-month.

Nevertheless, it can be observed that the WAG process simulated by compositional model provides a higher recovery factor than that simulated by the black oil model. In the compositional model, every WAG case has higher recovery factor than the waterflood. The reason for this observation is discussed when recovery factor is plotted as a function of water-gas ratio.

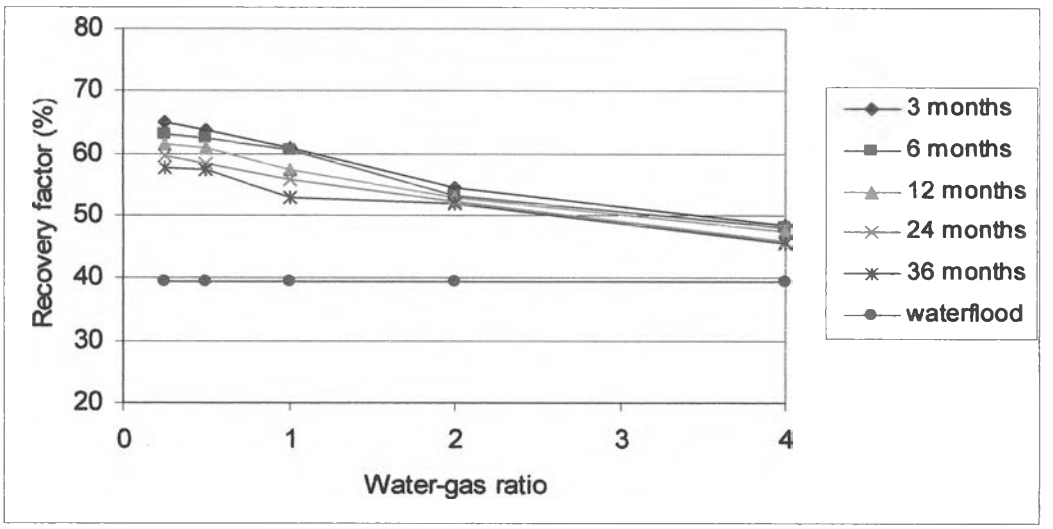

Figure 5.70: Recovery factor of WAG process when varying water-gas ratio for cases with k_h = 50 md.

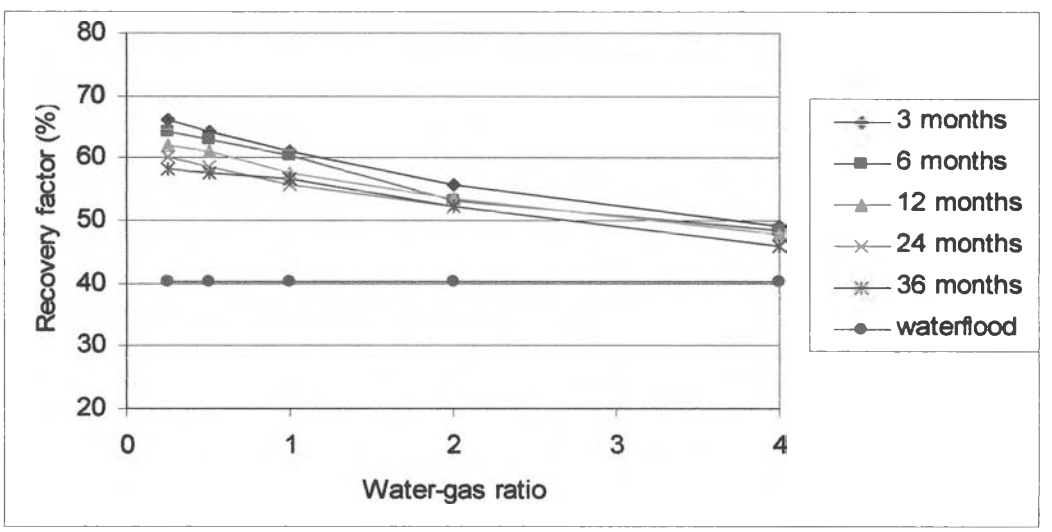

Figure 5.71: Recovery factor of WAG process when varying water-gas ratio for cases with k_h = 100 md.

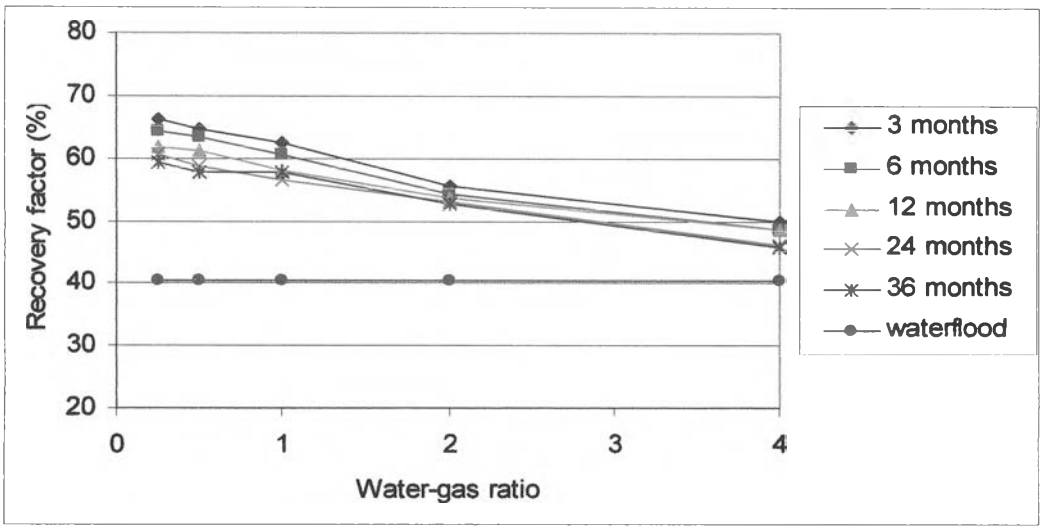

Figure 5.72: Recovery factor of WAG process when varying water-gas ratio for cases with k_h = 200 md.

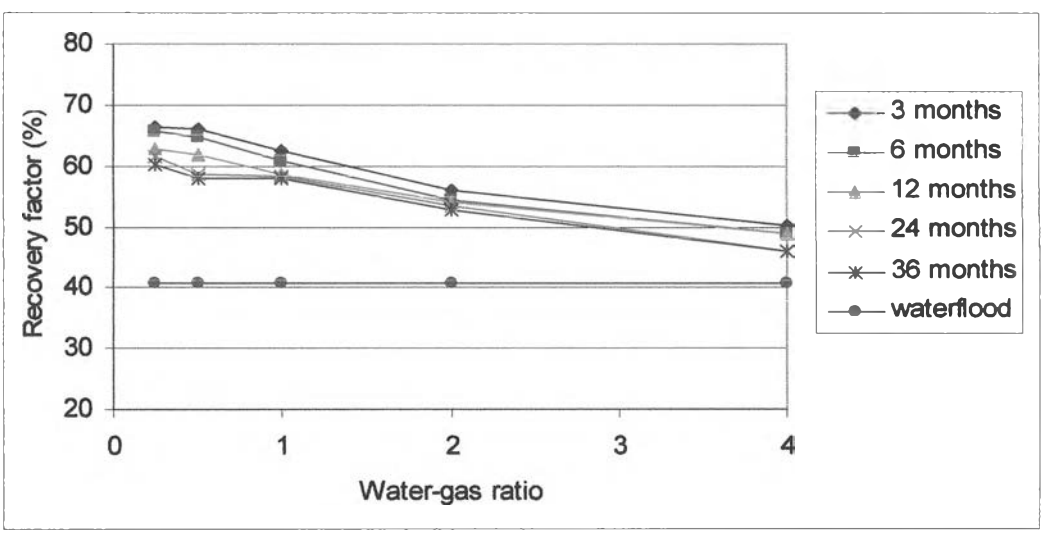

Figure 5.73: Recovery factor of WAG process when varying water-gas ratio for cases with k_h = 500 md.

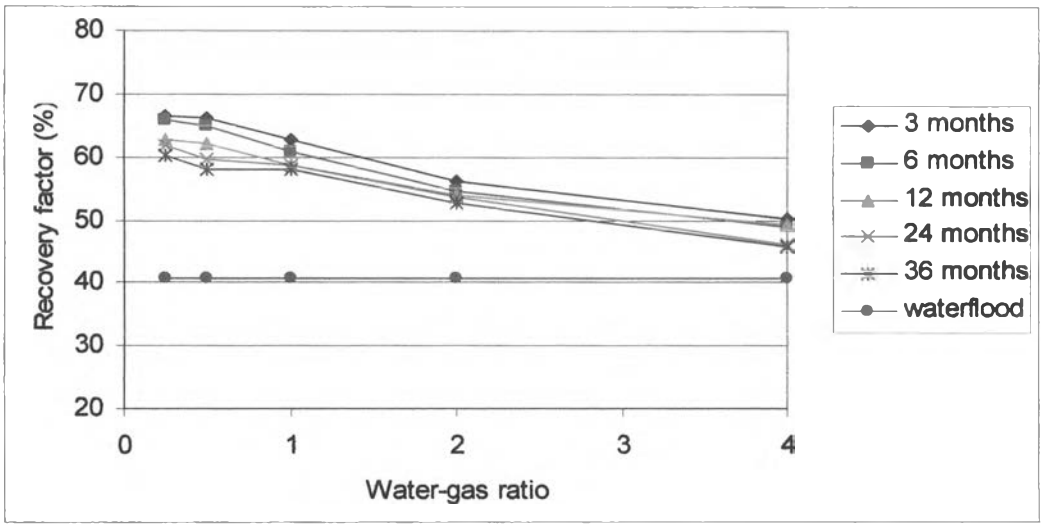

Figure 5.74: Recovery factor of WAG process when varying water-gas ratio for cases with k_h = 1,000 md.

Figures 5.70-5.74 present the recovery factor as a function of water-gas ratio for different cycle sizes. The recovery factor varies in the range of 46-66 %, which is much higher than recovery factors obtained from the black oil model. Another observation is that the difference between the recovery factors of WAG process and waterfood is higher in the compositional reservoir model. The waterflood cases have a recovery factor around 40.5 %. The WAG cases have higher recovery factor than the waterflood. In the compositional model, gas injection causes the oil saturation to reduce to zero. Thus, a higher recovery factor can be obtained from the compositional model.

It is found from these figures that the optimum water-gas ratio is 0.25 which is different from the result from the black oil model. The recovery factor decreases when the water-gas ratio increases for every cycle size. This means that more gas has to be injected in the compositional model in order to achieve higher recovery factor. The similarity between black oil and compositional models is found on the optimum cycle size which is 3-months. That is the smaller the cycle size, the higher the recovery factor is. Another similarity is that the horizontal permeability has no effect on the optimizing WAG process or the injection strategy in terms of cycle size and water-gas ratio for WAG process is the same when the horizontal permeability changes.

Like the black oil model, the effect of horizontal permeability can be observed when the production rate is investigated.

Figure 5.75 is a plot of period of plateau rate as a function of horizontal permeability. It is found that duration of plateau production increases with the horizontal permeability. Such increase is obviously seen from cases having horizontal permeability in the range of 50 to 200 md. For the cases with horizontal permeability exceeding 200 md, the plateau rate increases slightly due to the limit of ability to flow of the reservoir. However, it is found that WAG cases with higher water-gas ratio have longer plateau rate periods than cases with lower water-gas ratio. This observation shows the inverse trend comparing to the results from the black oil reservoir model in which cases with lower water-gas oil ratio can maintain the plateau rate longer. This is because, in the compositional model, large amount of injected gas transfers to the light component of reservoir fluid, resulting in ineffective pressure support.

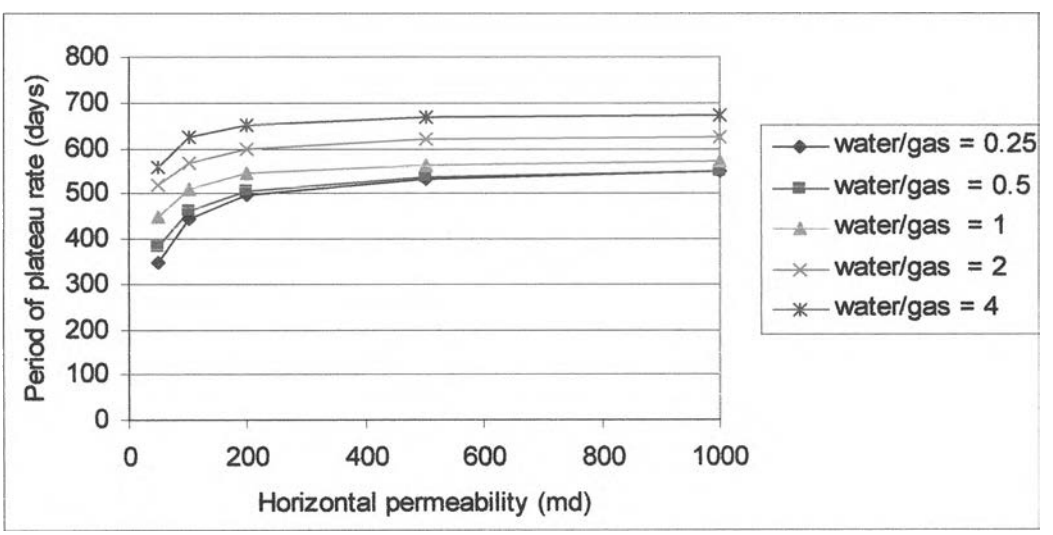

Figure 5.75: Effect of horizontal permeability on the period of plateau rate for WAG cases with 24 months cycle size.

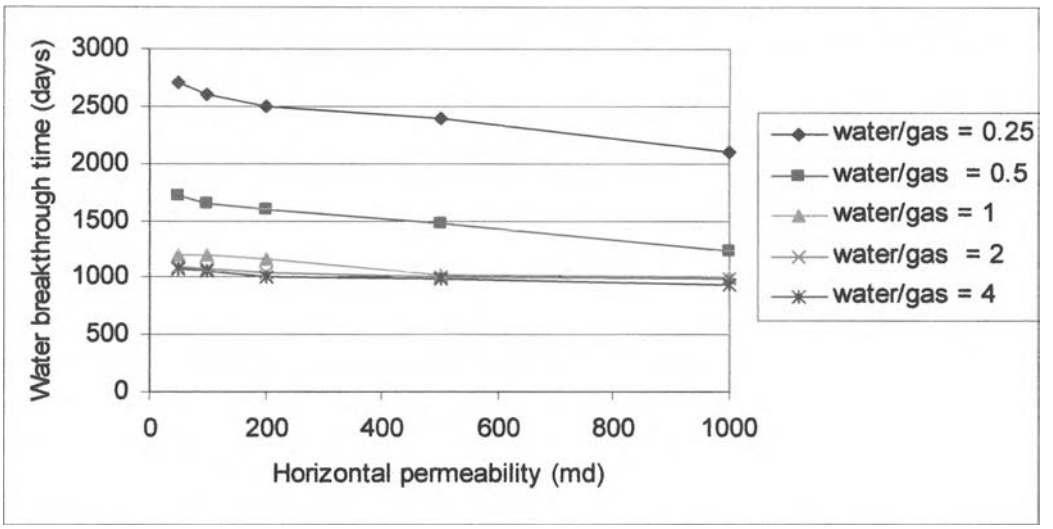

Figure 5.76: Effect horizontal permeability on water breakthrough time for WAG cases with 24 months cycle size.

The effect of horizontal permeability on water breakthrough time is shown in the Figure 5.76. It is seen that the result is similar to the result from the black oil model. Cases with higher horizontal permeability have an earlier water breakthrough than cases with lower horizontal permeability. Moreover, cases with lower water-gas ratio produce longer before water breakthrough. It is also observed that when water-gas ratio is 0.25, the compositional model gives later water breakthrough than in the black oil model whereas for other water-gas ratio values, water breakthroughs earlier in the compositional model.

In the previous section, cases having a large amount of injected water such as water-gas ratio of 2 and 4 were stopped when the water cut is 0.7 before reaching the oil economic limit of 200 STB/day and cases with water-gas ratio of 0.25, 0.5, and 1 was terminated when the oil rate reaches the economic limit of 200 STB/day. In this section, the effect of different criteria of stopping the production is also investigated.

The effect of having only 200 STB/day oil economic limit can be presented in Figure 5.77. It is found that cases which stop producing due to the water cut limit, can achieve higher recovery when using only oil rate economic limit. In this scenario, the recovery factor of the water flood case increases to 45.88 %. It is seen that the WAG process still performs much better than waterflood. In addition, the optimum cases is still the case with 3-month cycle size and water-gas ratio of 0.25. Therefore, it can be concluded that changing the economic criteria from limiting both oil rate and

water cut to limiting only the oil rate does not affect the optimization of WAG process.

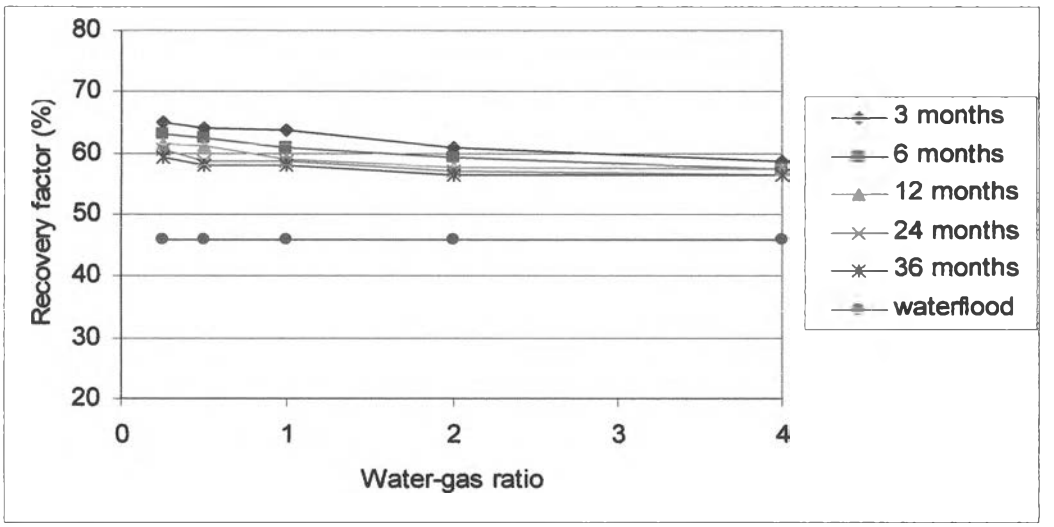

Figure 5.77: Recovery factor of WAG process when varying water-gas ratio for cases terminated by minimum oil rate of 200 STB/day.

5.2.2.2 Effect of vertical to horizontal permeability ratio

In the previous section, the effect of vertical to horizontal permeability ratio was investigated using the black oil model. The recovery factor is almost the same when the ratio varies. In the black oil model, vertical to horizontal permeability ratio does not affect the recovery factor of the WAG cases at all. However, it is interesting to see if the same kind of result is obtained when the compositional model is used.

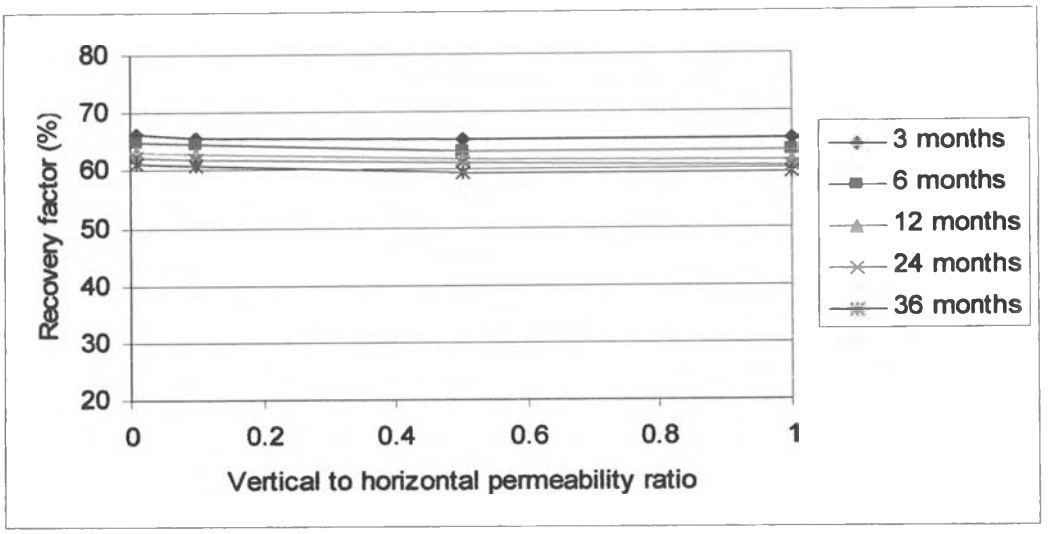

Figure 5.78: Effect of k_v/k_h on WAG cases with water-gas ratio = 0.25, k_h = 200 md.

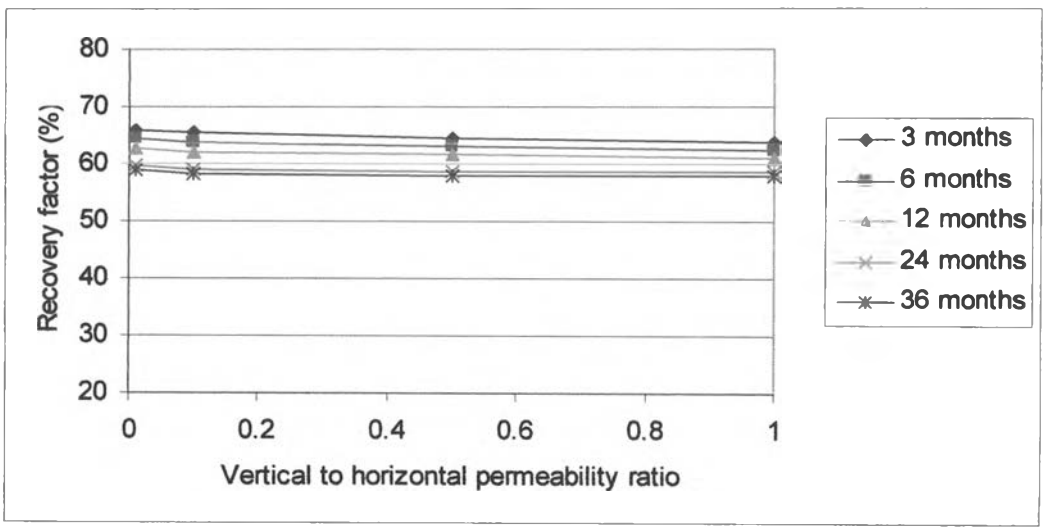

Figure 5.79: Effect of k_v/k_h on WAG cases with water-gas ratio = 0.5, k_h = 200 md.

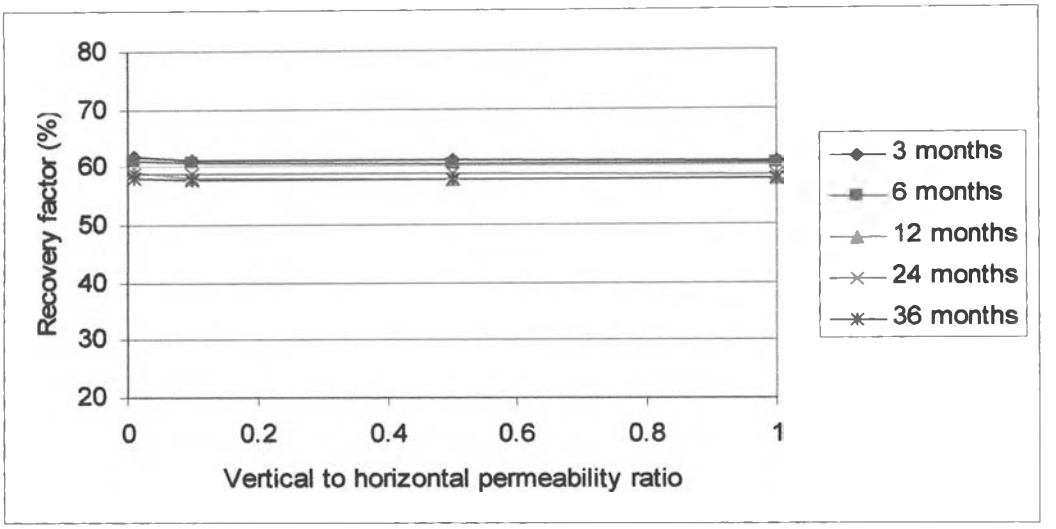

Figure 5.80: Effect of k_v/k_h on WAG cases with water-gas ratio = 1, k_h = 200 md.

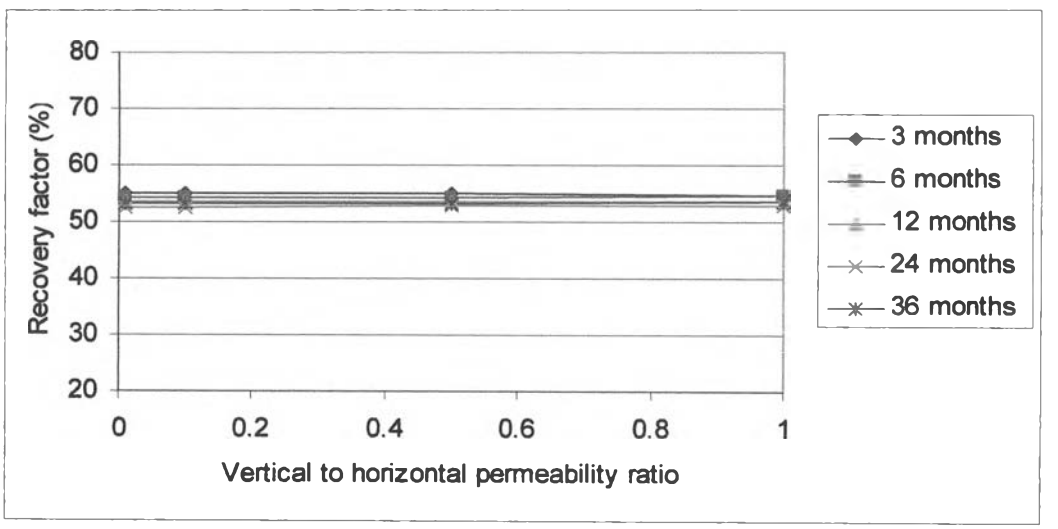

Figure 5.81: Effect of k_v/k_h on WAG cases with water-gas ratio = 2, k_h = 200 md.

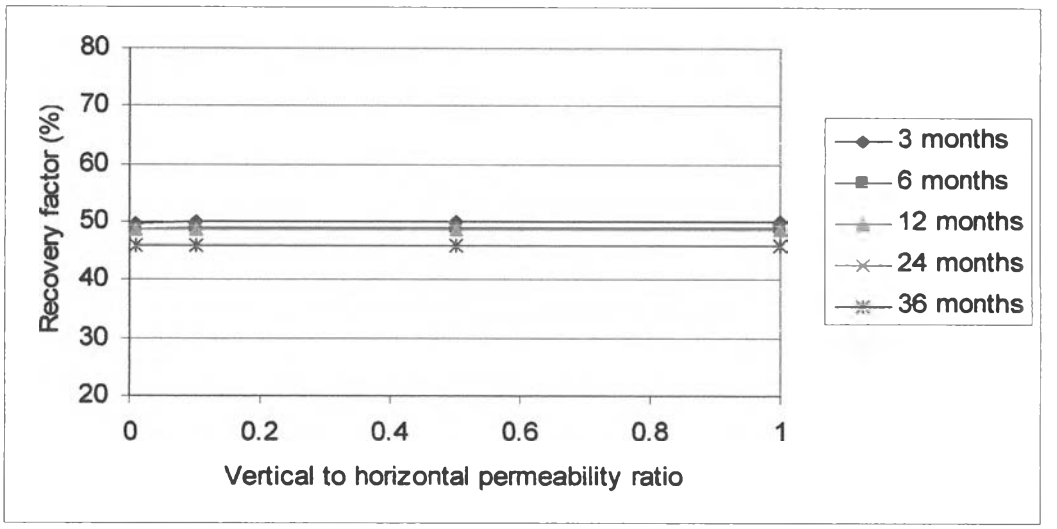

Figure 5.82: Effect of k_v/k_h on WAG cases with water-gas ratio = 4, k_h = 200 md.

Figures 5.78-.82 depict the recovery factor as a function of vertical to horizontal permeability ratio for different water-gas ratio and cycle sizes. It is observed from these figures that when water-gas ratio is 0.25, 0.5 and 1, the recovery factor slightly decreases with the vertical to horizontal permeability ratio. However, cases with water-gas ratio equal to 2 and 4 show similar results to that obtained from black oil model that the vertical to horizontal permeability ratio does not have an effect on the recovery factor. The slight decrease in recovery factor when there is a larger amount of injected gas (low water-gas ratio) may come from the reason that gas can flow better in the vertical direction when the vertical to horizontal permeability ratio increases. This causes the gravity override that reduces the areal sweep efficiency of gas.

Since the vertical to horizontal permeability ratio has some effect on some WAG cases, it is necessary to investigate the effect of vertical to horizontal permeability ratio on the optimization of WAG process. This investigation is shown in Figures 5.83-5.85.

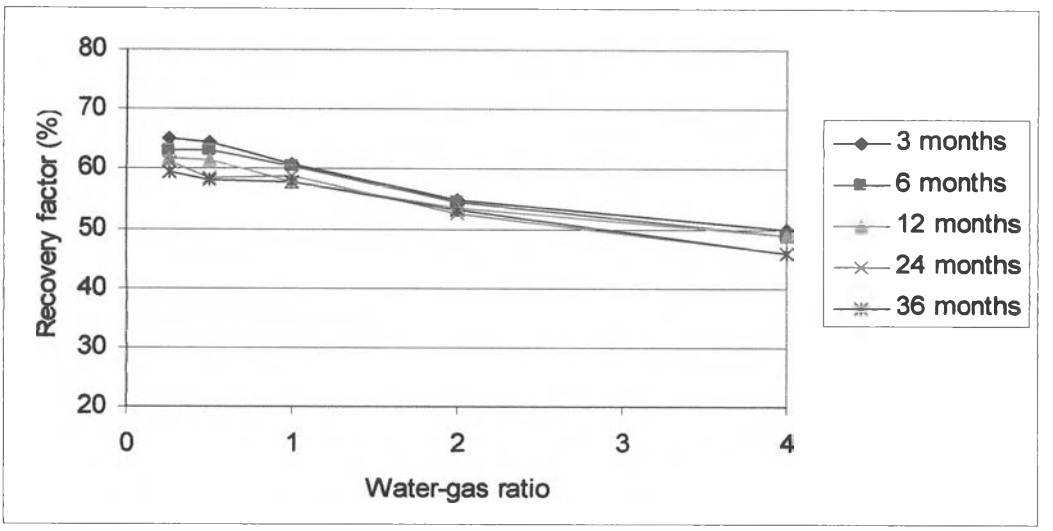

Figure 5.83: Recovery factor of WAG process when varying water-gas ratio for cases with $k_v/k_h = 0.1$.

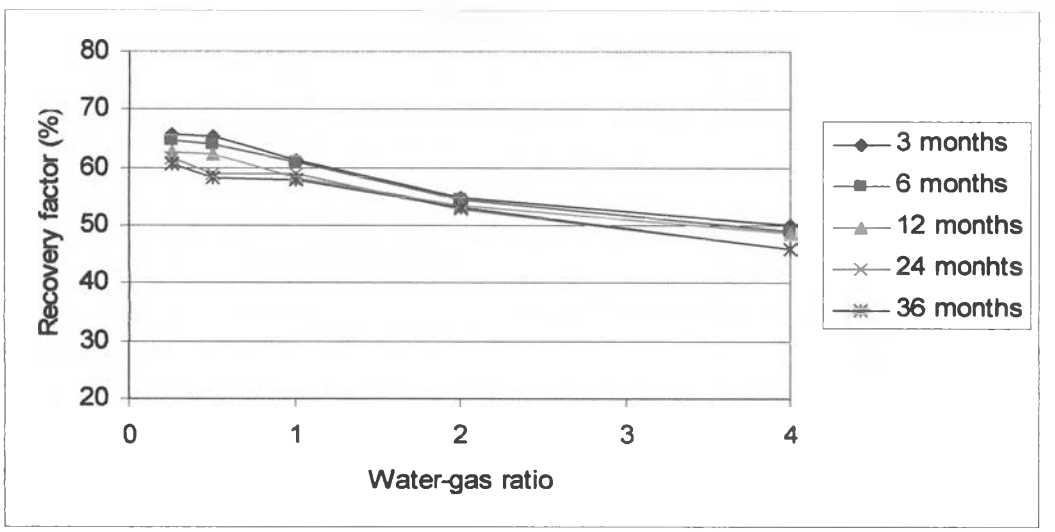

Figure 5.84: Recovery factor of WAG process when varying water-gas ratio for cases with $k_v/k_h = 0.5$.

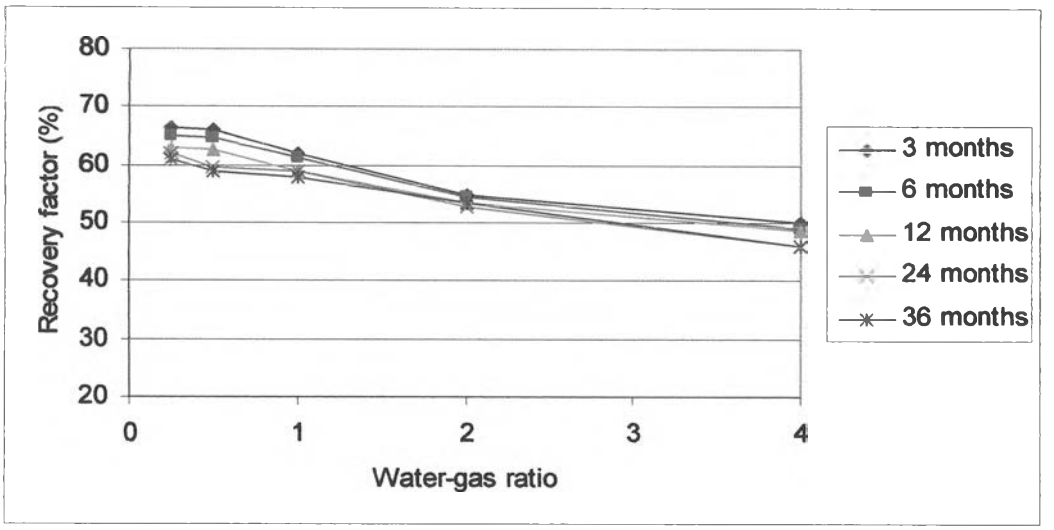

Figure 5.85: Recovery factor of WAG process when varying water-gas ratio for cases with $k_v/k_h = 1$.

In Figures 5.83-5.85, it is clear that changing the vertical to horizontal permeability ratio does not change the optimum WAG case. The optimum case is still the case with water-gas ratio of 0.25 and 3-month cycle size. All the cases show the same trend for different values of vertical to horizontal permeability ratio. The recovery factor decreases with the water-gas ratio and cycle size. Therefore, it can be concluded that in compositional reservoir model, vertical to horizontal permeability ratio does not affect the optimization of WAG process.

5.2.2.3 Effect of locations of producer and injector

The effect of locations of the producer and injector was studied using the black oil model in the previous section. It is found that the recovery factor increases when the two wells are located far apart. Nevertheless, the optimization of WAG process is not affected by the locations of the producer and injector.

This part of the chapter studies the effect of locations of the producer and injector using the compositional reservoir model. The investigation was conducted by using the scenarios mentioned in the Table 5.2. Cases with k_h = 200 md and k_v = 2 md were selected as well as in the previous section. The results from the compositional model are presented in Figures 5.86-5.88.

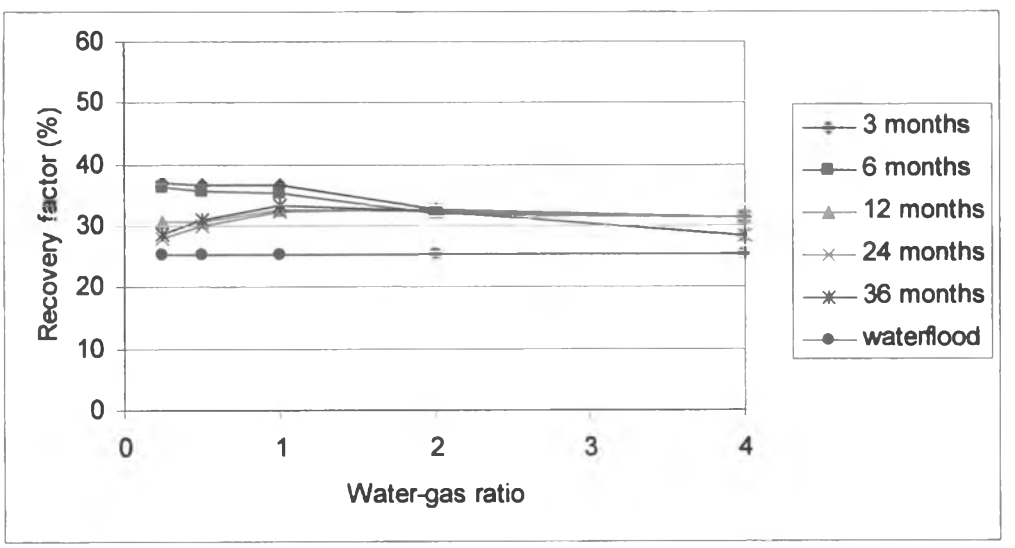

Figure 5.86: Recovery factor of WAG process when varying water-gas ratio for cases with scenario 1.

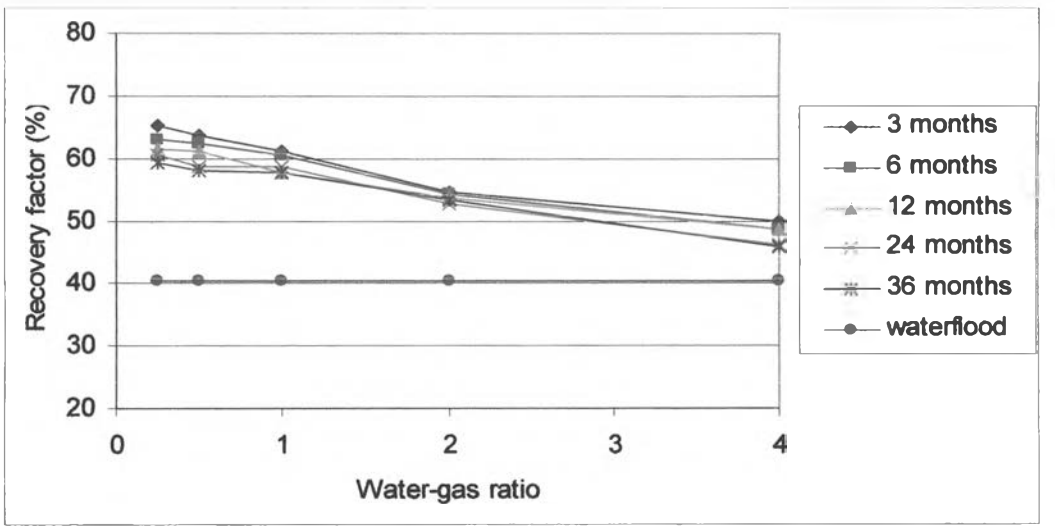

Figure 5.87: Recovery factor of WAG process when varying water-gas ratio for cases with scenario 2.

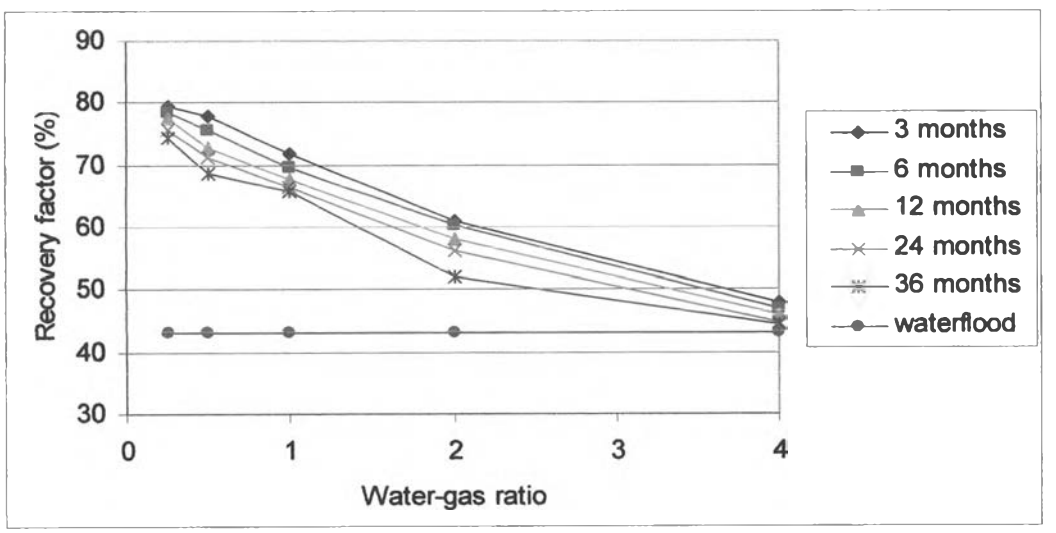

Figure 5.88: Recovery factor of WAG process when varying water-gas ratio for cases with scenario 3.

In scenario 1, cases with 24 and 36 month cycle size achieve the highest recovery at the water-gas ratio of 4. This observation is different from the results obtained from scenario 2 and 3 in which every WAG case achieve the maximum recovery factor at water-gas ratio of 0.25. The reason was already stated in the previous section. Moreover, like the black oil model, the recovery factor of the water flood process in scenario 1 is higher than many WAG cases especially cases with a large cycle size and low water-gas ratio. It is also found that the results in scenario 2 and 3 show similar behavior, that is, recovery factor decreases with water-gas ratio and cycle size. The optimum WAG cases of these two scenarios are still the cases with water–gas ratio of 0.25 and cycle size of 3 months. Similar to black oil model, there is an observation that the longer distance between producer and injector is, the less amount of oil is left between the well and along the boundaries. This is illustrated by Figures 5.89-5.91 in which production period is longer and production profile have more peaks of oil production rate if the distance between the production and injection well is further. This observation is also found in the black oil reservoir model.

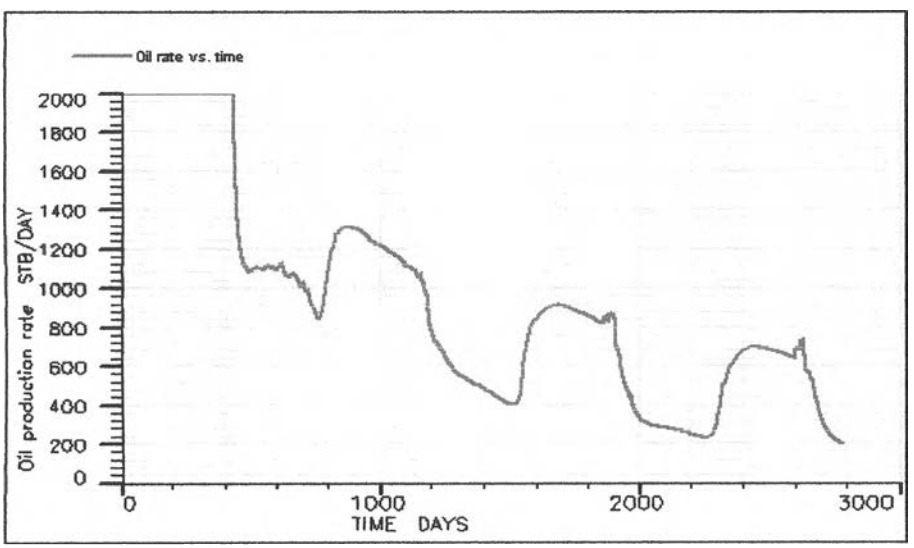

Figure 5.89: Production profile for scenario 1.

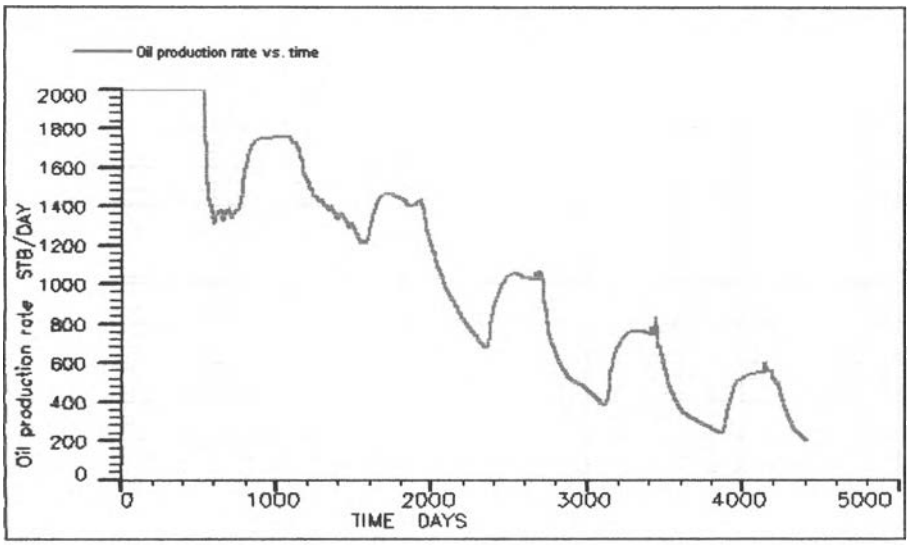

Figure 5.90: Production profile for scenario 2.

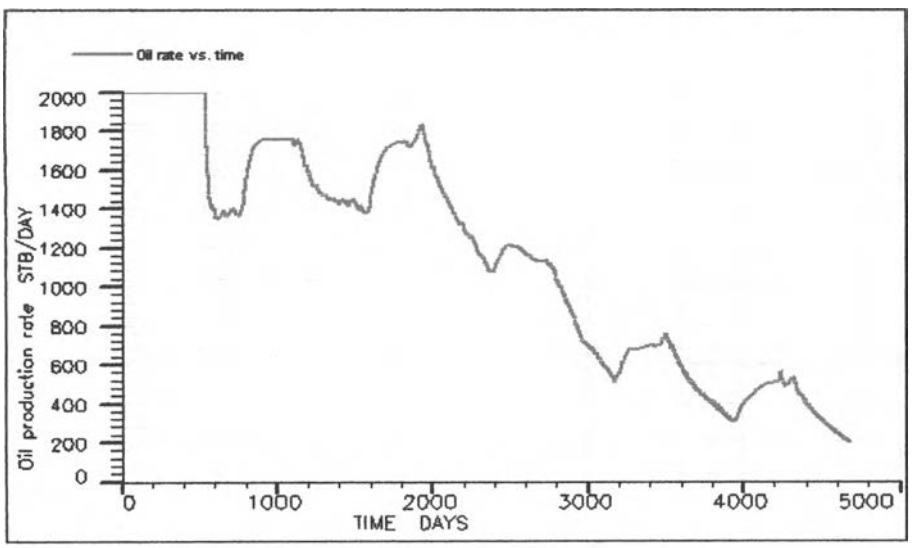

Figure 5.91: Production profile for scenario 3.

From results of the study shown in this section, it can be concluded that the optimal values of cycle size for WAG process obtained from black oil and compositional models is the same. The water-gas ratio is 0.25 whereas the optimum value for the black oil model is 1. It can be said for the compositional model that the higher the amount of injected gas, the higher the recovery factor. Furthermore, we also see that the horizontal permeability, vertical to horizontal permeability ratio, and the position of the production and injection wells do not have an effect on optimization of WAG process.

5.3 Relative permeability hysteresis model

As mentioned before that WAG process contains changes in displacement mechanism between drainage and imbibition, this part of the study focuses on the investigation of relative permeability hysteresis models existing in reservoir simulation. In the optimization of WAG process, Killough model was used because only this model is available in both black oil and compositional reservoir simulation. In this section, another relative permeability hysteresis model, Larsen and Skauge model, which is available in the black oil simulation model, is used. As stated earlier that this model is specially developed for WAG process, it is interesting to examine the results from this model in comparison to those from Killough model.

The investigation of relative permeability hysteresis model is performed on WAG cases simulated by both black oil and compositional reservoir simulation. Three cases were simulated in order to observe the effect of hysteresis model. These three cases are summarized in Table 5.5.

Table 5.5: Summary of cases used to investigate the effect of relative permeability hysteresis model.

Case	1	2	3
Reservoir simulation model	Black oil	Compositional	Black oil
Relative permeability hysteresis model	Killough	Killough	Larsen and Skauge
Water-gas ratio	1	1	1
Cycle size (month)	24	24	24
Horizontal permeability (md)	200	200	200
Vertical permeability (md)	2	2	2

The input parameter for Killough model is a modified trapped non-wetting phase saturation (a) which is set default to 0.1 as stated in Chapter 4. For Larsen and Skauge model, the input parameter are Land's constant (C) and reduction exponent (a) which are both specified to 2. Note that for Killough model, Land constant can be calculated using Equation (3.38).

The behavior of relative permeability hystersis can be investigated by plotting the relative permeability and saturation obtained from the simulation. The

investigation is performed on gas and water phases. The relative permeability to oil does not have hysteresis effect since oil decreases all the time during the WAG process. Grid block (25,11,5) was selected for this observation since it is located at the injection well position. The change of saturation and relative permeability is the most obvious at this grid block.

The first model that was investigated is Killough model in black oil simulation. Since the reservoir rock is a water-wet, the non-wetting phase in this study is gas. Figure 5.92 shows the relative permeability to gas as a function of gas saturation constructed from Killlough model. The input drainage and imbibition data are also plotted. Four cycles of injection are shown in the figure, starting with water injection which represents the first imbibition process, followed by gas injection which represents the first drainage process. During the first imbibition process, the gas saturation and relative permeability to gas are both 0 since no gas is presented in reservoir. The gas relative permeability then dramatically increases with the gas saturation along the input drainage curve during the first drainage process. The first drainage curve does not reach the maximum gas saturation of 0.75 specified in the model due to the injection of the second water slug. During the second imbibition process, the relative permeability to gas decreases along the scanning curve shown in orange in Figure 5.92. The second drainage process then traces along another scanning curve shown in blue in Figure 5.92. When the scanning curve reaches the input drainage curve, it then takes the value of input drainage curve and stops at the maximum saturation point (S_{hy}) which is 0.47 for the second drainage. After that, the third imbibition process proceeds backward along another scanning curve. This process goes on alternately until the injection stops. It is found that this maximum saturation slightly increases to 0.479 and 0.48 during the third and the fourth drainage respectively.

The hysteresis behavior of relative permeability to water of Killough model in black oil simulation is shown in Figure 5.93. Since water is the wetting phase, the input imbibition curve lies above the input drainage curve. The initial water saturation is 0.2. During the WAG process, water relative permeability retraces along the input imbibition only. This comes from the fact that hysteresis is only implemented in the non-wetting phase. Therefore, hysteresis effect cannot be seen from the water phase.

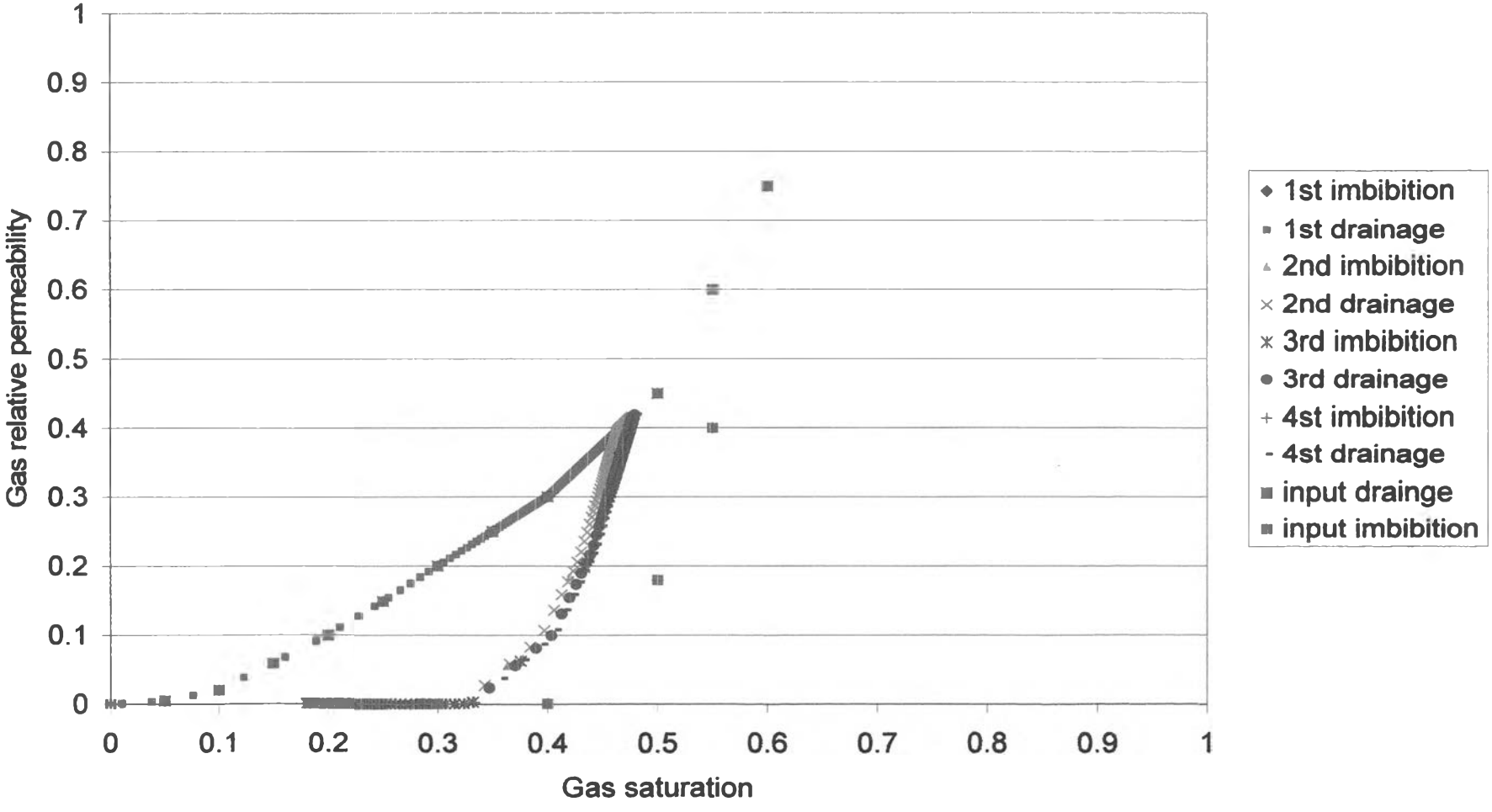

Figure 5.92: Plot of gas relative permeability vs. gas saturation of case 1.

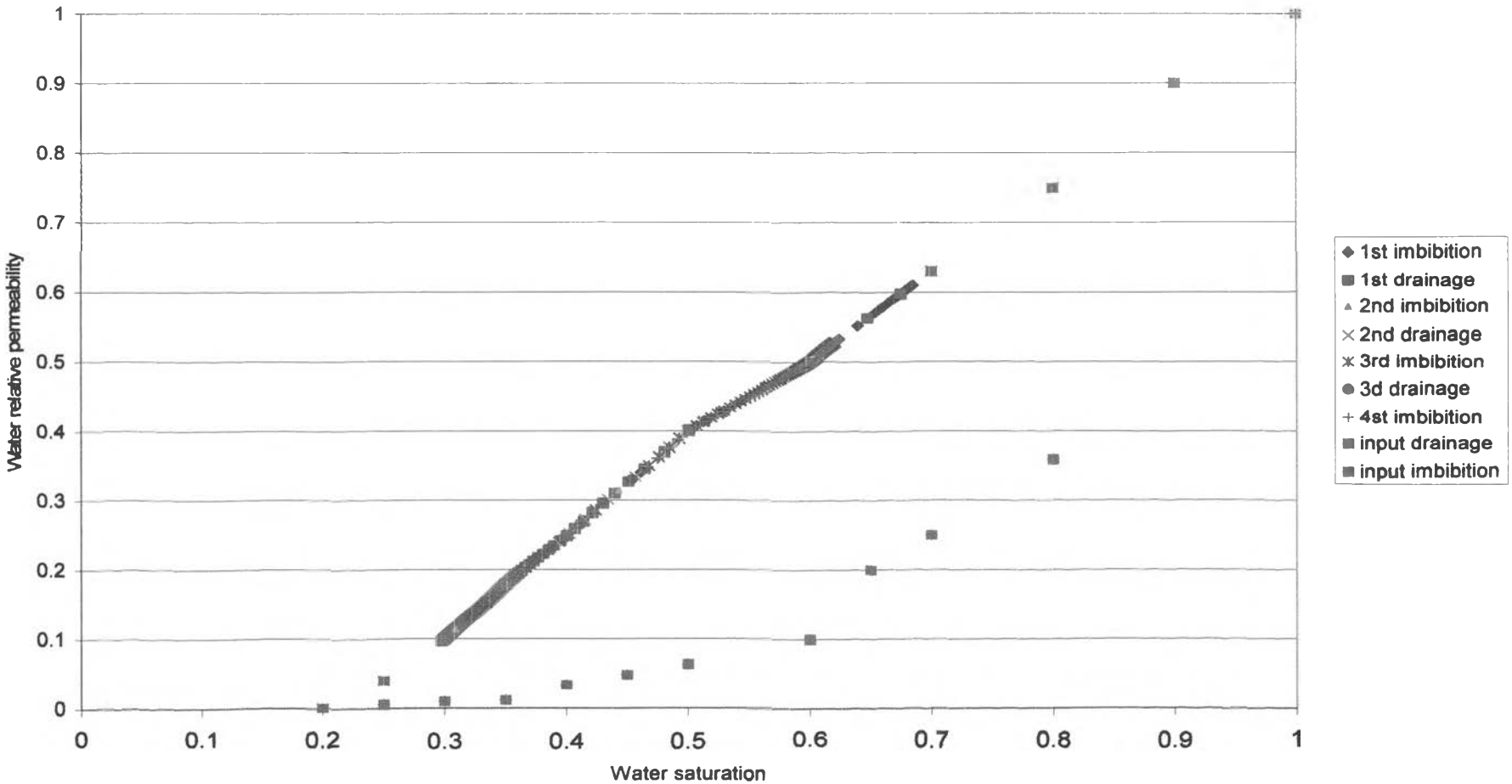

Figure 5.93: Plot of water relative permeability vs. water saturation of case 1.

Figure 5.94 presents the effect of Killough model on gas relative permeability in the compositional model. The characteristic is different from case 1. During the first drainage process, gas saturation increases along the input drainage curve exceeding the end-point saturation specified in the model of 0.6. Gas saturation increases to 0.756. Then, during the second imbibition process, relative permeability to gas abruptly decreases from this point towards 0 at S_g = 0.39. This path of the second imbibition process becomes the scanning curve. The scanning curve of the compositional reservoir model is shifted to the right hand side of the input imbibition curve. The gas saturation of this block increases beyond the maximum input gas saturation which is the end-point saturation of the relative permeability function. Hence, the relative permeability cannot increase much more than the end point value as can be seen from the figure. The next drainage and imbibition proceeds along the scanning curve in the same manner as the black oil model. It is further found that the maximum gas saturation of the scanning curve (S_{hy}) is about 0.72 which is higher than the value in black oil reservoir model whereas its correspondent gas relative permeability is about 0.55.

Figure 5.95 shows similar results as seen in Figure 5.93. The water relative permeability value proceeds and retraces along the input imbibition curve regardless of which phase is injected since Killough model implements the hysteresis effect on the non-wetting phase only.

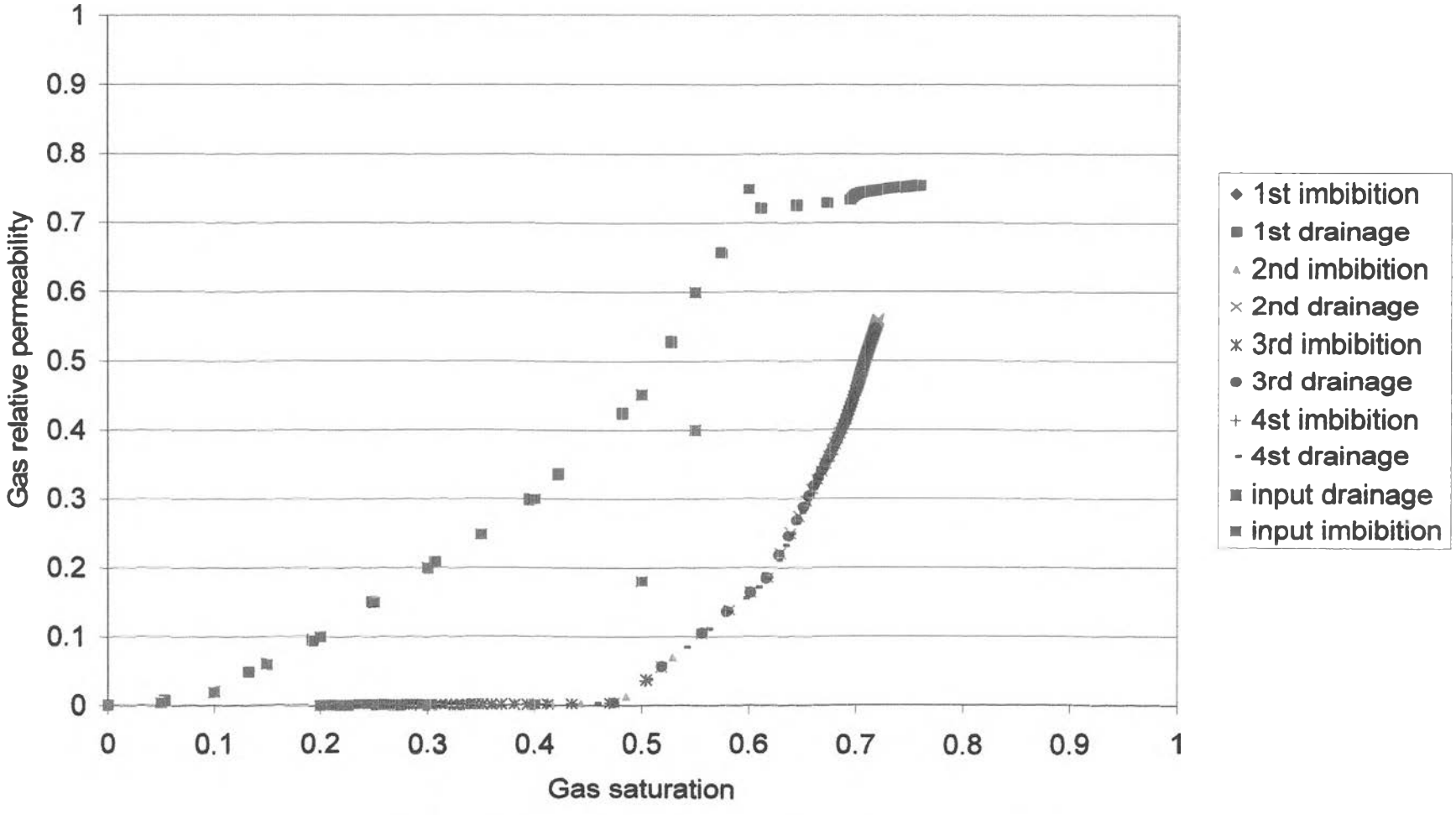

Figure 5.94: Plot of gas relative permeability vs. gas saturation of case 2.

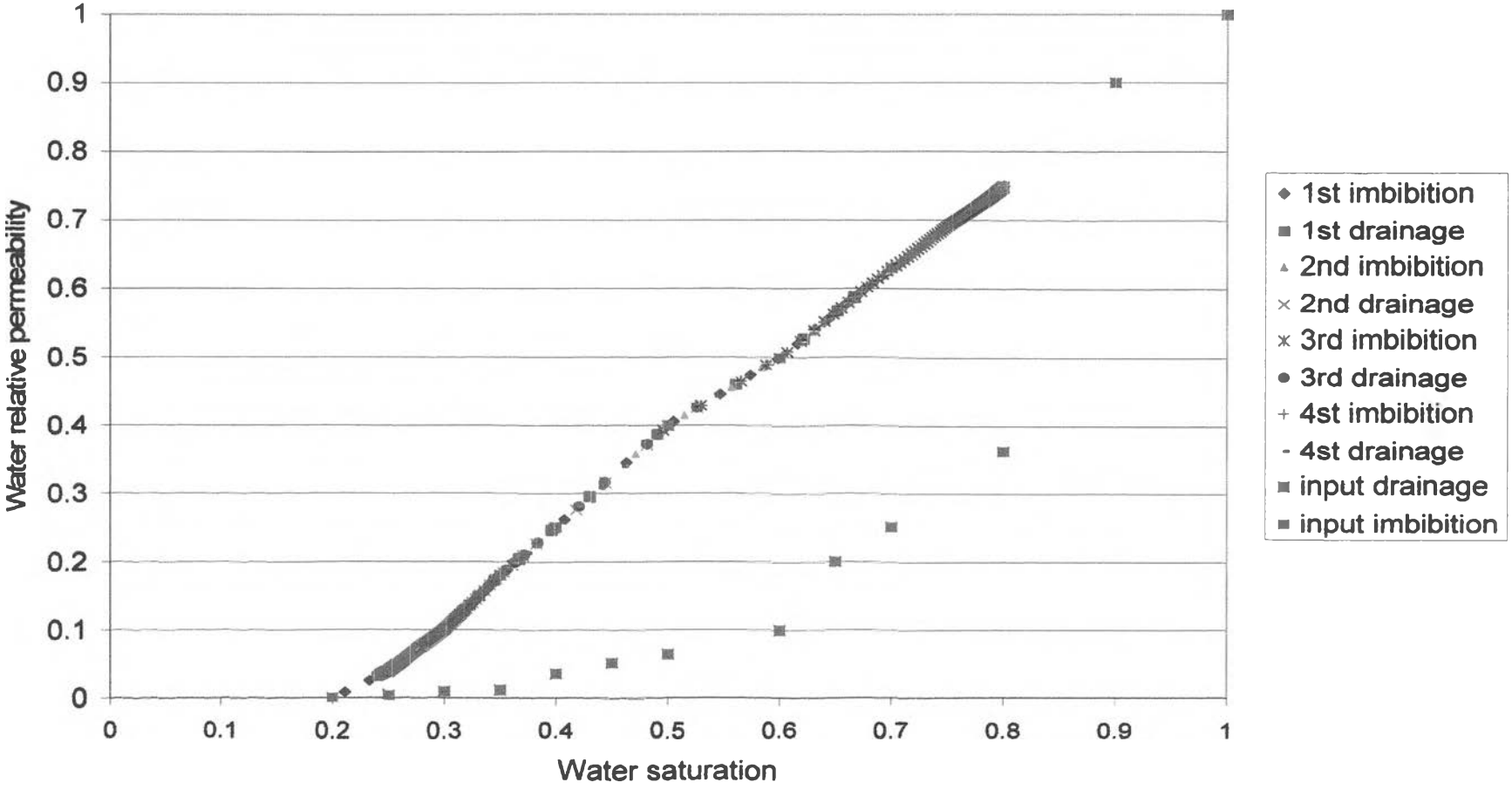

Figure 5.95: Plot of water relative permeability vs. water saturation of case 2.

Figure 5.96 illustrates the behavior of Larsen and Skauge relative permeability hysteresis model on the gas phase. The gas relative permeability stays at 0 during the first imbibition process. During the first drainage process, gas relative permeability slowly increases from S_g of 0 to S_g of 0.6. The drainage curve is constructed by damping the gas relative permeability curve by a factor which depends on water saturation at the beginning of the drainage phase. During the second imbibition process, gas relative permeability decreases to 0 at gas saturation = 0.273. During the next drainage and imbibition processes, gas relative permeability proceeds along the path which is not far away from each other. However, it is observed that damping of gas relative permeability results in a very low value of gas relative permeability for every drainage and imbibition curve. This may cause an underestimating of gas relative permeability. In general, the bottom hole pressure of the injection well during the gas injection process is lower than the pressure during water injection since gas has higher compressibility than water. If the gas injectivity problem occurs, the bottom hole pressure of the injection well may be higher than that during water injection. But the results from the Larsen and Skauge model show that the bottom hole pressure of the injector increases during gas injection. This is a direct result from underestimation of relative permeability to gas. Therefore, Larsen and Skauge relative permeability hysteresis model should be used with great care.

Figure 5.97 shows the hysteresis behavior of Larsen and Skauge model of the water phase. It was mentioned in Chapter 3 that the input curves are taken to be the two- phase curves and three-phase curves. The top curve the is two-phase curve whereas the bottom curve is the three-phases curve. During the first imbibition curve, water relative permeability proceeds along the three-phase. The first drainage process then begins at S_w = 0.7. The drainage curve proceeds toward the two-phase curve. This is because gas saturation during the imbibition is lower than gas saturation at the start of the drainage process. The subsequent drainage and imbibition processes then proceed along the two-phase curve.

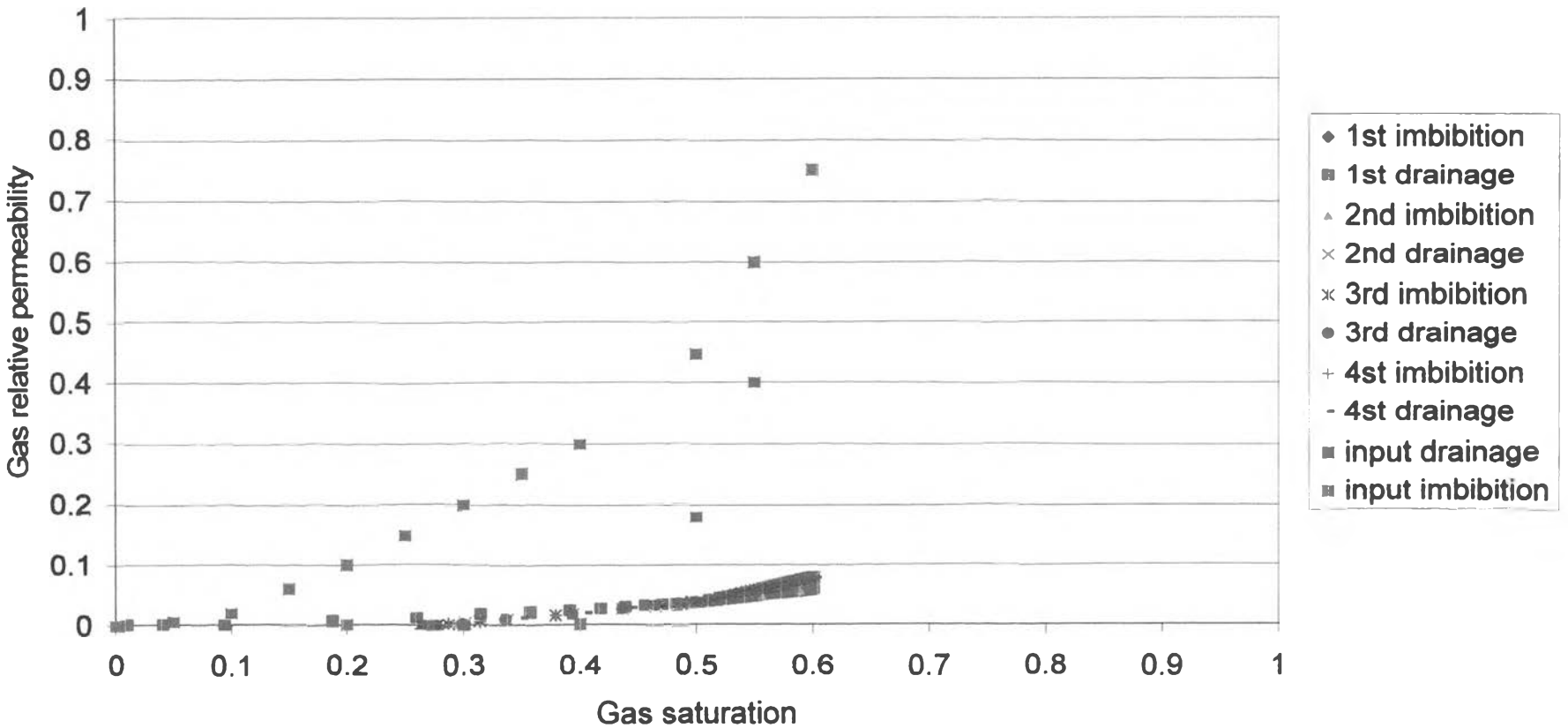

Figure 5.96: Plot of gas relative permeability vs. gas saturation of case 3.

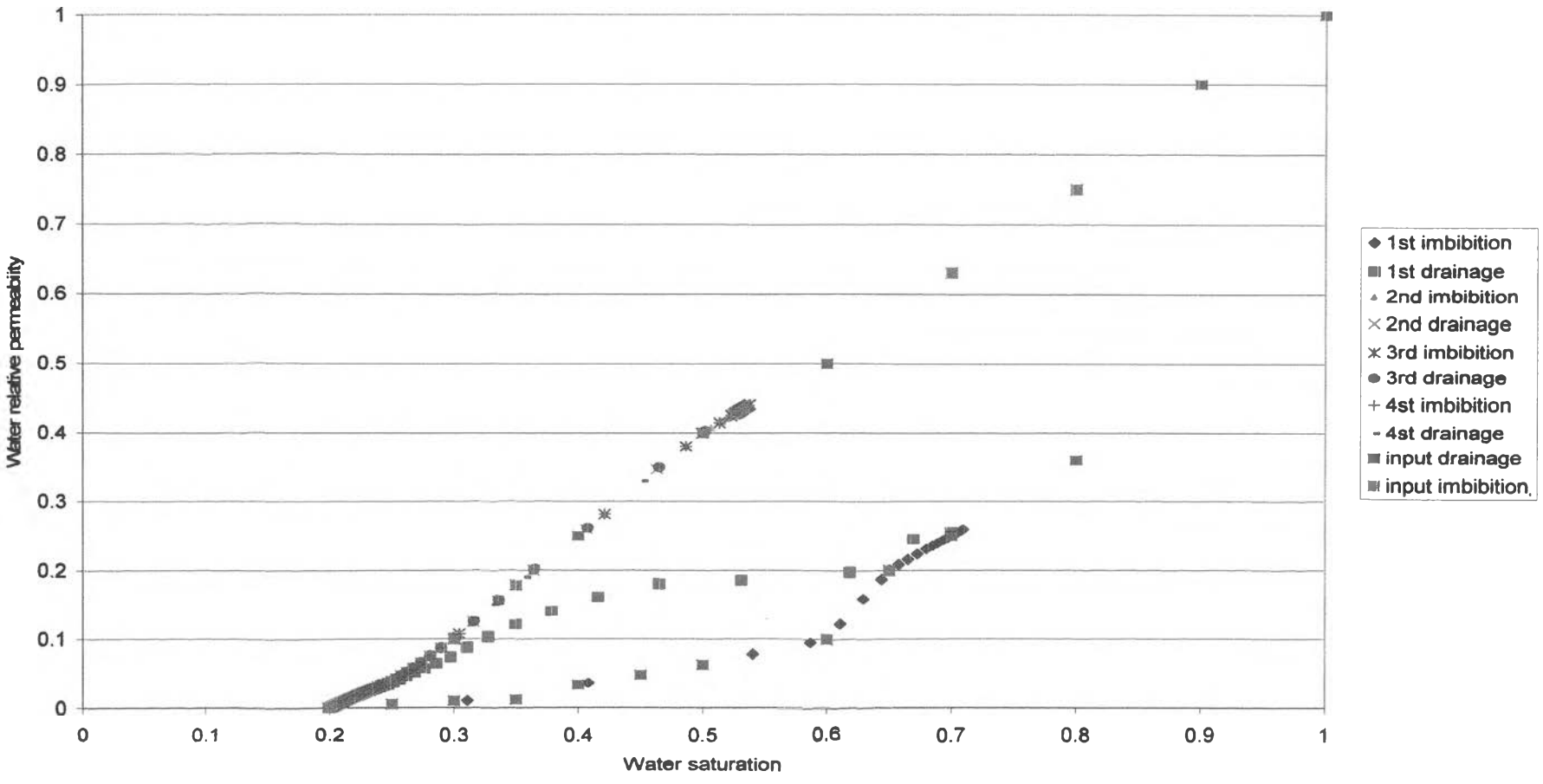

Figure 5.97: Plot of water relative permeability vs. water saturation of case 3.

The effect of relative permeability hysteresis model on the recovery factor was then investigated. Table 5.6 presented the results obtained from different relative permeability hysteresis models. For case 1 and 2, as already discussed in section 5.2, the difference in recovery factor comes from the miscibility of injected gas in case 2 which is a compositional model. The impact of using difference relative permeability hysteresis models is seen when comparing the recovery factor of case 1 and 3. The Larsen and Skauge model provides 12 % higher recovery factor than the Killough model. This is because gas relative permeability is damped to a very low value as seen in Figure 5.93. This is coupled by the fact that water relative permeability during the first imbibition and drainage process is lower than that of the Killough model. The lower value of gas and water relative permeability results in a decrease in the mobility ratio, giving the WAG process a more favorable flooding condition.

Table 5.6: Recovery factor of three cases.

Case	Recovery factor (%)
1	45.74
2	58.54
3	57.86

Since the results obtained from these cases come from a particular set of input parameters specified in the relative permeability hysteresis models, it is interesting to examine the effect of these parameters on the recovery factor.

Table 5.7: Recovery factors of case 1 and 2 when varying trapped gas saturation (a).

a	Recovery factor of case 1 (%)	Recovery factor of case 2 (%)
0.1	45.74	58.54
0.5	45.62	58.42
0.9	45.54	58.36

Table 5.8: Recovery factors of case 3 when varying Land's constant (C).

C	Recovery factor (%)
2	57.86
3	57.55
4	57.31

Table 5.9: Recovery factors of case 3 when varying reduction factor (α).

α	Recovery factor (%)
2	57.86
3	58.9
4	59.02

Table 5.7 shows the effect of trapped gas saturation parameter in the Killogh model on the recovery factor. It is seen that recovery factor decreases slightly when trapped gas saturation increases. This can be explained from the Eq. 3.36 and 3.37. If this parameter increases, the critical gas saturation (S_{gcrt}) will decrease. This allows gas to flow at lower saturation, increasing the ability of gas to flow from the injector to producer which may cause an early breakthrough.

Table 5.8 presents the effect of Land's constant in the Larsen and Skauge model on the recovery factors. The recovery factor decreases when this constant increases. As seen in Eq. 3.45, lowering the Land's constant causes the trapped gas saturation to decrease. This allows gas to flow more efficiently leading to a early gas breakthrough. However, the change of the recovery factor is very small.

The effect of reduction factor in Larsen and Skauge model is shown in Table 5.9. Increasing the reduction factor improves the recovery factor because the gas relative permeability is damped by a larger degree resulting in a better mobility ratio similar to the effects of the previous two parameters, the reduction factor has only small effect on the recovery factor.

The effect of relative permeability hysteresis model is investigated in this section. It can be concluded that Killough model implements the hysteresis effect on the non-wetting phase only. The black oil and compositional reservoir models show some different behaviors on gas relative permeability when Killough model is used. Hysteresis effect is implemented on both non-wetting and wetting phases in Larsen and Skauge model. Nevertheless, using Larsen and Skauge model can cause underestimation of relative permeability to gas.